ELSEVIER

Comput. Methods Appl. Mech. Engrg. 191 (2002) 3669–3750

Computer methods in applied mechanics and engineering

www.elsevier.com/locate/cma

Continuous/discontinuous finite element approximations of fourth-order elliptic problems in structural and continuum mechanics with applications to thin beams and plates, and strain gradient elasticity

G. Engel [a,1], K. Garikipati [b,*], T.J.R. Hughes [a], M.G. Larson [a,2], L. Mazzei [a,3], R.L. Taylor [c]

[a] *Division of Mechanics and Computation, Durand Building, Stanford University, Stanford, CA 94305-4040, USA*
[b] *Department of Mechanical Engineering, 3003B EECS, 2350 Hayward Street, University of Michigan, Ann Arbor, MI 48109-2125, USA*
[c] *Structural Engineering, Mechanics and Materials, Department of Civil and Environmental Engineering, 721 Davis Hall, University of California, Berkeley, CA 94720-1710, USA*

Received 28 February 2002; accepted 5 March 2002

Abstract

A new finite element method for fourth-order elliptic partial differential equations is presented and applied to thin bending theory problems in structural mechanics and to a strain gradient theory problem. The method combines concepts from the continuous Galerkin (CG) method, the discontinuous Galerkin (DG) method and stabilization techniques.

A brief review of the CG method, the DG method and stabilization techniques highlights the advantages and disadvantages of these methods and suggests a new approach for the solution of fourth-order elliptic problems. A continuous/discontinuous Galerkin (C/DG) method is proposed which uses C^0-continuous interpolation functions and is formulated in the primary variable only. The advantage of this formulation over a more traditional mixed approach is that the introduction of additional unknowns and related difficulties can be avoided. In the context of thin bending theory, the C/DG method leads to a formulation where displacements are the only degrees of freedom, and no rotational degrees of freedom need to be considered.

The main feature of the C/DG method is the weak enforcement of continuity of first and higher-order derivatives through stabilizing terms on interior boundaries. Consistency, stability and convergence of the method are shown analytically. Numerical experiments verify the theoretical results, and applications are presented for Bernoulli–Euler beam bending, Poisson–Kirchhoff plate bending and a shear layer problem using Toupin–Mindlin strain gradient theory.

* Corresponding author.
[1] Present address: Government of Singapore Investment Corporation, Singapore 068912.
[2] Present address: Department of Mathematics, Chalmers University of Technology, SE-412 96 Göteborg, Sweden.
[3] Present address: Bain and Company Italy, Via Crocefisso 10, 20122 Milano, Italy.

0045-7825/02/$ - see front matter
PII: S0045-7825(02)00286-4

1. Introduction

The solution of fourth-order elliptic problems with finite element methods has been the topic of research in computational mechanics for over 40 years. The objective of this paper is to devise a new technique for solving fourth-order elliptic problems which is superior to traditional finite element procedures. In the past, two methods have established themselves as standard approaches for solving fourth-order elliptic problems: C^1-continuous methods and mixed finite element methods. We wish to step back from these conventional schemes and take a new start by studying basic underlying finite element formulations. In particular, we wish to identify advantages and disadvantages of continuous Galerkin (CG), discontinuous Galerkin (DG) and stabilized methods. Based on these findings, we attempt to combine these techniques in order to retain their advantageous features, which will allow us to design a superior finite element formulation for fourth-order elliptic problems.

The approach suggested in this work has been termed the continuous/discontinuous Galerkin (C/DG) method, as it combines principles of the CG and DG schemes. The main feature of the C/DG method is that it involves only the primary variable, eliminating first derivatives and Lagrange multipliers as unknowns. For the case of thin bending theories, the C/DG method therefore allows for rotation-free finite element implementations. Another key feature of the C/DG method is that it employs only C^0-continuous shape functions and hence leads to discontinuities in first- and higher-order derivatives. Continuity requirements for the derivatives are satisfied weakly, as they are built into the variational equation via stabilizing residual terms on interior boundaries.

1.1. Fourth-order elliptic problems

Fourth-order elliptic problems are problems which can be described by partial differential equations with derivatives of up to fourth order. A problem is said to be of elliptic type when the characteristic equation of its governing partial differential equation possesses only complex roots [1]. We want to focus in this work on two examples from thin bending theory, namely the Bernoulli–Euler beam and the Poisson–Kirchhoff plate, and on the Toupin–Mindlin shear layer as an example from strain gradient theory. The thin beam theory obtained its name from its originators Johann Bernoulli (1717), Daniel Bernoulli (1742) and Leonhard Euler (1744), whereas the thin plate theory honors the fundamental contributions by Siméon-Denis Poisson (1811) and Gustav Robert Kirchhoff (1850) [2]. The strain gradient shear layer formulation is more recent and based on the developments of Toupin [3] and Mindlin [4] in the 1960s.

Descriptions of thin bending theories can be found in most textbooks on structural mechanics, see for examples [5–9], and [10,11] for a description in the context of finite elements. For an introduction to strain gradient theory, we refer to a review article by Fleck and Hutchinson [12].

1.2. Traditional finite element methods and continuity

Finite element methods have become the most widely used technique in computational structural mechanics and today dominate commercially available software as well as research endeavors into basic theory. It is interesting to look back at the early days and at the decisions that were tacitly made which have had a strong influence on the development of the methodology and the directions it ultimately took. In particular, we are interested in examining the role played by continuity in the evolution of the subject.

The generally agreed upon foundation of finite element methods is variational formulations of partial differential equations stated in terms of precisely defined infinite-dimensional trial solution and weighting function spaces. Familiar examples are Sobolev spaces, which are appropriate for many linear and nonlinear problems. The standard finite element approximations involve posing the variational formulation in terms of finite-dimensional subspaces of piecewise polynomials which inherit the regularity (i.e., differen-

tiability) properties of the in finite-dimensional spaces. Typically, these conditions amount to continuity of the polynomials across element boundaries. One speaks of C^0-continuous elements for the case when only the primary variable is continuous between elements and of C^1-continuous elements for the case when both the primary variable and its first derivative are continuous on element interfaces.

Researchers in the early days were challenged to develop elements which satisfied continuity requirements appropriate for various classes of problems. For example, the standard formulations require C^0-continuity of displacements for problems of elasticity, but more stringent C^1-continuity for problems involving thin beams, plates and shells, where we define thin to mean that we have no transverse shear deformation. It turned out that C^0-continuity for arbitrarily shaped elements was quite easy to achieve whereas C^1-continuity was not. C^1-continuous methods are feasible for one-dimensional problems. The standard approach for solving Bernoulli–Euler beam problems is by employing C^1-continuous Hermite cubic shape functions, interpolating both displacements and rotations (i.e., slopes). For two-dimensional problems, such as from plate and shell analysis, C^1-continuous methods are very complicated, and formulations for three-dimensional problems as they arise from strain gradient theories become intractable.

Despite some elegant albeit very complex successes for plates and shells, these efforts almost completely vanished about 20 years ago when researchers began focusing on the more promising shear-deformable bending theories in which rotations are independent fields and are not constrained to match the slopes of the transverse displacement field. This framework allowed use of independent C^0-continuous interpolations for displacements and rotations, which were ubiquitous for all element shapes and polynomial orders and which proved to be very convenient from an implementational viewpoint. Today, this mixed approach is a well-established method with a rich mathematical foundation and good accuracy and stability behavior [13]. However, formulations involve both displacements and derivatives as unknowns, and stability requirements arise for the combination of interpolation functions for the different fields.

The common approach for solving thin plate bending problems with mixed methods is to apply Reissner–Mindlin thick plate theory. The shear-locking difficulties arising for many combinations of low-order interpolation functions have been solved, but lead to more complicated formulations and theories. Remedies against shear-locking are, for example, satisfying inf-sup considerations [14,15], uniform/selective reduced integration [16], stabilized formulations [17] and non-conforming elements [18].

Mixed methods for strain gradient theories are more problematic, involving displacements and displacement gradients as unknowns. A recent method by Shu et al. [19], for example, invokes in addition Lagrange multipliers for enforcing kinematic constraints, and their lowest-order triangular element requires 28 unknowns per element, and their lowest-order quadrilateral element 38 unknowns. From these numbers it is evident that currently, no efficient finite element methods are available for strain gradient theory formulations.

1.3. Rotation-free thin bending elements

Today, C^0-continuous theories dominate commercial software and theoretical research, see Batoz et al. [20] for a survey on triangular plate bending elements. However, in the last decade a few efforts have attempted to reverse this trend. It is interesting to note that there have been many elements developed over the years which have violated the continuity requirements of the governing variational formulation. However, for the most part, elements of this type are viewed pejoratively; they are frequently described as non-conforming, incompatible, and variational crimes [21]. The penchant for respecting continuity requirements in structural mechanics, established in the early days, lives on, but some opportunities may be lost in the process.

In the thin bending theories, there is no need for independent rotation fields. Consequently, it is possible to develop methods which do not involve rotational degrees of freedom. This spirit was well established in

finite difference formulations [8], but finite element counterparts to this idea seemed impossible due to the necessity of employing slope degrees of freedom in order to satisfy continuity requirements. In the last decade, a number of procedures have been proposed, based on a combination of finite difference, finite element, finite volume and ad hoc concepts, leading to elements with only displacement degrees of freedom. Typically, these elements are very simple—the three-node triangle has dominated—and they all involve non-locality. By non-locality we mean that the curvature in an element depends on the displacement field in that element and its neighbors. Consequently, these elements fall outside the classical framework. Furthermore, C^1-continuity requirements are simply ignored, but these elements seem to perform fairly well and have the great advantage of eliminating altogether the rotational degrees of freedom. In the linear case, this leads to a saving of computer solution time, and in the non-linear case it additionally amounts to a substantial reduction in complexity. The reason for this is that in the linear case, rotations have a vector space structure (i.e., R^3), whereas in the non-linear case they have a non-linear group structure (i.e., SO(3)). Algorithms to preserve the group structure are very complicated, especially in dynamics. Thus, eliminating the rotation field ab initio is a very attractive proposition.

We would like to mention in this context the work on thin bending elements without rotational degrees of freedom of Phaal and Calladine [22,23] and of Oñate et al. [24,25], the latter blending finite volume concepts with traditional finite elements. Other interesting methods for fourth-order elliptic problems, for which error analyses are also presented, are a penalty method by Babuška and Zlámal [26] and a non-conforming discontinuous formulation by Baker [27].

Given the value of the rotation-free procedures mentioned before, we have set for ourselves the objective of establishing what we would describe as a consistent variational/finite element framework of thin bending elements accommodating C^0-continuous polynomial interpolations. It is possible to do this in the context of DG formulations, which have come under increasing attention of late, primarily in computational fluid dynamics. In the DG method, no continuity is required across element boundaries, but the variational formulations are more complex than classical ones. Agreement as to canonical DG formulations for even the simplest problems is not yet established, so it is appropriate to say that the method is still in its infancy, despite the fact that initiatory versions go back about 30 years.

1.4. Finite element techniques

The C/DG method suggested in this paper for the solution of fourth-order elliptic problems combines features of the three basic finite element techniques of CG methods, DG methods and stabilization. Let us consider a brief overview of these techniques. In the following, it has not been attempted to give a complete survey of the evolution of the respective fields. Rather, contributions of major importance for the areas as a whole or for the purpose of the developments in this paper have been mentioned in order to place the C/DG method in the context of previous investigations.

1.4.1. Continuous Galerkin methods

CG methods have been pioneered by Argyris [28,29] and Zienkiewicz [30] (also see [31]). They consist of recasting the strong form of the boundary value problem in its variational (or weak) form by means of integration by parts. One then chooses finite-dimensional trial and weighting function spaces for the approximation functions, leading to a matrix system which can be solved for the unknown nodal quantities, see [10] for a detailed description. The main feature of the CG method is the assumption of continuity in the primary variable, and for fourth-order problems also of the first derivatives, across interior boundaries.

The CG method is a well-established and efficient formulation for second-order elliptic problems with a rich mathematical foundation, and error estimates are available [32–35]. Difficulties, however, arise for fourth-order elliptic problems due to the stronger continuity requirements, as well as for constrained problems.

1.4.2. Discontinuous Galerkin methods

DG methods can be separated into two main categories: methods which are discontinuous in time, and methods which are discontinuous in space. Time-DG methods have been developed for first- and second-order hyperbolic equations, and are often encountered in fully discrete space–time finite element formulations; [36,37].

In this work we will not consider time-DG methods further and focus on methods which are discontinuous in space. The DG method has established itself as a viable method for solving first-order hyperbolic partial differential equations in fluid mechanics. Discontinuities may be present in the solution, and the DG method seems to be the natural approach for capturing these numerically. The first DG method was introduced by Reed and Hill for the neutron transport equation in 1973 [38]. Their method was analyzed extensively, first by Lesaint and Raviart [39,40] and later by Johnson et al. [41] and Johnson and Pitkäaranta [42].

The introduction of non-conforming (or incompatible) finite elements for bending problems in 1973 can be considered as a precursor to the DG method in structural mechanics. Wilson et al. [43] designed an incompatible modes finite element which was discontinuous on the interior boundaries between the nodes. This construction resulted in improved bending behavior of the element. The convergence behavior of the non-conforming element was analyzed by Lesaint [44]. Kikuchi and Ando [45] presented a formulation for thin plates and shells with non-conforming normal rotations.

Most of the development of the DG method has been motivated by problems from fluid mechanics. Cockburn and Shu [46] introduced a Runge–Kutta DG method for the solution of first-order non-linear hyperbolic conservation laws. An *hp*-adaptive DG method for first-order problems was developed and analyzed by Bey and Oden [47], and a more detailed analysis was presented by Houston et al. [48]. Bassi and Rebay [49] presented a DG method for the solution of the Euler equations, which paved the way for research efforts aimed at solving the Navier–Stokes equations.

The initial approach for solving second-order hyperbolic equations was to rewrite the equation as a system of first-order equations. Introducing the flux as an auxiliary variable, which is the first derivative of the primary variable, one can numerically solve the first-order system of equations. The advantage of this mixed approach is that one can solve a second-order equation with a method originally designed for first-order problems. The disadvantage, however, is a considerable increase in the unknowns due to the introduction of auxiliary variables. Bassi and Rebay [50] extended their method to a mixed approach for solving the compressible Navier–Stokes equations. Their method was analyzed by Brezzi et al. [51] and generalized by Cockburn and Shu [52].

A different approach to second-order problems has been motivated by a method by Nitsche introduced in 1973 [53]. Nitsche's method features two crucial characteristics, namely the elimination of a Lagrange multiplier by means of an energetically consistent flux weighting function and the introduction of a stabilization term. Dirichlet boundary conditions are built into the weak form. Rather than invoking an unknown Lagrange multiplier, however, Nitsche chose a flux-like weighting function instead. In addition, Nitsche introduced a stabilizing term on the boundary for enforcing the homogeneous Dirichlet boundary condition he considered. This choice for the weighting function and the stabilization on the boundary led to optimal convergence rates for the elliptic Poisson equation. A penalty method by Babuška [54] had the same goal of building the boundary condition into the weak form.

Douglas and Dupont [55] extended Nitsche's idea to DG methods for linear elliptic and parabolic problems. They applied Nitsche's approach on an element level, and summing all element contributions, it resulted in a modified weak form with flux-weighted and penalized inter-element conditions. In particular, jump terms in the unknown variable across interior boundaries arose, which were penalized to approximately enforce continuity across element interfaces. Wheeler [56] analyzed this method, and Percell and Wheeler [57] recognized the significance of this method for *hp*-adaptive finite element strategies. Arnold [58,59] investigated these interior penalty methods for linear and non-linear parabolic boundary value

problems. A method by Delves and Hall [60], which the authors termed the 'global element method', also features flux-weighted interface conditions. However, it lacks the stabilization (or interior penalty) term, which results in the matrix being indefinite.

A strong influence on the development of the DG method for second-order equations was the work of Baumann [61]. By reversing the sign of the flux-weighted interface conditions in the global element method, which can be traced back to the original work by Nitsche, he obtained a method amenable to a variety of elliptic and hyperbolic problems of fluid mechanics. The sign reversal renders the originally symmetric formulation of Delves and Hall and Nitsche non-symmetric. For the application of Baumann's method to advective–diffusive problems, which was the ultimate goal, symmetry of the system is, however, unimportant, as the contribution of the advective operator leads to a non-symmetric system. In addition, the sign reversal results in advantages for the analysis of the method. Another benefit of Baumann's method is the fact that no auxiliary variables need to be introduced, as was the case for mixed methods, which reduces the number of unknowns. The disadvantage of the method, however, is that stability and convergence could only be established analytically for cubic or higher-order interpolation. Babuška et al. [62] provide numerical evidence that the method is also stable for quadratic interpolation by numerically evaluating the inf-sup condition in a one-dimensional setting. An interesting detail worth mentioning is their observation of a loss of accuracy of Baumann's method in the L^2-norm for even orders of interpolation. Various contributions by Oden et al. [63] and Baumann and Oden [64–66] explore Baumann's method numerically and analytically and apply it to the solution of the Euler and Navier–Stokes equations in an *hp*-adaptive environment. Prudhomme et al. establish *hp* a priori error estimates [67]. Recent research efforts have been aimed at stabilizing Baumann's method and thereby linking it back to the original development by Nitsche and to the interior penalty methods discussed earlier. Arnold et al. [68] have presented a general framework for stabilized and non-stabilized DG methods for elliptic equations.

A rich mathematical foundation has been established for DG methods. However, the disadvantage of DG methods is that they necessitate the introduction of new programming structures into current finite element codes. DG methods involve contributions on interior boundaries, which require the introduction of a loop over interior boundaries in addition to the loop over elements. Furthermore, due to the discontinuous nature of the approximation functions, additional unknowns are introduced, which most current finite element codes cannot accommodate. The increase in the number of unknowns often leads to DG methods being inefficient when compared to CG methods. This fact has been recognized by Freund [69] who suggested an approach for combining CG and DG methods on different parts of the domain for the advection–diffusion problem.

1.4.3. Stabilization

Stabilization enhances stability without sacrificing accuracy by changing the weak formulation of the boundary value problem under consideration. Weighted residual terms are added to the variational equation, which involve a mesh-dependent stabilization parameter. These extra terms usually are functions of the Euler–Lagrange equations on an element level to ensure consistency of the method. Stabilized methods were proposed in the 1980s to account for the fact that CG methods for certain boundary value problems do not inherit the stability properties of the continuous problem. They were originally introduced for the advection–diffusion equation by Brooks and Hughes [70] and subsequently generalized by Hughes et al. [71]. Stabilized methods have been analyzed extensively, and the theoretical foundations are still being explored. Two frameworks for deriving stabilized methods and stabilization parameters have been established, namely the variational multiscale approach [72] and the residual-free bubbles approach [73,74]. The two approaches have been shown to be equivalent under certain circumstances [75]. Several applications and generalizations of residual-free bubbles have been presented by Franca and Russo [76–79]. For a review of the evolution of stabilized methods and a survey of techniques, see [80].

1.5. Objectives

Knowing about the difficulties as they arise from traditional C^1-continuous and mixed finite element approaches, and based on the advantages and disadvantages of the basic finite element techniques of CG methods, DG methods and stabilization, we attempt to combine these three basic techniques in order to retain their advantageous features and to obtain a superior finite element method for solving fourth-order elliptic problems. In particular, we want the C/DG method to have the following characteristics:

1. The formulation involves only the primary variable. In the case of thin bending theories, we insist on rotation-free descriptions. For strain gradient theories, we want to avoid Lagrange multipliers and obtain a displacement gradient-free formulation. This leads to greater simplicity and reduces the number of unknowns.
2. The approximation functions only need to satisfy C^0-continuity requirements across interior boundaries, leading to discontinuities in first and higher-order derivatives. Therefore, we need to change the variational formulation to enforce the continuity requirements for the derivatives weakly. We wish to employ low-order interpolation functions on the element level (linear, quadratic, cubic).
3. The method needs to be consistent, stable, convergent and simple. To ensure stability, we add weighted residual terms on interior boundaries, utilizing stabilization techniques.

1.6. Outline of the paper

In Section 2, we introduce the CG method and its stabilized counterpart. For this purpose we present the advection, diffusion and advection–diffusion model problems. CG methods are introduced for advection–diffusion, and we examine stabilized versions for the advection–diffusion and diffusion problems.

Section 3 covers DG methods for the three model problems introduced in Section 2 and their stabilized equivalents. An error analysis is presented for stabilized DG methods for advection, diffusion and advection–diffusion. The section closes with an investigation of the efficiency of DG methods.

In Section 4, we introduce C/DG methods for thin bending theories for the example of the Bernoulli–Euler beam and its two-dimensional generalization, the Poisson–Kirchhoff plate. For both examples, an error analysis of the C/DG method is performed.

Section 5 establishes the C/DG method for a strain gradient theory. The method is stated for the Toupin–Mindlin shear layer, and a convergence proof is given. The results from this one-dimensional problem provide a foundation for future generalizations to two and three dimensions, as well as to nonlinear applications such as strain gradient plasticity.

The numerical validation of the C/DG methods is presented in Section 6 for several example problems. In particular, we investigate cantilever beams loaded by an end moment, an end shear force and a distributed force for different orders of interpolation. We present convergence studies for square and circular plates with distributed and center point loads for different boundary conditions. We end the section with a numerical validation of the theoretical convergence results for the Toupin–Mindlin shear layer fixed on one side and loaded by a traction on the other side.

Section 7 summarizes the main findings of this work, draws some conclusions and suggests directions for future research.

Appendix A assembles basic definitions for the finite element method as well as estimates used frequently in the error analyses in the body of this paper. We present interpolation estimates, inverse estimates and a trace inequality.

Appendix B gives a definition of the stabilization parameter. An analytical way for determining the constants of the stabilization parameters is outlined for linear interpolation in one dimension by comparing the finite element equations with finite difference approximations.

Appendix C briefly discusses implementation considerations of DG and C/DG methods. Existing finite element programs for CG methods require modifications which are delineated.

2. Stabilized continuous Galerkin methods

The CG method has established itself as the method of choice for numerically solving partial differential equations in structural mechanics. Through the introduction of stabilization techniques, the CG method, which in its original form is unstable for hyperbolic problems and elliptic problems with significant first derivatives, is capable of accurately approximating the solution of such partial differential equations, which has extended the reach of finite element methods into the realm of computational fluid mechanics. Stabilized methods not only allow the solution of new problem classes with finite elements, but also opened up new possibilities for constrained problems in structural mechanics.

We start this section with an outline of the model problems we will use for the discussion of stabilized CG and DG methods, and introduce some notation employed throughout this paper. We then comment on the weak formulation of a boundary value problem and give a brief account of the CG method. We end this section with a review of stabilized methods for the advection–diffusion and diffusion equations, and analyze the streamline/upwind Petrov–Galerkin (SUPG) method, the Galerkin least squares (GLS) method and a method by Nitsche as examples.

2.1. Model problems and definitions

The three model problems outlined in this section are the basic ones used in computational fluid mechanics, namely advection, diffusion and advection–diffusion. The advection–diffusion equation is the problem for which stabilized CG methods were originally developed, and most of our exposition in Sections 2.2 and 2.3 is based on this equation. In Section 2.3 we discuss in addition a stabilized formulation introduced by Nitsche for the diffusion problem.

2.1.1. Advection

Let us consider the scalar linear hyperbolic boundary value problem

$$-\nabla \cdot \boldsymbol{\sigma}^{\mathrm{a}}(\phi) = f \quad \text{in } \Omega, \tag{1}$$

$$\phi = g \quad \text{on } \Gamma^{-}, \tag{2}$$

where

$$\boldsymbol{\sigma}^{\mathrm{a}}(\phi) = -\boldsymbol{u}\phi \tag{3}$$

is the advective flux, $\boldsymbol{u} = \boldsymbol{u}(\boldsymbol{x})$ is the velocity field, assumed smooth and solenoidal, i.e.,

$$\nabla \cdot \boldsymbol{u} = 0, \tag{4}$$

ϕ is the unknown we wish to solve for, and f and g are given forcing and boundary condition functions, respectively. The domain Ω is assumed to be open and bounded in $\mathbb{R}^d$, $d = 1$, 2 or 3, and its boundary Γ to be Lipschitz-continuous [32]. Let Γ^{-} indicate the inflow boundary, i.e.,

$$\Gamma^{-} = \{\boldsymbol{x} \in \Gamma : \boldsymbol{u} \cdot \boldsymbol{n} < 0\}, \tag{5}$$

where $\boldsymbol{n} = \boldsymbol{n}(\boldsymbol{x})$ is the outward unit normal vector to Γ. The outflow boundary is denoted by $\Gamma^{+} = \Gamma \setminus \Gamma^{-}$, see Fig. 1 for an illustration of the boundary partition and the outward unit normal vector. Let us also define the component of the advective flux along $\boldsymbol{n}$

$$\sigma_n^{\mathrm{a}}(\phi) = \boldsymbol{n} \cdot \boldsymbol{\sigma}^{\mathrm{a}}(\phi) = -(\boldsymbol{n} \cdot \boldsymbol{u})\phi = -u_n\phi, \tag{6}$$

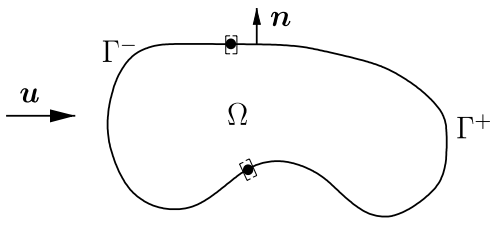

Fig. 1. Boundary partition for advection.

where $u_n = \boldsymbol{n} \cdot \boldsymbol{u}$, and the advection operator

$$\mathscr{L}_{\mathrm{a}}(\cdot) = \boldsymbol{u} \cdot \boldsymbol{\nabla}(\cdot). \tag{7}$$

The advection equation (1) governs basic transport phenomena.

2.1.2. Diffusion

The scalar linear diffusion equation with both Dirichlet and Neumann boundary conditions can be written as

$$-\boldsymbol{\nabla} \cdot \boldsymbol{\sigma}^{\mathrm{d}}(\phi) = f \quad \text{in } \Omega, \tag{8}$$

$$\phi = g \quad \text{on } \Gamma_g, \tag{9}$$

$$\sigma_n^{\mathrm{d}}(\phi) = h \quad \text{on } \Gamma_h, \tag{10}$$

where, similarly to the advection case, we define the diffusive flux as

$$\boldsymbol{\sigma}^{\mathrm{d}}(\phi) = \boldsymbol{A}\boldsymbol{\nabla}\phi \tag{11}$$

and its component along $\boldsymbol{n}$ as

$$\sigma_n^{\mathrm{d}}(\phi) = \boldsymbol{n} \cdot \boldsymbol{\sigma}^{\mathrm{d}}(\phi) = \boldsymbol{n} \cdot (\boldsymbol{A}\boldsymbol{\nabla}\phi). \tag{12}$$

The boundary Γ consists of the two parts Γ_g, where the Dirichlet boundary condition function g is specified, and Γ_h, where the Neumann boundary condition function h is given, and we have $\Gamma_g \cap \Gamma_h = \emptyset$, $\overline{\Gamma_g \cup \Gamma_h} = \Gamma$, see Fig. 2. The diffusivity matrix $\boldsymbol{A}$ in (11) is assumed to be symmetric, bounded and such that there exists a positive constant diffusivity A satisfying

$$A\boldsymbol{v}^{\mathrm{T}}\boldsymbol{v} \leqslant \boldsymbol{v}^{\mathrm{T}}\boldsymbol{A}(\boldsymbol{x})\boldsymbol{v} \quad \forall \boldsymbol{v}, \boldsymbol{x} \in \mathbb{R}^d. \tag{13}$$

The diffusion operator is defined as

$$\mathscr{L}_{\mathrm{d}}(\cdot) = -\boldsymbol{\nabla} \cdot \boldsymbol{A}\boldsymbol{\nabla}(\cdot). \tag{14}$$

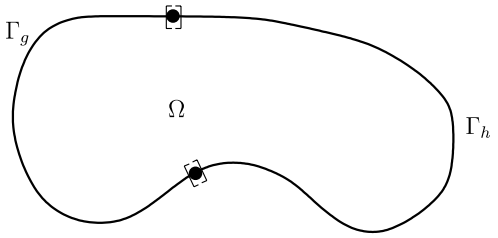

Fig. 2. Boundary partition for diffusion.

The diffusion problem is of elliptic type and governs physical phenomena such as heat conduction and Brownian motion.

2.1.3. Advection–diffusion

Let us introduce the scalar linear advection–diffusion boundary value problem

$$-\nabla \cdot \boldsymbol{\sigma}^{\mathrm{ad}}(\phi) = f \quad \text{in } \Omega, \tag{15}$$

$$\phi = g \quad \text{on } \Gamma_g, \tag{16}$$

$$\sigma_n^{\mathrm{d}}(\phi) = h \quad \text{on } \Gamma_h, \tag{17}$$

where

$$\boldsymbol{\sigma}^{\mathrm{ad}}(\phi) = \boldsymbol{\sigma}^{\mathrm{a}}(\phi) + \boldsymbol{\sigma}^{\mathrm{d}}(\phi) \tag{18}$$

denotes the advective–diffusive flux and consists of the previously defined advective flux $\boldsymbol{\sigma}^{\mathrm{a}}(\phi)$ and the diffusive flux $\boldsymbol{\sigma}^{\mathrm{d}}(\phi)$, see (3) and (11). The component of the advective–diffusive flux along $\boldsymbol{n}$ is defined as

$$\sigma_n^{\mathrm{ad}}(\phi) = \boldsymbol{n} \cdot \boldsymbol{\sigma}^{\mathrm{ad}}(\phi) = \sigma_n^{\mathrm{a}}(\phi) + \sigma_n^{\mathrm{d}}(\phi). \tag{19}$$

The assumptions for the Dirichlet and Neumann parts of the boundary are the same as the ones introduced in the diffusion case (see Section 2.1.2), and we also extend most of the other previous conditions, namely that the velocity field is incompressible as in the advection case, see (4), and that the diffusivity matrix $\boldsymbol{A}$ is symmetric, bounded and such that (13) holds as in the diffusion case.

For simplicity, we introduce the additional assumption $\Gamma^- \subseteq \Gamma_g$, where Γ^- denotes again the inflow part of the boundary as defined in (5). The advection–diffusion operator can be written as

$$\mathscr{L}_{\mathrm{ad}}(\cdot) = \mathscr{L}_{\mathrm{a}}(\cdot) + \mathscr{L}_{\mathrm{d}}(\cdot), \tag{20}$$

where we have used the definitions of the advection and diffusion operators in (7) and (14), respectively.

2.2. Continuous Galerkin methods

In this section we restrict our attention to the advection–diffusion model problem with homogeneous Dirichlet boundary condition on $\Gamma_g \equiv \Gamma$. In the context of finite element methods and variational calculus, (15)–(17) are referred to as the strong form of the boundary value problem. The CG method is a finite-dimensional approximation to the solution of the corresponding weak form, which we introduce now.

The weak form can be stated as: Find $\phi \in \mathscr{V}$ such that

$$B(w, \phi) = L(w) \quad \forall w \in \mathscr{V}, \tag{21}$$

where the bilinear form $B(\cdot,\cdot)$ and the linear form $L(\cdot)$ are defined as

$$B(w, \phi) = (\nabla w, \boldsymbol{\sigma}^{\mathrm{ad}}(\phi)), \tag{22}$$

$$L(w) = (w, f) \tag{23}$$

for w, $\phi \in \mathscr{V}$ sufficiently smooth. For the advection–diffusion problem considered, we have $\mathscr{V} = H_0^1(\Omega)$, where H_0^1 denotes the Sobolev space of square-integrable functions vanishing on the boundary and with square-integrable first derivatives. The notation $(\cdot,\cdot)$ indicates the L^2-inner product on the domain Ω. In the remainder of this paper it will be assumed that the notation $(\cdot,\cdot)$ corresponds to the L^2-inner product on the entire domain Ω; otherwise, the domain on which the inner product is to be taken will be explicitly stated as a subscript. Solutions of (21) are called weak solutions, as they only need to satisfy less restrictive

smoothness requirements. It can be shown that under certain assumptions, solutions of (15)–(17) and (21) are equivalent [10].

Let us introduce at this point the partition

$$\mathscr{P}(\Omega) = \{\Omega_e\}_{e=1}^{N_{\mathrm{el}}} \tag{24}$$

of the domain Ω into N_{el} elements Ω_e, which is illustrated in Fig. 3 for the example of triangular elements. We assume that the family of elements resulting from the partition is regular (see Definition A.6 in Appendix A), and we use $h_e = \mathrm{diam}(\Omega_e)$ as the element characteristic dimension. For any element $\Omega_e \in \mathscr{P}(\Omega)$ define $P_k(\Omega_e)$ to be the finite-dimensional space of all polynomials of degree less than or equal to k defined on Ω_e. We can now define

$$\mathscr{V}^h = \{v^h \in H_0^1(\Omega) |\ v^h|_{\Omega_e} \in P_k(\Omega_e)\ \forall \Omega_e \in \mathscr{P}(\Omega)\} \tag{25}$$

as the finite-dimensional space for our CG approximations, i.e., $\mathscr{V}^h \subset \mathscr{V}$. Fig. 4 illustrates the continuous nature of the approximation functions across interior boundaries for a four element patch of linear quadrilaterals.

We can now state the CG method as: Find $\phi^h \in \mathscr{V}^h$ such that

$$B(w^h, \phi^h) = L(w^h) \quad \forall w^h \in \mathscr{V}^h, \tag{26}$$

where $B(\cdot,\cdot)$ and $L(\cdot)$ are defined in (22) and (23), respectively, and where w^h is a weighting function and ϕ^h the finite element approximation to ϕ. The CG method possesses the best approximation property for certain problems [10,21,32], but is unstable for the advection–diffusion equation. In particular, spurious

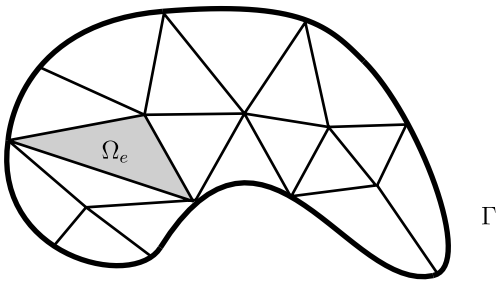

Fig. 3. Illustration of domain partition.

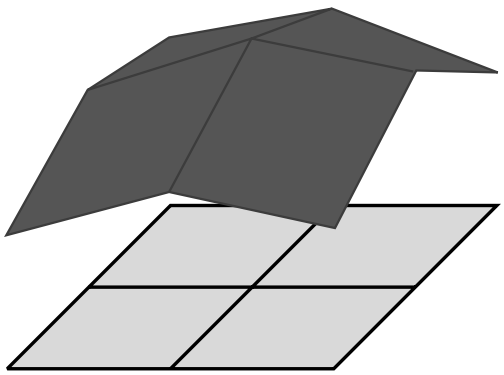

Fig. 4. Illustration of approximation functions for CG method on a four element patch of linear quadrilaterals.

oscillations arise in the solution for coarse discretizations and advection–dominated flows, and the classical CG method is unable to adequately approximate the solution in those cases.

2.3. Stabilization

The technique of stabilization entails the addition of weighted residuals to the weak form of the equation and appropriately selecting a stabilization parameter to be introduced in the formulation. We first consider two classical stabilization techniques for the advection–diffusion equation, namely SUPG and GLS, and then examine a method by Nitsche [53] for the diffusion equation with stabilization on the exterior boundary.

Brooks and Hughes introduced SUPG for the advection–diffusion equations (15)–(17) in 1982 [70]. SUPG for advection–diffusion with homogeneous Dirichlet boundary conditions on $\Gamma_g \equiv \Gamma$ can be written as: Find $\phi^h \in \mathscr{V}^h$ such that

$$B_{\mathrm{SUPG}}(w^h, \phi^h) = L_{\mathrm{SUPG}}(w^h) \quad \forall w^h \in \mathscr{V}^h, \tag{27}$$

where

$$B_{\mathrm{SUPG}}(w^h, \phi^h) = B(w^h, \phi^h) + (\tau \mathscr{L}_{\mathrm{a}} w^h, \mathscr{L}_{\mathrm{ad}} \phi^h)_{\tilde{\Omega}}, \tag{28}$$

$$L_{\mathrm{SUPG}}(w^h) = L(w^h) + (\tau \mathscr{L}_{\mathrm{a}} w^h, f)_{\tilde{\Omega}}. \tag{29}$$

The approximation space $\mathscr{V}^h$ for SUPG is the same as for the CG method, see (25). In (28) and (29), also $B(\cdot,\cdot)$ and $L(\cdot)$ are the same as in the CG method, see (22) and (23). A residual of the advection–diffusion equation has been added to the weak form on element interiors, which are defined as

$$\tilde{\Omega} = \bigcup_{e=1}^{N_{\mathrm{el}}} \Omega_e \tag{30}$$

and are illustrated in Fig. 5. For the L^2-inner product on element interiors, we have adopted the notation

$$(a,b)_{\tilde{\Omega}} = \sum_{e=1}^{N_{\mathrm{el}}} (a,b)_{\Omega_e} \tag{31}$$

for suitably defined a, b. The stabilization parameter τ introduced in (28) and (29) was originally defined as

$$\tau|_{\Omega_e} = \frac{h_e}{2|\boldsymbol{u}|}\tilde{\xi}, \tag{32}$$

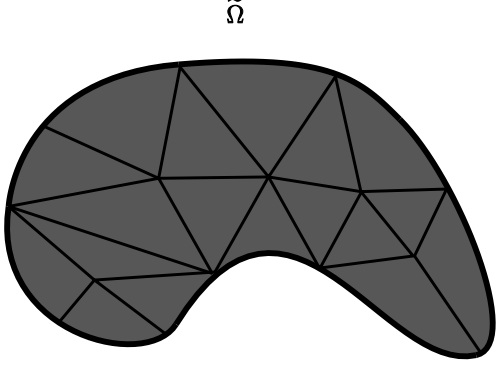

Fig. 5. Definition of element interiors, $\tilde{\Omega}$.

where

$$\tilde{\xi} = \coth Pe - \frac{1}{Pe}, \tag{33}$$

and

$$Pe = \frac{|\boldsymbol{u}|h_e}{2|\boldsymbol{A}|} \tag{34}$$

denotes the Péclet number for appropriately defined vector and matrix norms [81]. Alternative definitions for the stabilization parameter have been suggested by Franca et al. [82].

SUPG has subsequently been generalized to GLS by Hughes et al. [71]. GLS for the same model problem can be stated as: Find $\phi^h \in \mathscr{V}^h$ such that

$$B_{\mathrm{GLS}}(w^h, \phi^h) = L_{\mathrm{GLS}}(w^h) \quad \forall w^h \in \mathscr{V}^h, \tag{35}$$

where

$$B_{\mathrm{GLS}}(w^h, \phi^h) = B(w^h, \phi^h) + (\tau \mathscr{L}_{\mathrm{ad}} w^h, \mathscr{L}_{\mathrm{ad}} \phi^h)_{\tilde{\Omega}}, \tag{36}$$

$$L_{\mathrm{GLS}}(w^h) = L(w^h) + (\tau \mathscr{L}_{\mathrm{ad}} w^h, f)_{\tilde{\Omega}}. \tag{37}$$

Note that the only difference between GLS and SUPG is that in GLS, the advection–diffusion operator is applied to the weighting function in (36) and (37) rather than the advection operator as in SUPG, see (28) and (29). This generalization provides advantages in certain situations.

The stabilization techniques considered so far added weighted residual terms to the weak form of the advection–diffusion equation on element interiors. Let us now consider stabilization on the exterior boundary. Nitsche [53] added dimensionally consistent terms to the weak form of the diffusion equation for weakly enforcing the g-boundary condition on Γ_g. For the diffusion problem (8)–(10), the method reads: Find $\phi^h \in \mathscr{V}^h$ such that

$$B_N(w^h, \phi^h) = L_N(w^h) \quad \forall w^h \in \mathscr{V}^h, \tag{38}$$

where

$$B_N(w^h, \phi^h) = (\nabla w^h, \boldsymbol{\sigma}^{\mathrm{d}}(\phi^h)) - (w^h, \sigma_n^{\mathrm{d}}(\phi^h))_{\Gamma_g} - (\sigma_n^{\mathrm{d}}(w^h), \phi^h)_{\Gamma_g} + (\tau w^h, \phi^h)_{\Gamma_g}, \tag{39}$$

$$L_N(w^h) = (w^h, f) + (w^h, h)_{\Gamma_h} - (\sigma_n^{\mathrm{d}}(w^h), g)_{\Gamma_g} + (\tau w^h, g)_{\Gamma_g}. \tag{40}$$

The approximation space for this method is defined as

$$\mathscr{V}^h = \{v^h \in H^1(\Omega) |\ v^h|_{\Omega_e} \in P_k(\Omega_e)\ \forall \Omega_e \in \mathscr{P}(\Omega)\}.$$

Note that the first two terms on the right-hand side of (39) and the second term on the right-hand side of (40) arise from integration by parts (see, e.g., [10,83]), whereas the last two terms on the second line of each equation were added to weakly enforce the g-boundary condition on Γ_g. For the stabilization term τ, dimensional analysis indicates that it is of the form

$$\tau|_{\Omega_e} = \mathscr{O}(|\boldsymbol{A}|/h_e). \tag{41}$$

The weak enforcement of the boundary condition in (38) has been interpreted here as a GLS- type stabilization technique on the exterior boundary. In the next section, we will generalize this idea to the weak enforcement of continuity conditions on interior boundaries.

3. Stabilized discontinuous Galerkin methods

The combination of the DG approach with stabilization leads to optimally convergent schemes for a variety of problems. Only recently have research efforts started to examine and analyze DG methods for general differential equations beyond first order, and the application area has been so far mostly confined to problems of fluid mechanics. Investigating stabilized DG methods in the context of fluid mechanics will allow us to identify advantages and disadvantages of the resulting methods and will offer guidance on how to combine finite element techniques to develop numerical schemes for fourth-order elliptic problems which are consistent, stable, convergent and computationally efficient.

In this section, we first want to introduce DG methods in the context of fluid mechanics for the advection, diffusion and advection–diffusion problem, which will serve as a basis for their stabilized versions. Next, we discuss the adaptation of stabilization to the discontinuous case. In particular, rather than adding stabilization terms on element interiors only, we add terms on interior boundaries which weakly enforce continuity requirements for the diffusion and advection–diffusion model problems. This approach leads to optimal convergence in all three problem cases, which is proven analytically. Finally, we consider the efficiency of stabilized DG methods. We will see that the resulting methods lead to an increased number of unknowns, which will serve as motivation to look beyond stabilization and DG methods to create a numerical scheme which is computationally more attractive.

3.1. Discontinuous Galerkin methods

DG methods allow the approximation functions in the finite element space to be discontinuous between adjacent elements. This is in contrast to CG methods, for which continuity between neighboring elements is assumed. Consider again the partition (24) of the domain into finite elements. Let us define

$$\mathscr{V}^h = \{v^h \in L^2(\Omega) |\ v^h|_{\Omega_e} \in P_k(\Omega_e)\ \forall \Omega_e \in \mathscr{P}(\Omega)\} \tag{42}$$

as the finite-dimensional space for our discontinuous approximations. Fig. 6 illustrates the discontinuous nature of the approximation functions across interior boundaries for a four element patch of linear quadrilaterals. We can now introduce a DG formulation for each of the three model problems from Section 2.1.

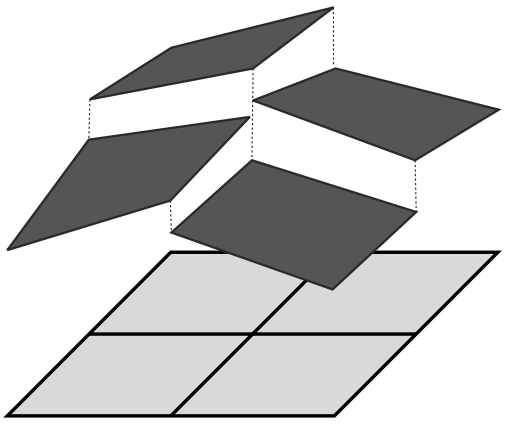

Fig. 6. Illustration of approximation functions for DG method on a four element patch of linear quadrilaterals.

3.1.1. Advection

The DG method was originally developed for the advection problem [38]. Consider the following DG formulation for (1) and (2): Find $\phi^h \in \mathscr{V}^h$ such that

$$B_{\mathrm{a}}(w^h, \phi^h) = L_{\mathrm{a}}(w^h) \quad \forall w^h \in \mathscr{V}^h, \tag{43}$$

where

$$B_{\mathrm{a}}(w^h, \phi^h) = (\nabla w^h, \boldsymbol{\sigma}^{\mathrm{a}}(\phi^h))_{\tilde{\Omega}} - ([\![w^h]\!], \sigma_n^{\mathrm{a}}(\phi^{h-}))_{\tilde{\Gamma}} - (w^{h-}, \sigma_n^{\mathrm{a}}(\phi^{h-}))_{\Gamma^+}, \tag{44}$$

$$L_{\mathrm{a}}(w^h) = (w^h, f)_{\tilde{\Omega}} + (w^{h+}, \sigma_n^{\mathrm{a}}(g))_{\Gamma^-} \tag{45}$$

and where the union of interior boundaries can be expressed as the intersection of the boundaries $\partial\Omega_e$ of individual elements Ω_e by

$$\tilde{\Gamma} = \bigcup_{\substack{r,s=1 \\ s>r}}^{N_{\mathrm{el}}} (\partial\Omega_r \cap \partial\Omega_s), \tag{46}$$

see Fig. 7. Alternatively, one can write the interior boundaries as

$$\tilde{\Gamma} = \bigcup_{i=1}^{N_{\mathrm{i}}} \Gamma_i, \tag{47}$$

where N_{i} is the number of interior boundaries Γ_i. Analogous to (31), we define the L^2-inner product on interior boundaries as

$$(a, b)_{\tilde{\Gamma}} = \sum_{i=1}^{N_{\mathrm{i}}} (a, b)_{\Gamma_i}. \tag{48}$$

In (44) we have adopted the notation

$$[\![a]\!] = a^+ - a^- \tag{49}$$

for the jump operator on interior boundary $\Gamma_i = \partial\Omega_r \cap \partial\Omega_s \subseteq \tilde{\Gamma}$, where

$$a^{\pm}|_{\Gamma_i} = \lim_{\varepsilon \to 0} a(\boldsymbol{x} \pm \varepsilon \boldsymbol{u}) \tag{50}$$

is the value of a on either side of interior boundary Γ_i. The normal fluxes appearing in the formulation are computed on the exterior boundaries with respect to the outward unit normal vector on Γ^+ and Γ^-. On interior boundaries, any of the two opposite normals could be chosen for the normal flux, and (44) reflects the sign convention $\boldsymbol{u} \cdot \boldsymbol{n} < 0$ we have employed here for the unit normal vector $\boldsymbol{n}$. For an analysis of the DG method for the advection equation, see Lesaint and Raviart [39,40], Johnson et al. [41] and Johnson and Pitkäranta [42].

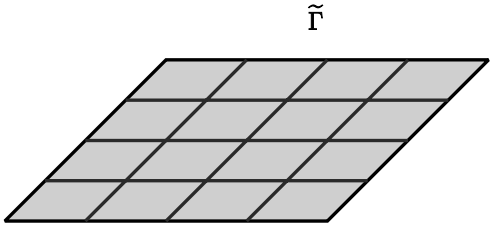

Fig. 7. Definition of interior boundaries, $\tilde{\Gamma}$.

3.1.2. Diffusion

The utility of DG methods for elliptic problems was strongly influenced and enhanced by the work of Baumann [61]. Let us present here a generalization of his method. For any $\alpha \in \mathbb{R}$, consider the following DG formulation for (8)–(10): Find $\phi^h \in \mathscr{V}^h$ such that

$$B_{\mathrm{d}}(w^h, \phi^h) = L_{\mathrm{d}}(w^h) \quad \forall w^h \in \mathscr{V}^h, \tag{51}$$

where

$$\begin{aligned} B_{\mathrm{d}}(w^h, \phi^h) = {} & (\nabla w^h, \boldsymbol{\sigma}^{\mathrm{d}}(\phi^h))_{\tilde{\Omega}} - (\llbracket w^h \rrbracket, \langle \sigma_n^{\mathrm{d}}(\phi^h) \rangle)_{\tilde{\Gamma}} + \alpha(\langle \sigma_n^{\mathrm{d}}(w^h) \rangle, \llbracket \phi^h \rrbracket)_{\tilde{\Gamma}} \\ & - (w^h, \sigma_n^{\mathrm{d}}(\phi^h))_{\Gamma_g} + \alpha(\sigma_n^{\mathrm{d}}(w^h), \phi^h)_{\Gamma_g} \end{aligned} \tag{52}$$

and

$$L_{\mathrm{d}}(w^h) = (w^h, f)_{\tilde{\Omega}} + (w^h, h)_{\Gamma_h} + \alpha(\sigma_n^{\mathrm{d}}(w^h), g)_{\Gamma_g}. \tag{53}$$

In this case, the jump operator (49) on $\Gamma_i \subseteq \tilde{\Gamma}$ is computed using

$$a^{\pm}|_{\Gamma_i} = \lim_{\varepsilon \to 0} a(\boldsymbol{x} \mp \varepsilon \boldsymbol{n}), \tag{54}$$

where $\boldsymbol{n} \perp \Gamma_i$ is any of the two unit normals to Γ_i. Note that we have introduced in (52) the notation

$$\langle a \rangle = \tfrac{1}{2}(a^+ + a^-) \tag{55}$$

for the average operator.

In this family of discontinuous formulations for the diffusion problem (8)–(10), $\alpha \in \mathbb{R}$ is a parameter differentiating the various methods. In particular, for $\alpha = -1$, (51) yields the symmetric method of Delves and Hall [60]. Choosing $\alpha = 1$ we obtain the method of Baumann [61], in which the interface terms constitute a skew-symmetric operator.

3.1.3. Advection–diffusion

A DG method for this model problem can be expressed as a combination of the two previous methods for advection and diffusion. For any $\alpha \in \mathbb{R}$, we consider the following family of DG formulations for (15)–(17): Find $\phi^h \in \mathscr{V}^h$ such that

$$B_{\mathrm{ad}}(w^h, \phi^h) = L_{\mathrm{ad}}(w^h) \quad \forall w^h \in \mathscr{V}^h, \tag{56}$$

where

$$B_{\mathrm{ad}}(w^h, \phi^h) = B_{\mathrm{a}}(w^h, \phi^h) + B_{\mathrm{d}}(w^h, \phi^h), \tag{57}$$

$$L_{\mathrm{ad}}(w^h) = (w^h, f)_{\tilde{\Omega}} + (w^{h+}, \sigma_n^{\mathrm{a}}(g))_{\Gamma^-} + (w^h, h)_{\Gamma_h} + \alpha(\sigma_n^{\mathrm{d}}(w^h), g)_{\Gamma_g}, \tag{58}$$

and $B_{\mathrm{a}}(\cdot,\cdot)$ and $B_{\mathrm{d}}(\cdot,\cdot)$ are the bilinear forms defined previously in (44) and (52), respectively.

Eq. (56) represents a family of DG formulations for the advection–diffusion problem, where $\alpha \in \mathbb{R}$ is the parameter differentiating the various methods for the treatment of the diffusion term, and the normal fluxes appearing in the formulation are computed with the same convention adopted for the advection case in Section 3.1.1, i.e., on $\tilde{\Gamma}$, the unit normal vector $\boldsymbol{n}$ employed is the one for which $\boldsymbol{u} \cdot \boldsymbol{n} < 0$.

3.2. Stabilization

The DG methods presented in the previous section are widely used in practice. For certain problems, however, they can exhibit instabilities, and the numerical results fail to approximate the exact solution. For

practitioners, it is important to have methods available which yield reliable results for a wide variety of problems. By using stabilization techniques, many of the shortcomings of non-stabilized DG methods can be overcome, and the resulting methods are attractive tools in common situations such as advection–dominated flows, where non-stabilized methods fail. We limit our discussion in this section to analytical considerations and refer to published work [84] for numerical verification.

3.2.1. Advection

We consider the following stabilized version of method (43) for the advection problem (1) and (2): Find $\phi^h \in \mathscr{V}^h$ such that

$$B_{\mathrm{a}}^{(s)}(w^h, \phi^h) = L_{\mathrm{a}}^{(s)}(w^h) \quad \forall w^h \in \mathscr{V}^h, \tag{59}$$

where

$$B_{\mathrm{a}}^{(s)}(w^h, \phi^h) = B_{\mathrm{a}}(w^h, \phi^h) + (\tau_{\mathrm{a}} \mathscr{L}_{\mathrm{a}} w^h, \mathscr{L}_{\mathrm{a}} \phi^h)_{\tilde{\Omega}} \tag{60}$$

and

$$L_{\mathrm{a}}^{(s)}(w^h) = L_{\mathrm{a}}(w^h) + (\tau_{\mathrm{a}} \mathscr{L}_{\mathrm{a}} w^h, f)_{\tilde{\Omega}}. \tag{61}$$

In (60) and (61) we have introduced the stabilization parameter τ_{a}, for which we have, using the natural length and velocity scales on each element,

$$\tau_{\mathrm{a}}|_{\Omega_e} = \mathscr{O}(h_e / u_e^{\mathrm{M}}) > 0, \tag{62}$$

where u_e^{M} denotes the maximum magnitude of the velocity field of element Ω_e. The presence of the stabilization terms will result in optimal rates of convergence.

3.2.2. Diffusion

For any $\alpha \in \mathbb{R}$ we examine the following stabilized DG formulation for (8)–(10): Find $\phi^h \in \mathscr{V}^h$ such that

$$B_{\mathrm{d}}^{(s)}(w^h, \phi^h) = L_{\mathrm{d}}^{(s)}(w^h) \quad \forall w^h \in \mathscr{V}^h, \tag{63}$$

where

$$B_{\mathrm{d}}^{(s)}(w^h, \phi^h) = B_{\mathrm{d}}(w^h, \phi^h) + (\tau_{\mathrm{d}} [\![w^h]\!], [\![\phi^h]\!])_{\tilde{\Gamma}} + (\tau_{\mathrm{d}} w^h, \phi^h)_{\Gamma_g} \tag{64}$$

and

$$L_{\mathrm{d}}^{(s)}(w^h) = L_{\mathrm{d}}(w^h) + (\tau_{\mathrm{d}} w^h, g)_{\Gamma_g}. \tag{65}$$

In this family of stabilized DG formulations for the diffusion problem (8)–(10), $\alpha \in \mathbb{R}$ is the parameter differentiating the various methods and τ_{d} the stabilization parameter. For this case

$$\tau_{\mathrm{d}}|_{\Omega_e} = \mathscr{O}(A_e^{\mathrm{M}} / h_e), \tag{66}$$

where $A_e^{\mathrm{M}} = |\boldsymbol{A}|$ is the maximum diffusivity on element Ω_e and the matrix norm is defined as

$$|\boldsymbol{A}| = \sup_{\substack{v \in \mathbb{R}^d \\ v \neq 0}} \frac{|\boldsymbol{A}\boldsymbol{v}|}{|\boldsymbol{v}|}. \tag{67}$$

If we choose $\alpha = -1$ in (63), we obtain Nitsche's method [53,85,86] generalized to the discontinuous case, see Section 2.3. The stabilization terms, similar to the term introduced by Nitsche in his CG method, can be interpreted as the weak enforcement of continuity across interior boundaries and on the exterior boundary.

This weak enforcement of continuity is illustrated in Fig. 8 and contrasted with C^0-continuity in the CG method for the one-dimensional case. On the left, continuity on the interior boundary between the two

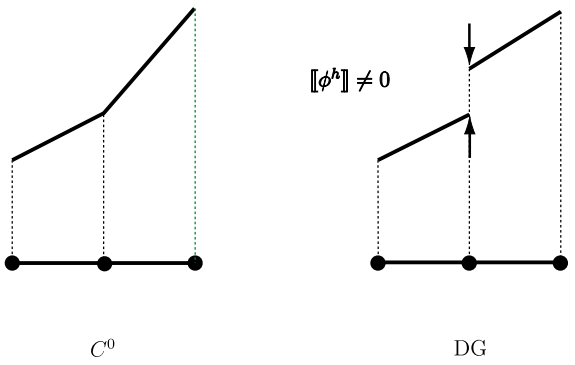

Fig. 8. Illustration of C^0-continuity and weak enforcement of continuity in the DG method across interior boundaries.

adjacent linear elements is achieved in the CG method via the definition of the approximation functions. On the right, the discontinuous nature of the approximation spaces in the DG method is displayed, and the action of the weak enforcement term is illustrated by the two arrows, resulting in a reduction of the discontinuity.

3.2.3. Advection–diffusion

For any $\alpha \in \mathbb{R}$ we introduce the following stabilized version of (56) for the advection–diffusion problem (15)–(17): Find $\phi^h \in \mathscr{V}^h$ such that

$$B_{\mathrm{ad}}^{(s)}(w^h, \phi^h) = L_{\mathrm{ad}}^{(s)}(w^h) \quad \forall w^h \in \mathscr{V}^h, \tag{68}$$

where

$$B_{\mathrm{ad}}^{(s)}(w^h, \phi^h) = B_{\mathrm{ad}}(w^h, \phi^h) + (\tau_{\mathrm{ad}} \mathscr{L}_{\mathrm{a}} w^h, \mathscr{L}_{\mathrm{ad}} \phi^h)_{\tilde{\Omega}} + (\tau_{\mathrm{d}} [\![w^h]\!], [\![\phi^h]\!])_{\tilde{\Gamma}} + (\tau_{\mathrm{d}} w^h, \phi^h)_{\Gamma_g} \tag{69}$$

and

$$L_{\mathrm{ad}}^{(s)}(w^h) = L_{\mathrm{ad}}(w^h) + (\tau_{\mathrm{ad}} \mathscr{L}_{\mathrm{a}} w^h, f)_{\tilde{\Omega}} + (\tau_{\mathrm{d}} w^h, g)_{\Gamma_g}. \tag{70}$$

Eq. (68) represents a family of stabilized discontinuous formulations for the advection–diffusion problem, where $\alpha \in \mathbb{R}$ is the parameter differentiating the various methods for the treatment of the diffusion term, τ_{d} is the stabilization parameter on interior and exterior boundaries with dimension (66), τ_{ad} is the stabilization parameter on element interiors defined in (32) with $|\boldsymbol{u}| = u_e^{\mathrm{M}}$ and $|\boldsymbol{A}| = A_e^{\mathrm{M}}$, and the normal fluxes on interior boundaries appearing in the formulation are computed with the same convention adopted for the advection case in Section 3.1.1, i.e., we have $\boldsymbol{u} \cdot \boldsymbol{n} < 0$ for $\boldsymbol{n}$ on $\tilde{\Gamma}$.

3.3. Error analysis

The stabilized DG methods from Section 3.2 exhibit optimal convergence rate behavior for all three model problems, which we show analytically in this section. By optimal convergence rate we mean that no function in the finite element space converges at a faster rate than the approximate DG solution. For this purpose, we first prove the consistency of the methods. Consistency requires that the exact solution of the boundary value problem needs to satisfy the C/DG formulation. Next, we show stability. In particular, a method is stable when its bilinear form induces a norm which can be bounded from below. With the results from consistency and stability we can prove convergence of the methods. Freund [69] presented an error

analysis for the advection–diffusion model problem in which the approximation functions are allowed to be discontinuous on parts of the domain. His analysis is based on earlier developments by Stenberg [86].

3.3.1. Advection

Consistency. Let us begin by verifying that (59) is consistent in the usual weighted residual sense. Integration by parts of (59) yields $\forall w^h \in \mathscr{V}^h$

$$\begin{aligned} 0 &= B_{\mathrm{a}}^{(s)}(w^h, \phi^h) - L_{\mathrm{a}}^{(s)}(w^h), \\ &= (w^h, \mathscr{L}_{\mathrm{a}}\phi^h - f)_{\tilde{\Omega}} + (\sigma_n^{\mathrm{a}}(w^{h+}), \phi^{h+} - g)_{\Gamma^-} + (\sigma_n^{\mathrm{a}}(w^{h^+}), [\![\phi^h]\!])_{\tilde{\Gamma}} + (\tau_{\mathrm{a}}\mathscr{L}_{\mathrm{a}}w^h, \mathscr{L}_{\mathrm{a}}\phi^h - f)_{\tilde{\Omega}}. \end{aligned} \tag{71}$$

Therefore, for ϕ sufficiently smooth, and using the fact that $\phi^+ = \phi^- = g$ on Γ^-, we have

$$0 = B_{\mathrm{a}}^{(s)}(w^h, \phi) - L_{\mathrm{a}}^{(s)}(w^h) \quad \forall w^h \in \mathscr{V}^h, \tag{72}$$

i.e., the exact solution ϕ satisfies (59). Hence, subtracting (59) from (72) and defining the error of the finite element solution as

$$e = \phi - \phi^h, \tag{73}$$

we obtain

$$B_{\mathrm{a}}^{(s)}(w^h, e) = 0 \quad \forall w^h \in \mathscr{V}^h, \tag{74}$$

i.e., the "Galerkin orthogonality" of the error to the finite element space.

Stability. The relevant norm for $\mathscr{V}^h$ corresponding to (59) is

$$|||w^h|||_{\mathrm{a}}^2 = \|\tau_{\mathrm{a}}^{1/2}\boldsymbol{u}\cdot\nabla w^h\|_{\tilde{\Omega}}^2 + \tfrac{1}{2}\||u_n|^{1/2}[\![w^h]\!]\|_{\tilde{\Gamma}}^2 + \tfrac{1}{2}\||u_n|^{1/2}w^{h-}\|_{\Gamma^+}^2 + \tfrac{1}{2}\||u_n|^{1/2}w^{h+}\|_{\Gamma^-}^2, \tag{75}$$

where $\|\cdot\|_{\Psi}$ denotes the L^2-norm on Ψ, and we define the norms on element interiors and interior boundaries as

$$\|\cdot\|_{\tilde{\Omega}}^2 = \sum_{e=1}^{N_{\mathrm{el}}} \|\cdot\|_{\Omega_e}^2, \tag{76}$$

$$\|\cdot\|_{\tilde{\Gamma}}^2 = \sum_{i=1}^{N_{\mathrm{i}}} \|\cdot\|_{\Gamma_i}^2. \tag{77}$$

A norm which can be derived from the bilinear form of a method, such as (75), is also referred to as the energy norm of the method. Note that above norm is mesh-dependent.

Lemma 3.1. *Assume that u vanishes at most at isolated points. Then* $|||\cdot|||_{\mathrm{a}}^2$ *is a norm on* $\mathscr{V}^h$.

Proof. The only non-trivial functions in $\mathscr{V}^h$ for which $|||w^h|||_{\mathrm{a}}^2$ could vanish are the piecewise constants $w^h(x) = \sum_{e=1}^{N_{\mathrm{el}}} c_e\chi_e(x)$, where χ_e is the characteristic function of element e and c_e a constant. The two possibilities, therefore, are that either w^h is a non-zero constant or at least two of the c_e's are distinct. In the former case, $w^h \neq 0$ and so $\||u_n|^{1/2}w^{h-}\|_{\Gamma^+}^2 > 0$ and $\||u_n|^{1/2}w^{h+}\|_{\Gamma^-}^2 > 0$; in the latter case, $[\![w^h]\!] \neq 0$ on one or more interior boundaries, so that $\||u_n|^{1/2}[\![w^h]\!]\|_{\tilde{\Gamma}}^2 > 0$. Consequently, $|||w^h|||_{\mathrm{a}}^2 > 0\ \forall w^h \in \mathscr{V}^h$. □

Lemma 3.2. *The bilinear form* (60) *in* (59) *is coercive and we have*

$$B_{\mathrm{a}}^{(s)}(w^h, w^h) = |||w^h|||_{\mathrm{a}}^2 \quad \forall w^h \in \mathscr{V}^h. \tag{78}$$

Proof. The result follows directly from (60) using the relationship

$$(\nabla w^h, \boldsymbol{\sigma}^{\mathrm{a}}(w^h))_{\Omega_e} = -\tfrac{1}{2}(w^h, u_n w^h)_{\partial\Omega_e}, \tag{79}$$

which can be obtained from integration by parts and invoking the incompressibility condition (4). □

Convergence. Let $\tilde{\phi}^h$ denote any interpolant of ϕ in the finite-dimensional space $\mathscr{V}^h$. Let us specify the interpolation error by $\eta = \phi - \tilde{\phi}^h$. Thus, we can decompose the error e as

$$e = \phi - \phi^h = (\phi - \tilde{\phi}^h) + (\tilde{\phi}^h - \phi^h) = \eta + e^h, \tag{80}$$

where $e^h = \tilde{\phi}^h - \phi^h$ is the part of the error in the finite element space, i.e., $e^h \in \mathscr{V}^h$.

Theorem 3.1. *Assume the consistency and stability conditions* (74) *and* (78), *respectively*, *hold. Given that conditions are satisfied for the interpolation estimates* (A.12), (A.13) *and the trace inequality* (A.18) *to hold*, *the error estimate for the stabilized DG method* (59) *can be written as*

$$|||e|||_{\mathrm{a}}^2 \leqslant C \sum_{e=1}^{N_{\mathrm{el}}} h_e^{2k+1} |\phi|^2_{H^{k+1}(\Omega_e)}, \tag{81}$$

where C is a constant [4], *and* $|\cdot|_{H^{k+1}(\Omega_e)}$ *denotes the* H^{k+1}*-seminorm on* Ω_e, *see* [32] *for a definition.*

Proof. First, we estimate e^h as

$$\begin{aligned} |||e^h|||_{\mathrm{a}}^2 &= B_{\mathrm{a}}^{(s)}(e^h, e^h), \\ &= B_{\mathrm{a}}^{(s)}(e^h, e - \eta), \\ &= -B_{\mathrm{a}}^{(s)}(e^h, \eta), \\ &\leqslant |B_{\mathrm{a}}^{(s)}(e^h, \eta)|, \\ &\leqslant |(\nabla e^h, \boldsymbol{\sigma}^{\mathrm{a}}(\eta))_{\tilde{\Omega}}| + |(\tau_{\mathrm{a}} \mathscr{L}_{\mathrm{a}} e^h, \mathscr{L}_{\mathrm{a}} \eta)_{\tilde{\Omega}}| + |(\llbracket e^h \rrbracket, \sigma_n^{\mathrm{a}}(\eta^-))_{\tilde{\Gamma}}| + |(e^{h-}, \sigma_n^{\mathrm{a}}(\eta^-))_{\Gamma^+}|. \end{aligned} \tag{82}$$

Applying the ε-inequality

$$|(a,b)|_{\Psi}| \leqslant \frac{\varepsilon}{2}\|a\|_{\Psi}^2 + \frac{1}{2\varepsilon}\|b\|_{\Psi}^2, \tag{83}$$

which holds for arbitrary $\varepsilon > 0$, on each term in (82), we obtain

$$|||e^h|||_{\mathrm{a}}^2 \leqslant 2(\|\tau_{\mathrm{a}}^{-1/2}\eta\|_{\tilde{\Omega}}^2 + \||u_n|^{1/2}\eta^-\|_{\Gamma^+}^2 + \||u_n|^{1/2}\eta^-\|_{\tilde{\Gamma}}^2 + \|\tau_{\mathrm{a}}^{1/2}\boldsymbol{u}\cdot\nabla\eta\|_{\tilde{\Omega}}^2). \tag{84}$$

Recognizing the local behavior (62) of τ_{a} and invoking the interpolation estimate (A.13) and trace inequality (A.18), we can estimate the terms appearing in (84) as

$$\|\tau_{\mathrm{a}}^{-1/2}\eta\|_{\tilde{\Omega}}^2 \leqslant C \sum_{e=1}^{N_{\mathrm{el}}} h_e^{2k+1} |\phi|^2_{H^{k+1}(\Omega_e)}, \tag{85}$$

$$\||u_n|^{1/2}\eta^-\|_{\Gamma^+}^2 + \||u_n|^{1/2}\eta^-\|_{\tilde{\Gamma}}^2 \leqslant C \sum_{e=1}^{N_{\mathrm{el}}} h_e^{2k+1} |\phi|^2_{H^{k+1}(\Omega_e)}, \tag{86}$$

[4] In the following, we will denote all constants by C, which, in general, will have different values in different situations. Whenever we want to refer to a specific constant, that constant will be distinguished by a subscript, e.g. C_{I} for the constant resulting from an inverse estimate.

$$\|\tau_{\mathrm{a}}^{1/2}\boldsymbol{u}\cdot\nabla\eta\|_{\tilde{\Omega}}^2 \leqslant C\sum_{e=1}^{N_{\mathrm{el}}} h_e^{2k+1}|\phi|_{H^{k+1}(\Omega_e)}^2. \tag{87}$$

Substituting (85)–(87) in (84) yields

$$|||e^h|||_{\mathrm{a}}^2 \leqslant C\sum_{e=1}^{N_{\mathrm{el}}} h_e^{2k+1}|\phi|_{H^{k+1}(\Omega_e)}^2, \tag{88}$$

where

$$C \propto \max_e u_e^{\mathrm{M}}. \tag{89}$$

With similar arguments it can be proven that we also have

$$|||\eta|||_{\mathrm{a}}^2 \leqslant C\sum_{e=1}^{N_{\mathrm{el}}} h_e^{2k+1}|\phi|_{H^{k+1}(\Omega_e)}^2, \tag{90}$$

and the result follows by the triangle inequality. □

3.3.2. Diffusion

Consistency. Consistency of (63) can be verified by integration by parts and is independent of the value of the parameter α. We obtain $\forall w^h \in \mathscr{V}^h$

$$\begin{aligned} 0 &= B_{\mathrm{d}}^{(s)}(w^h,\phi^h) - L_{\mathrm{d}}^{(s)}(w^h),\\ &= (w^h, \mathscr{L}_{\mathrm{d}}\phi^h - f)_{\tilde{\Omega}} + (w^h, \sigma_n^{\mathrm{d}}(\phi^h) - h)_{\Gamma_h} + \alpha(\sigma_n^{\mathrm{d}}(w^h), \phi^h - g)_{\Gamma_g}\\ &\quad + (\tau_{\mathrm{d}}w^h, \phi^h - g)_{\Gamma_g} + \alpha(\langle\sigma_n^{\mathrm{d}}(w^h)\rangle, [\![\phi^h]\!])_{\tilde{\Gamma}}\\ &\quad + (\langle w^h\rangle, [\![\sigma_n^{\mathrm{d}}(\phi^h)]\!])_{\tilde{\Gamma}} + (\tau_{\mathrm{d}}[\![w^h]\!], [\![\phi^h]\!])_{\tilde{\Gamma}}, \end{aligned} \tag{91}$$

where we have taken advantage of the equality

$$[\![ab]\!] = [\![a]\!]\langle b\rangle + \langle a\rangle[\![b]\!], \tag{92}$$

which holds for all a, b. Thus, for ϕ sufficiently smooth, we have that the exact solution of (8)–(10) satisfies (63), i.e.,

$$0 = B_{\mathrm{d}}^{(s)}(w^h,\phi) - L_{\mathrm{d}}^{(s)}(w^h) \quad \forall w^h \in \mathscr{V}^h, \tag{93}$$

and hence the Galerkin orthogonality of the error to the finite element space

$$B_{\mathrm{d}}^{(s)}(w^h, e) = 0 \quad \forall w^h \in \mathscr{V}^h \tag{94}$$

follows by the same argument used to obtain (74).

Stability. An appropriate generalization of the norms employed for some of the methods included in our parameterized family of formulations shows that a suitable norm for $\mathscr{V}^h$ corresponding to (63) is

$$|||w^h|||_{\mathrm{d}}^2 = \|\boldsymbol{A}^{1/2}\nabla w^h\|_{\tilde{\Omega}}^2 + \|\tau_{\mathrm{d}}^{1/2}[\![w^h]\!]\|_{\tilde{\Gamma}}^2 + \|\tau_{\mathrm{d}}^{1/2}w^h\|_{\Gamma_g}^2. \tag{95}$$

Note that this energy norm is independent of the particular method and does not depend on the parameter α.

Lemma 3.3. $|||\cdot|||_{\mathrm{d}}^2$ *is a norm on* $\mathscr{V}^h$.

Proof. The only non-trivial functions in $\mathscr{V}^h$ for which $|||w^h|||_{\mathrm{d}}^2$ could vanish are, as in Lemma 3.1, the piecewise constants $w^h(x) = \sum_{e=1}^{N_{\mathrm{el}}} c_e \chi_e(x)$. Hence, either w^h is a non-zero constant on the entire domain Ω, or at least two of the c_e's are distinct. In the former case, $w^h \neq 0$ and so $\|\tau_{\mathrm{d}}^{1/2} w^h\|_{\Gamma_g}^2 > 0$; in the latter case, $[\![w^h]\!] \neq 0$ on one or more element interfaces, so that $\|\tau_{\mathrm{d}}^{1/2}[\![w^h]\!]\|_{\tilde{\Gamma}}^2 > 0$. Consequently, $|||w^h|||_{\mathrm{d}}^2 > 0\ \forall w^h \in \mathscr{V}^h$. □

We then have the following

Lemma 3.4. *The bilinear form* (64) *is stable, that is, for any* $\alpha \in \mathbb{R}$ *there exists a positive constant m such that*

$$B_{\mathrm{d}}^{(s)}(w^h, w^h) \geqslant m|||w^h|||_{\mathrm{d}}^2 \quad \forall w^h \in \mathscr{V}^h. \tag{96}$$

Proof. Substituting w^h for ϕ^h in (64) we obtain the estimate

$$\begin{aligned} B_{\mathrm{d}}^{(s)}(w^h, w^h) \geqslant{}& \|\boldsymbol{A}^{1/2}\boldsymbol{\nabla} w^h\|_{\Omega}^2 - |(\alpha-1)|(w^h, \sigma_n^{\mathrm{d}}(w^h))_{\Gamma_g}| - |(\alpha-1)|([\![w^h]\!], \langle\sigma_n^{\mathrm{d}}(w^h)\rangle)_{\tilde{\Gamma}}| \\ &+ \|\tau_{\mathrm{d}}^{1/2}[\![w^h]\!]\|_{\tilde{\Gamma}}^2 + \|\tau_{\mathrm{d}}^{1/2} w^h\|_{\Gamma_g}^2. \end{aligned} \tag{97}$$

One can see from (97) that a positive inferior bound needs to be found for the two terms in inner product notation. Invoking (83) and the inequality

$$\|\langle a\rangle\|_{\Psi}^2 \leqslant \|a^+\|_{\Psi}^2 + \|a^-\|_{\Psi}^2, \tag{98}$$

we have

$$|(w^h, \sigma_n^{\mathrm{d}}(w^h))_{\Gamma_g}| + |([\![w^h]\!], \langle\sigma_n^{\mathrm{d}}(w^h)\rangle)_{\tilde{\Gamma}}| \leqslant \frac{\varepsilon}{2}\sum_{e=1}^{N_{\mathrm{el}}} \|\sigma_n^{\mathrm{d}}(w^h)\|_{\partial\Omega_e}^2 + \frac{1}{2\varepsilon}[\|w^h\|_{\Gamma_g}^2 + \|[\![w^h]\!]\|_{\tilde{\Gamma}}^2]. \tag{99}$$

We now can use trace inequality (A.18) and inverse estimate (A.17) to obtain

$$\sum_{e=1}^{N_{\mathrm{el}}} \|\sigma_n^{\mathrm{d}}(w^h)\|_{\partial\Omega_e}^2 \leqslant C\sum_{e=1}^{N_{\mathrm{el}}} h_e^{-1}\|\boldsymbol{A}^{1/2}\boldsymbol{\nabla} w^h\|_{\Omega_e}^2, \tag{100}$$

where the constant C increases with the order of interpolation k. Let us choose ε and τ_{d} within each element as

$$\tau_{\mathrm{d}}|_{\Omega_e} = \frac{A_e^{\mathrm{M}}}{h_e}(1 + C|\alpha-1|^2), \tag{101}$$

$$\varepsilon|_{\Omega_e} = \frac{h_e}{A_e^{\mathrm{M}}}\left(\frac{|\alpha-1|}{1+C|\alpha-1|^2}\right), \tag{102}$$

and we obtain

$$B_{\mathrm{d}}^{(s)}(w^h, w^h) \geqslant \sum_{e=1}^{N_{\mathrm{el}}} \frac{2 + C|\alpha-1|^2}{2 + 2C|\alpha-1|^2}\|\boldsymbol{A}^{1/2}\boldsymbol{\nabla} w^h\|_{\Omega_e}^2 + \tfrac{1}{2}[\|\tau_{\mathrm{d}}^{1/2} w^h\|_{\Gamma_g}^2 + \|\tau_{\mathrm{d}}^{1/2}[\![w^h]\!]\|_{\tilde{\Gamma}}^2], \tag{103}$$

i.e., (96) holds with $m = 1/2$ when $\alpha \neq 1$, since

$$\frac{1}{2} \leqslant \frac{2 + C|\alpha-1|^2}{2 + 2C|\alpha-1|^2} \leqslant 1,$$

and as an equality with $m = 1$ when $\alpha = 1$, as can be seen directly from (97). □

The presence of the stabilization term on interior boundaries allows convergence for a wide variety of methods. The parameter α permits, in addition, "tuning" of the different methods in order to obtain improved convergence properties.

Convergence. With the notation introduced in Section 3.3.1 and the results from the previous consistency and stability considerations, we can prove convergence for the family of methods (63) independent of the parameter α. We have the following.

Theorem 3.2. *Assume the consistency and stability conditions* (94) and (96), *respectively*, *hold. Given that conditions are satisfied for the interpolation estimates* (A.12), (A.13) *and the trace inequality* (A.18) *to hold*, *the error estimate for the stabilized DG method* (63) *can be written as*

$$|||e|||_{\mathrm{d}}^2 \leqslant C \sum_{e=1}^{N_{\mathrm{el}}} h_e^{2k} |\phi|_{H^{k+1}(\Omega_e)}^2, \tag{104}$$

where C is a constant.

Proof. We use the same approach as in the proof of Theorem 3.1 and estimate e^h as

$$\begin{aligned} m|||e^h|||_{\mathrm{d}}^2 &\leqslant B_{\mathrm{d}}^{(s)}(e^h, e^h), \\ &= B_{\mathrm{d}}^{(s)}(e^h, e - \eta), \\ &= -B_{\mathrm{d}}^{(s)}(e^h, \eta), \\ &\leqslant |B_{\mathrm{d}}^{(s)}(e^h, \eta)|, \\ &\leqslant |(\nabla e^h, \boldsymbol{\sigma}^{\mathrm{d}}(\eta))_{\tilde{\Omega}}| + |(\llbracket e^h \rrbracket, \langle \sigma_n^{\mathrm{d}}(\eta) \rangle)_{\tilde{\Gamma}}| + |\alpha(\langle \sigma_n^{\mathrm{d}}(e^h) \rangle, \llbracket \eta \rrbracket)_{\tilde{\Gamma}}| \\ &\quad + |(\tau_{\mathrm{d}} \llbracket e^h \rrbracket, \llbracket \eta \rrbracket)_{\tilde{\Gamma}}| + |(e^h, \sigma_n^{\mathrm{d}}(\eta))_{\Gamma_g}| + |\alpha(\sigma_n^{\mathrm{d}}(e^h), \eta)_{\Gamma_g}| + |(\tau_{\mathrm{d}} e^h, \eta)_{\Gamma_g}|. \end{aligned} \tag{105}$$

As before, we apply the ε-inequality (83) on each term. Invoking (98), trace inequality (A.18) and inverse estimate (A.17), we can rewrite

$$\|\sigma_n^{\mathrm{d}}(e^h)\|_{\Gamma_g}^2 + \|\langle \sigma_n^{\mathrm{d}}(e^h) \rangle\|_{\tilde{\Gamma}}^2 \leqslant C \sum_{e=1}^{N_{\mathrm{el}}} h_e^{-1} \|\boldsymbol{A}^{1/2} \nabla e^h\|_{\Omega_e}^2. \tag{106}$$

By similar arguments, but noting that inverse inequality (A.17) does not hold for the interpolation error since $\eta \notin \mathscr{V}^h$, we also have

$$\|\sigma_n^{\mathrm{d}}(\eta)\|_{\Gamma_g}^2 + \|\langle \sigma_n^{\mathrm{d}}(\eta) \rangle\|_{\tilde{\Gamma}}^2 \leqslant C \sum_{e=1}^{N_{\mathrm{el}}} \|\boldsymbol{A}^{1/2} \nabla \eta\| \Omega_e \|\boldsymbol{A}^{1/2} \nabla \eta\|_{H^1(\Omega_e)}, \tag{107}$$

where $\|\cdot\|_{H^1(\Omega_e)}$ is the H^1-norm on Ω_e, see [32]. Using

$$\|\llbracket a \rrbracket\|_{\Psi}^2 \leqslant 2(\|a^+\|_{\Psi}^2 + \|a^-\|_{\Psi}^2) \tag{108}$$

and trace inequality (A.18), we can write

$$\|\eta\|_{\Gamma_g}^2 + \|\llbracket \eta \rrbracket\|_{\tilde{\Gamma}}^2 \leqslant C \sum_{e=1}^{N_{\mathrm{el}}} (h_e^{-1} \|\eta\|_{\Omega_e}^2 + h_e \|\nabla \eta\|_{\Omega_e}^2). \tag{109}$$

Dividing (105) by m and recalling the local behavior (101) of τ_{d}, we obtain with (106)–(109)

$$|||e^h|||_{\mathrm{d}}^2 \leqslant C \sum_{e=1}^{N_{\mathrm{el}}} \{\|\boldsymbol{A}^{1/2} \nabla \eta\|_{\Omega_e}^2 + h_e \|\boldsymbol{A}^{1/2} \nabla \eta\|_{\Omega_e} \|\boldsymbol{A}^{1/2} \nabla \eta\|_{H^1(\Omega_e)} + A_e^{\mathrm{M}} h_e^{-1} (h_e^{-1} \|\eta\|_{\Omega_e}^2 + h_e \|\nabla \eta\|_{\Omega_e}^2)\}. \tag{110}$$

Application of interpolation estimates (A.12) and (A.13) yields for the terms in (110)

$$\|\boldsymbol{A}^{1/2}\nabla\eta\|^2_{\Omega_e} \leqslant Ch_e^{2k}|\phi|^2_{H^{k+1}(\Omega_e)}, \tag{111}$$

$$h_e\|\boldsymbol{A}^{1/2}\nabla\eta\|_{\Omega_e}\|\boldsymbol{A}^{1/2}\nabla\eta\|_{H^1(\Omega_e)} \leqslant Ch_e^{2k}|\phi|^2_{H^{k+1}(\Omega_e)}, \tag{112}$$

$$A_e^{\mathrm{M}}h_e^{-1}(h_e^{-1}\|\eta\|^2_{\Omega_e} + h_e\|\nabla\eta\|^2_{\Omega_e}) \leqslant Ch_e^{2k}|\phi|^2_{H^{k+1}(\Omega_e)}. \tag{113}$$

Substitution of (111)–(113) in (110) leads to

$$|||e^h|||^2_{\mathrm{d}} \leqslant C\sum_{e=1}^{N_{\mathrm{el}}} h_e^{2k}|\phi|^2_{H^{k+1}(\Omega_e)}, \tag{114}$$

where

$$C \propto \max_e A_e^{\mathrm{M}}. \tag{115}$$

By similar arguments we can bound $|||\eta|||^2_{\mathrm{d}}$, and the triangle inequality yields the conclusion

$$|||e|||^2_{\mathrm{d}} \leqslant C\sum_{e=1}^{N_{\mathrm{el}}} h_e^{2k}|\phi|^2_{H^{k+1}(\Omega_e)}, \tag{116}$$

which proves the theorem. □

3.3.3. Advection–diffusion

Consistency. Consistency of (68) follows from integration by parts. We have $\forall w^h \in \mathscr{V}^h$

$$\begin{aligned} 0 &= B^{(s)}_{\mathrm{ad}}(w^h,\phi^h) - L^{(s)}_{\mathrm{ad}}(w^h),\\ &= (w^h, \mathscr{L}_{\mathrm{ad}}\phi^h - f)_{\tilde{\Omega}} + (w^h, \sigma_n^{\mathrm{d}}(\phi^h) - h)_{\Gamma_h}\\ &\quad + \alpha(\sigma_n^{\mathrm{d}}(w^h), \phi^h - g)_{\Gamma_g} + \alpha(\langle\sigma_n^{\mathrm{d}}(w^h)\rangle, [\![\phi^h]\!])_{\tilde{\Gamma}}\\ &\quad + (\langle w^h\rangle, [\![\sigma_n^{\mathrm{d}}(\phi^h)]\!])_{\tilde{\Gamma}} + (\sigma_n^{\mathrm{a}}(w^{h+}), \phi^h - g)_{\Gamma^-} + (\sigma_n^{\mathrm{a}}(w^{h+}), [\![\phi^h]\!])_{\tilde{\Gamma}}\\ &\quad + (\tau_{\mathrm{d}}w^h, \phi^h - g)_{\Gamma_g} + (\tau_{\mathrm{d}}[\![w^h]\!], [\![\phi^h]\!])_{\tilde{\Gamma}} + (\tau_{\mathrm{ad}}\mathscr{L}_{\mathrm{a}}w^h, \mathscr{L}_{\mathrm{ad}}\phi^h - f)_{\tilde{\Omega}}. \end{aligned} \tag{117}$$

Therefore, for ϕ sufficiently smooth, and using the fact that $\phi^+ = \phi^- = g$ on Γ_g, on we conclude that the exact solution of (15)–(17) satisfies (68), i.e.,

$$0 = B^{(s)}_{\mathrm{ad}}(w^h,\phi) - L^{(s)}_{\mathrm{ad}}(w^h) \quad \forall w^h \in \mathscr{V}^h, \tag{118}$$

and we obtain the usual Galerkin orthogonality property

$$B^{(s)}_{\mathrm{ad}}(w^h, e) = 0 \quad \forall w^h \in \mathscr{V}^h. \tag{119}$$

Stability. The appropriate norm for $\mathscr{V}^h$ corresponding to (68) for the advection–diffusion case can be obtained by generalizing the norms employed for the previous two cases, yielding

$$\begin{aligned} |||w^h|||^2_{\mathrm{ad}} &= \|\boldsymbol{A}^{1/2}\nabla w^h\|^2_{\tilde{\Omega}} + \|\tau_{\mathrm{ad}}^{1/2}\boldsymbol{u}\cdot\nabla w^h\|^2_{\tilde{\Omega}} + \||u_n|^{1/2}[\![w^h]\!]\|^2_{\tilde{\Gamma}} + \|\tau_{\mathrm{d}}^{1/2}[\![w^h]\!]\|^2_{\tilde{\Gamma}} + \||u_n|^{1/2}w^{h-}\|^2_{\Gamma^+}\\ &\quad + \||u_n|^{1/2}w^{h+}\|^2_{\Gamma^-} + \|\tau_{\mathrm{d}}^{1/2}w^h\|^2_{\Gamma_g}. \end{aligned} \tag{120}$$

Note that above energy norm is independent of α.

Lemma 3.5. $|||\cdot|||_{\mathrm{ad}}^2$ *is a norm on* $\mathscr{V}^h$.

Proof. The proof follows directly from the arguments used to prove Lemmas 3.1 and 3.3. □

Lemma 3.6. *The bilinear form* (69) *is stable, that is, for any* $\alpha \in \mathbb{R}$ *there exists a positive constant m such that*

$$B_{\mathrm{ad}}^{(s)}(w^h, w^h) \geqslant m|||w^h|||_{\mathrm{ad}}^2 \quad \forall w^h \in \mathscr{V}^h. \tag{121}$$

Proof. Substituting (57) in (69) and recalling definition (64), we can write

$$B_{\mathrm{ad}}^{(s)}(w^h, w^h) = B_{\mathrm{a}}(w^h, w^h) + (\tau_{\mathrm{ad}}\mathscr{L}_{\mathrm{a}}w^h, \mathscr{L}_{\mathrm{a}}w^h)_{\tilde{\Omega}} + B_{\mathrm{d}}^{(s)}(w^h, w^h) + (\tau_{\mathrm{ad}}\mathscr{L}_{\mathrm{a}}w^h, \mathscr{L}_{\mathrm{d}}w^h)_{\tilde{\Omega}}. \tag{122}$$

All except for the last of above terms have been considered in Sections 3.3.1 and 3.3.2. By virtue of (83) and (A.17) we can express this last term for $\delta > 0$ as

$$(\tau_{\mathrm{ad}}\mathscr{L}_{\mathrm{a}}w^h, \mathscr{L}_{\mathrm{d}}w^h)_{\tilde{\Omega}} \geqslant \sum_{e=1}^{N_{\mathrm{el}}} \tau_{\mathrm{ad}} \left[-\frac{\delta}{2}\|\boldsymbol{u}\cdot\nabla w^h\|_{\Omega_e}^2 - \frac{C_{\mathrm{I}}^2|\boldsymbol{A}|h_e^{-2}}{2\delta}\|\boldsymbol{A}^{1/2}\nabla w^h\|_{\Omega_e}^2 \right]. \tag{123}$$

We now choose

$$\delta|_{\Omega_e} = 1, \tag{124}$$

$$\tau_{\mathrm{ad}}|_{\Omega_e} = \frac{h_e}{2u_e^{\mathrm{M}}}\tilde{\xi}, \tag{125}$$

where $\tilde{\xi}$ is defined as in (33), and the element Péclet number is

$$Pe = \frac{u_e^{\mathrm{M}}h_e}{2A_e^{\mathrm{M}}}, \tag{126}$$

see (34). We have used here the classical definition of the stabilization parameter τ_{ad} as in the CG method for advection–diffusion with SUPG stabilization, see Section 2.3. These choices yield, together with the results from Sections 3.3.1 and 3.3.2,

$$\begin{aligned} B_{\mathrm{ad}}^{(s)}(w^h, w^h) \geqslant \sum_{e=1}^{N_{\mathrm{el}}} \left(\frac{2 + C|\alpha-1|^2}{2 + 2C|\alpha-1|^2} - \frac{C_{\mathrm{I}}^2\tilde{\xi}}{8Pe} \right) \|\boldsymbol{A}^{1/2}\nabla w^h\|_{\Omega_e}^2 + \tfrac{1}{2}\Big[\|\tau_{\mathrm{ad}}^{1/2}\boldsymbol{u}\cdot\nabla w^h\|_{\tilde{\Omega}}^2 + \||u_n|^{1/2}[\![w^h]\!]\|_{\tilde{\Gamma}}^2 \\ + \|\tau_{\mathrm{d}}^{1/2}[\![w^h]\!]\|_{\tilde{\Gamma}}^2 + \||u_n|^{1/2}w^{h-}\|_{\Gamma^+}^2 + \||u_n|^{1/2}w^{h+}\|_{\Gamma^-}^2 + \|\tau_{\mathrm{d}}^{1/2}w^h\|_{\Gamma_g}^2 \Big]. \end{aligned} \tag{127}$$

To ensure that the coefficient of $\|\boldsymbol{A}^{1/2}\nabla w^h\|_{\Omega_e}^2$ on the first line of (127) is sufficiently large, we insist on

$$\frac{2 + C|\alpha-1|^2}{2 + 2C|\alpha-1|^2} - \frac{C_{\mathrm{I}}^2\tilde{\xi}}{8Pe} \geqslant \frac{1}{2}, \tag{128}$$

which restricts $\tilde{\xi}$ to satisfy

$$\tilde{\xi} \leqslant \frac{4Pe}{C_{\mathrm{I}}^2}\left(\frac{1}{1 + C|\alpha-1|^2} \right). \tag{129}$$

Note that C_{I} increases for higher-order interpolation. The restriction (129) on $\tilde{\xi}$ is primarily a condition on its slope at $Pe = 0$. It ensures that, in the diffusion-dominated case, the stabilization term on element interiors vanishes sufficiently fast as Pe approaches zero. Let us mention that we can always adjust the slope

of $\tilde{\xi}$ at the origin for any type of element to ensure that the stability condition (129) is satisfied. Given that condition (129) is met, we have that (121) holds with $m = 1/2$, which concludes the proof. □

Convergence. Convergence of the stabilized DG method (68) is independent of the parameter α as for the diffusion case and can be shown analogous to the proofs in Sections 3.3.1 and 3.3.2. We have the following.

Theorem 3.3. *Assume the consistency and stability conditions* (119) and (121), *respectively*, *hold. Given that the conditions are satisfied for the interpolation estimates* (A.12), (A.13) *and the trace inequality* (A.18) *to hold*, *the error estimate for the stabilized DG method* (68) *can be written as*

$$|||e|||_{\mathrm{ad}}^2 \leqslant C \sum_{e=1}^{N_{\mathrm{el}}} h_e^{2k} |\phi|_{H^{k+1}(\Omega_e)}^2, \tag{130}$$

where C is a constant.

Proof. As in the proofs of Theorems 3.1 and 3.2 we estimate $|||e^h|||_{\mathrm{ad}}^2$ as

$$\begin{aligned} m|||e^h|||_{\mathrm{ad}}^2 &\leqslant B_{\mathrm{ad}}^{(s)}(e^h, e^h), \\ &= B_{\mathrm{ad}}^{(s)}(e^h, e - \eta), \\ &= -B_{\mathrm{ad}}^{(s)}(e^h, \eta), \\ &\leqslant |B_{\mathrm{ad}}^{(s)}(e^h, \eta)|, \\ &\leqslant |B_{\mathrm{a}}(e^h, \eta)| + |(\tau_{\mathrm{ad}} \mathscr{L}_{\mathrm{a}} e^h, \mathscr{L}_{\mathrm{a}} \eta)_{\tilde{\Omega}}| + |B_{\mathrm{d}}^{(s)}(e^h, \eta)| + |(\tau_{\mathrm{ad}} \mathscr{L}_{\mathrm{a}} e^h, \mathscr{L}_{\mathrm{d}} \eta)_{\tilde{\Omega}}|. \end{aligned} \tag{131}$$

Of the four terms appearing in the last of the above inequalities, only the last term has not been previously analyzed and bounded from above. Using (83) and (A.13) and noting that (125) satisfies in the diffusion-dominated case

$$\tau_{\mathrm{ad}}|_{\Omega_e} \leqslant \frac{h_e^2}{12 A_e^{\mathrm{M}}}, \tag{132}$$

we obtain with the results from Sections 3.3.1 and 3.3.2

$$|||e^h|||_{\mathrm{ad}}^2 \leqslant C \sum_{e=1}^{N_{\mathrm{el}}} h_e^{2k} |\phi|_{H^{k+1}(\Omega_e)}^2. \tag{133}$$

Invoking interpolation estimates and similar arguments to bound $|||\eta|||_{\mathrm{ad}}^2$ and using the triangle inequality, we have

$$|||e|||_{\mathrm{ad}}^2 \leqslant C \sum_{e=1}^{N_{\mathrm{el}}} h_e^{2k} |\phi|_{H^{k+1}(\Omega_e)}^2, \tag{134}$$

which proves the theorem. □

3.4. Efficiency

We have seen from Section 3.3 that stabilized DG methods are a versatile approach for a variety of partial differential equations and that they converge at optimal rates for all model problems considered. However, the discontinuous nature of the shape functions introduces additional unknowns relative to the CG method, as we need to distinguish between values from different elements at the same node.

In one dimension, for scalar problems and linear elements, we have one unknown at each node in CG methods, whereas we have twice as many for DG methods. For higher-order interpolation, the ratio of the number of unknowns per element in the DG method versus the CG method improves, but for all orders of interpolation which are used in practice, the increased number of unknowns can suggest that DG may be expensive.

In Table 1 we compare the number of unknowns of DG and CG methods per element for different orders of interpolation, and a one-dimensional element patch of two elements is illustrated in Fig. 9 for linear and quadratic elements. Note that for the CG method, the nodes shared by e adjacent elements are counted as $1/e$ to each individual element in Table 1.

For two-dimensional elements, such as quadrilaterals and triangles, the ratio of the number of unknowns is even more unfavorable for DG methods. In Fig. 10 we display an element patch of four quadratic quadrilateral elements as example. Table 2 (panel a) compares the ratio for different quadrilateral elements and Table 2 (panel b) for triangular elements, which have been obtained from subdividing each quadrilateral into two triangles. For this case, each vertex node of a triangular element will be shared by six adjacent triangles, and each edge node by two adjacent triangles.

For three-dimensional elements, the corresponding comparison is given in Table 3 (panel a) for hexahedral Lagrangian elements, and in Table 3 (panel b) for tetrahedral Lagrangian elements, where the functions appearing in the table are defined as

$$f(\bar{k}) = 4 + 6(\bar{k}-1) + 4H(\bar{k}-2.5)\tfrac{1}{2}(\bar{k}-1)(\bar{k}-2) + H(\bar{k}-3.5)\sum_{\kappa=4}^{\bar{k}}\tfrac{1}{2}(\kappa-2)(\kappa-3), \tag{135}$$

$$g(\bar{k}) = 0.2 + 1.2(\bar{k}-1) + 2H(\bar{k}-2.5)\tfrac{1}{2}(\bar{k}-1)(\bar{k}-2) + H(\bar{k}-3.5)\sum_{\kappa=4}^{\bar{k}}\tfrac{1}{2}(\kappa-2)(\kappa-3), \tag{136}$$

Table 1
Comparison of number of unknowns of DG with CG methods for one-dimensional elements

k	DG	CG	DG/CG
0	1	–	–
1	2	1	2
2	3	2	1.5
3	4	3	1.33
⋮	⋮	⋮	⋮
$\bar{k}$ (>0)	$\bar{k}+1$	$\bar{k}$	$1+1/\bar{k}$

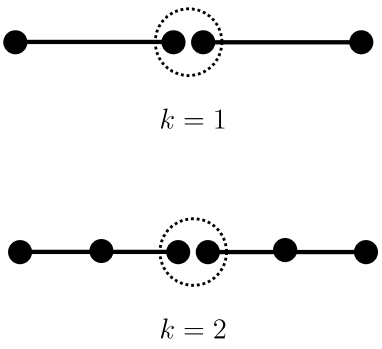

Fig. 9. One-dimensional element patch of two elements for linear ($k = 1$) and quadratic ($k = 2$) interpolation.

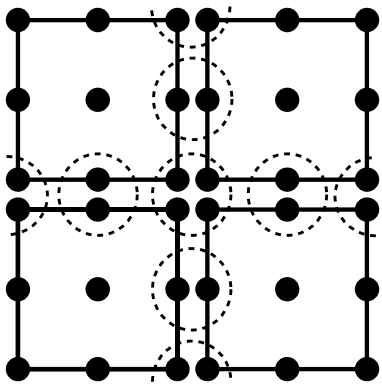

Fig. 10. Two-dimensional element patch of four quadratic elements ($k = 2$).

Table 2
Comparison of number of unknowns of DG with CG methods for (panel a) quadrilaterals and (panel b) triangles

k	DG	CG	DG/CG
(a) Quadrilaterals			
0	1	–	–
1	4	1	4
2	9	4	2.25
3	16	9	1.78
⋮	⋮	⋮	⋮
$\bar{k}$ (> 0)	$(\bar{k}+1)^2$	$\bar{k}^2$	$1 + 2/\bar{k}$
(b) Triangles			
0	1	–	–
1	3	1/2	6
2	6	2	3
3	10	9/2	2.22
⋮	⋮	⋮	⋮
$\bar{k}$ (> 0)	$\frac{1}{2}(\bar{k}+1)(\bar{k}+2)$	$\frac{1}{2}\bar{k}^2$	$1 + 3/\bar{k}$

and $H(\cdot)$ denotes the Heaviside function [10]. Similarly to the two-dimensional case, the comparison for tetrahedra is based on a subdivision of each hexahedral element into five tetrahedra.

In summary we conclude that the advantages of stabilized DG methods may be counterbalanced by the disadvantage resulting from the introduction of additional unknowns. For fourth-order elliptic problems, however, we can envision formulations which are continuous and only exhibit discontinuities in first- and higher-order derivatives. In many fourth-order elliptic problems, one is interested in solutions which are continuous in the variable and its derivatives, and by adopting a weak enforcement of the continuity of derivatives, while at the same time keeping interpolation functions C^0-continuous, one is able to overcome this disadvantage and retain the lower number of unknowns of CG methods. This approach will be discussed in Section 4.

Table 3
Comparison of number of unknowns of DG with CG methods for (panel a) hexahedra and (panel b) tetrahedra

k	DG	CG	DG/CG
(a) Hexahedra			
0	1	–	–
1	8	1	8
2	27	8	3.38
3	64	27	2.37
⋮	⋮	⋮	⋮
$\bar{k}$ (>0)	$(\bar{k}+1)^3$	$\bar{k}^3$	$1+3/\bar{k}$
(b) Tetrahedra			
0	1	–	–
1	4	0.2	20
2	10	1.4	7.14
3	20	4.6	4.35
⋮	⋮	⋮	⋮
$\bar{k}$ (>0)	$f(\bar{k})$	$g(\bar{k})$	$f(\bar{k})/g(\bar{k})$

4. C/DG methods for thin bending theories

In this section we introduce C/DG formulations for two thin bending theories. The C/DG methods have the following central features:

1. The approximation functions are C^0-continuous, a feature inherited from CG methods.
2. Therefore, we will encounter discontinuities in first and higher-order derivatives, which leads to the adoption of concepts from DG methods.
3. Continuity of first- and higher-order derivatives will be weakly enforced by adding weighted residual terms to the variational equation on interior boundaries, invoking stabilization techniques.

The C/DG methods are based on Bernoulli–Euler beam theory and Poisson–Kirchhoff plate theory, and are therefore rotation free. This reduces the number of unknowns and complexity of the methods considerably compared to traditional finite element approaches.

4.1. Bernoulli–Euler beam theory

We start our developments with the statement of the boundary value model problem and then suggest a C/DG method for the Bernoulli–Euler beam. The error analysis of our formulation comprises consistency and stability considerations, which imply convergence of the method. We give an interpretation of the Euler–Lagrange equations of the method in the context of continuity and discuss some implications of the C/DG method.

4.1.1. Model problem

Let $\Omega \subset \mathbb{R}$ be an open, bounded domain and Γ its boundary. Let Γ_g, Γ_h, Γ_M and Γ_Q denote the displacement, slope, moment and shear force boundaries, respectively. The strong form of the Bernoulli–Euler beam problem can be written as

$$(EI\phi_{,xx})_{,xx} = f \quad \text{in } \Omega, \tag{137}$$

$$\phi = g \quad \text{on } \Gamma_g, \tag{138}$$

$$\phi_{,x} \cdot n = h \quad \text{on } \Gamma_h, \tag{139}$$

$$EI\phi_{,xx} = M \quad \text{on } \Gamma_M, \tag{140}$$

$$(EI\phi_{,xx})_{,x} \cdot n = Q \quad \text{on } \Gamma_Q. \tag{141}$$

In the above, ϕ denotes the transverse displacement of the beam, EI is its bending stiffness, f is a given distributed load, and g, h, M and Q denote the prescribed boundary displacement, slope, moment and shear force, respectively. Note that we have the relationships

$$\Gamma_Q = \Gamma \setminus \Gamma_g, \tag{142}$$

$$\Gamma_M = \Gamma \setminus \Gamma_h \tag{143}$$

between the different parts of the boundary.

4.1.2. Method

Let us consider a partition of the domain into finite elements as in (24), and let us choose approximation functions which are continuous on the entire domain, but discontinuous in first and higher-order derivatives across interior boundaries, i.e., let us define the finite-dimensional trial solution and weighting function spaces as

$$\mathscr{S}^h = \{\phi^h \in H^1(\Omega) |\ \phi^h|_{\Omega_e} \in P_k(\Omega_e)\ \forall \Omega_e \in \mathscr{P}(\Omega), \phi^h|_{\Gamma_g} = g\}, \tag{144}$$

$$\mathscr{V}^h = \{w^h \in H^1(\Omega) |\ w^h|_{\Omega_e} \in P_k(\Omega_e)\ \forall \Omega_e \in \mathscr{P}(\Omega), w^h|_{\Gamma_g} = 0\}. \tag{145}$$

The method we propose for the solution of the Bernoulli–Euler beam problem (137)–(141) can be written as: Find $\phi^h \in \mathscr{S}^h$ such that

$$B_{\mathrm{b}}(w^h, \phi^h) = L_{\mathrm{b}}(w^h) \quad \forall w^h \in \mathscr{V}^h, \tag{146}$$

where the bilinear form is defined as

$$\begin{aligned} B_{\mathrm{b}}(w^h, \phi^h) = {} & (w^h_{,xx}, EI\phi^h_{,xx})_{\tilde{\Omega}} - [\![w^h_{,x}]\!]\langle EI\phi^h_{,xx}\rangle_{\tilde{\Gamma}} - \langle EIw^h_{,xx}\rangle[\![\phi^h_{,x}]\!]_{\tilde{\Gamma}} + \tau[\![w^h_{,x}]\!][\![\phi^h_{,x}]\!]_{\tilde{\Gamma}} \\ & - w^h_{,x} \cdot nEI\phi^h_{,xx}|_{\Gamma_h} - EIw^h_{,xx}\phi^h_{,x} \cdot n|_{\Gamma_h} + \tau_h w^h_{,x} \cdot n\phi^h_{,x} \cdot n|_{\Gamma_h} \end{aligned} \tag{147}$$

and the linear form as

$$L_{\mathrm{b}}(w^h) = (w^h, f)_{\tilde{\Omega}} + w^h_{,x} \cdot nM|_{\Gamma_M} - EIw^h_{,xx}h|_{\Gamma_h} - w^h Q|_{\Gamma_Q} + \tau_h w^h_{,x} \cdot nh|_{\Gamma_h}. \tag{148}$$

We have introduced in (147) and (148) the stabilization parameters τ on interior boundaries and τ_h on the exterior slope boundary, which will be further specified in Section 4.1.3. Note that we have extended in (147) our previous notational convention in that a subscript on any bracket indicates where the respective terms are to be evaluated.

The C/DG method (146) is similar to method (63) for the diffusion problem, extending the approach to a higher-order partial differential equation. The weighting functions in (147) and (148) have been chosen dimensionally consistent, adopting the ideas of Nitsche [53].

One can see from the definition of the bilinear form (147) that the C/DG method has non-local character. In addition to element contributions, we encounter terms on interior boundaries contributing to the two elements adjacent to the respective interfaces. This leads to the necessity of introducing a new programming structure into most current finite element codes. Formulation (146) suggests complementing the standard

assembly loop over elements by an additional loop over interior boundaries. One can avoid such extra loop by ad hoc concepts such as defining overlapping finite macro-elements. This approach, however, leads to non-intuitive formulations and requires additional virtual nodes and boundary elements beyond the computational domain for enforcement of the boundary conditions [24], and is therefore not recommended.

Let us emphasize that even though the C/DG method necessitates the introduction of an additional interior boundary assembly loop, as commonly exists in DG or finite volume codes, we circumvent the introduction of additional nodal unknowns of DG formulations as we retain C^0-continuity. Our approximation functions are continuous on element interfaces, and we can express the discontinuities in the derivatives on an interior boundary by the nodal quantities from the two elements sharing the interface only.

4.1.3. Error analysis

In this section we want to conduct an error analysis for the symmetric C/DG method (146). Let us assume for simplicity that the bending stiffness EI is continuous along the beam.

Consistency. Integration by parts of (146) yields

$$\begin{aligned} 0 &= B_{\mathrm{b}}(w^h,\phi^h) - L_{\mathrm{b}}(w^h),\\ &= (w^h,[(EI\phi^h_{,xx})_{,xx} - f])_{\tilde{\Omega}} - \langle EIw^h_{,xx}\rangle[\![\phi^h_{,x}]\!]_{\tilde{\Gamma}} + \langle w^h_{,x}\rangle[\![EI\phi^h_{,xx}]\!]_{\tilde{\Gamma}}\\ &\quad - \langle w^h\rangle[\![(EI\phi^h_{,xx})_{,x}]\!]_{\tilde{\Gamma}} - EIw^h_{,xx}[\phi^h_{,x}\cdot n - h]_{\Gamma_h} + w^h_{,x}\cdot n[EI\phi^h_{,xx} - M]_{\Gamma_M}\\ &\quad - w^h[(EI\phi^h_{,xx})_{,x}\cdot n - Q]_{\Gamma_Q} + \tau[\![w^h_{,x}]\!][\![\phi^h_{,x}]\!]_{\tilde{\Gamma}} + \tau_h w^h_{,x}\cdot n[\phi^h_{,x}\cdot n - h]_{\Gamma_h}. \end{aligned} \tag{149}$$

From (149) we deduce the Euler–Lagrange equations

$$(EI\phi^h_{,xx})_{,xx} = f \quad \text{in } \tilde{\Omega}, \tag{150}$$

$$\phi^h_{,x}\cdot n = h \quad \text{on } \Gamma_h, \tag{151}$$

$$EI\phi^h_{,xx} = M \quad \text{on } \Gamma_M, \tag{152}$$

$$(EI\phi^h_{,xx})_{,x}\cdot n = Q \quad \text{on } \Gamma_Q, \tag{153}$$

$$[\![\phi^h_{,x}]\!] = 0 \quad \text{on } \tilde{\Gamma}, \tag{154}$$

$$[\![EI\phi^h_{,xx}]\!] = 0 \quad \text{on } \tilde{\Gamma}, \tag{155}$$

$$[\![(EI\phi^h_{,xx})_{,x}]\!] = 0 \quad \text{on } \tilde{\Gamma}. \tag{156}$$

Note that (150) denotes the enforcement of the governing partial differential equation (137) on element interiors, (151)–(153) account for the enforcement of the boundary conditions, (154) ensures the continuity of the slope, (155) the continuity of the moment and (156) the continuity of the shear force across interior boundaries. Substituting the exact solution ϕ for ϕ^h in (146) yields the Galerkin orthogonality condition

$$B_{\mathrm{b}}(w^h,e) = 0 \quad \forall w^h \in \mathscr{V}^h(\Omega). \tag{157}$$

The implication of the weak enforcement of the continuity requirements, which is achieved in (146) through the terms corresponding to (154)–(156), is illustrated for the first derivative in Fig. 11. On the left we can see a two element patch for which C^1-continuity has been obtained by employing Hermite cubic

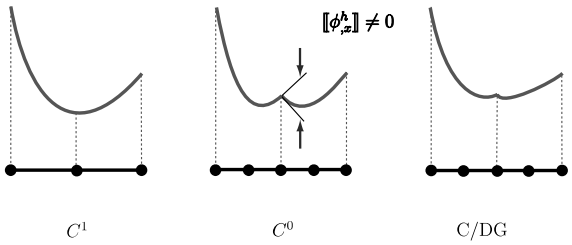

Fig. 11. Weak enforcement of continuity of first derivative.

approximation functions. In the middle, C^0-continuous quadratic shape functions lead to a discontinuity in slope on the interior boundary. The action of the weak enforcement of the continuity of the slope on the interior boundary is illustrated by the two arrows and results in an approximation which can be seen on the right. The C/DG method satisfies continuity of the slope in a weak sense, allowing for a small kink in the slope on the interior boundary.

Stability. To prove stability, define

$$|||w^h|||_{\mathrm{b}}^2 = \|(EI)^{1/2} w^h_{,xx}\|_{\bar{\Omega}}^2 + \|\tau^{1/2}[\![w^h_{,x}]\!]\|_{\bar{\Gamma}}^2 + \|\tau_h^{1/2} w^h_{,x}\|_{\Gamma_h}^2. \tag{158}$$

Proposition 4.1. $|||\cdot|||_{\mathrm{b}}^2$ *is a norm on* $\mathscr{V}^h$.

Proof. There are no non-trivial functions for which (158) could vanish by similar arguments as in the proofs of Lemmas 3.1 and 3.3. The only non-trivial functions in $\mathscr{V}^h$ for which $|||w^h|||_{\mathrm{b}}^2$ could vanish are the piecewise linears. The two possibilities, therefore, are that either w^h is linear over the entire domain Ω, i.e., possesses constant slope, or w^h changes slope at least once. In the former case, $w^h_{,x} \neq 0$ and so $\|\tau_h^{1/2} w^h_{,x}\|_{\Gamma_h}^2 > 0$; in the latter case, $[\![w^h_{,x}]\!] \neq 0$ on one or more element interfaces, so that $\|\tau^{1/2}[\![w^h_{,x}]\!]\|_{\bar{\Gamma}}^2 > 0$. Consequently, $|||w^h|||_{\mathrm{b}}^2 > 0\ \forall w^h \in \mathscr{V}^h$. $\square$

Proposition 4.2. *The C/DG method* (146) *is stable in the energy norm* (158), *that is, there exists a positive constant m such that*

$$B_{\mathrm{b}}(w^h, w^h) \geqslant m|||w^h|||_{\mathrm{b}}^2 \quad \forall w^h \in \mathscr{V}^h(\Omega). \tag{159}$$

Proof. From definition (147) we obtain

$$B_{\mathrm{b}}(w^h, w^h) \geqslant \|(EI)^{1/2} w^h_{,xx}\|_{\bar{\Omega}}^2 + \|\tau^{1/2}[\![w^h_{,x}]\!]\|_{\bar{\Gamma}}^2 + \|\tau_h^{1/2} w^h_{,x}\|_{\Gamma_h}^2 - 2(|[\![w^h_{,x}]\!]\langle EIw^h_{,xx}\rangle_{\bar{\Gamma}}| + |w^h_{,x} \cdot nEIw^h_{,xx}|_{\Gamma_h}|). \tag{160}$$

Similar to the approach in Section 3.3.2, we invoke the ε-inequality (83), inequality (98), trace inequality (A.18) and inverse estimate (A.17) and can write

$$|[\![w^h_{,x}]\!]\langle EIw^h_{,xx}\rangle_{\bar{\Gamma}}| + |w^h_{,x} \cdot nEIw^h_{,xx}|_{\Gamma_h}| \leqslant \sum_{e=1}^{N_{\mathrm{el}}} \frac{\varepsilon CEI}{2h_e} \|(EI)^{1/2} w^h_{,xx}\|_{\Omega_e}^2 + \sum_{i=1}^{N_{\mathrm{i}}} \frac{1}{2\varepsilon\tau} \|\tau^{1/2}[\![w^h_{,x}]\!]\|_{\Gamma_i}^2 + \sum_{j=1}^{N_h} \frac{1}{2\varepsilon\tau_h} \|\tau_h^{1/2} w^h_{,x}\|_{\Gamma_j}^2, \tag{161}$$

where N_h denotes the number of exterior slope boundary segments $\Gamma_j \subseteq \Gamma_h$. Using (161) in (160), we have

$$B_{\mathrm{b}}(w^h, w^h) \geqslant \sum_{e=1}^{N_{\mathrm{el}}} \left(1 - \frac{\varepsilon CEI}{h_e}\right) \|(EI)^{1/2} w^h_{,xx}\|^2_{\Omega_e} + \sum_{i=1}^{N_{\mathrm{i}}} \left(1 - \frac{1}{\varepsilon\tau}\right) \|\tau^{1/2} [\![w^h_{,x}]\!]\|^2_{\Gamma_i} + \sum_{j=1}^{N_h} \left(1 - \frac{1}{\varepsilon\tau_h}\right) \|\tau_h^{1/2} w^h_{,x}\|^2_{\Gamma_j} \geqslant m |||w^h|||^2_{\mathrm{b}}. \tag{162}$$

In particular, assuming that $\tau = \tau_h$, we can prove (159) for $m = 1/2$ if we choose $\varepsilon|_{\Omega_e} = h_e/(2CEI)$, in which case we obtain $\tau = \tau_h = 4CEI/h_e$. □

4.1.4. Convergence in energy norm

Theorem 4.1. *Assume that the consistency condition* (157) *and stability condition* (159) *of the method hold. Given that the conditions are satisfied for the interpolation estimates* (A.12), (A.13) *and the trace inequality* (A.18) *holds, the error estimate for the C/DG method* (146) *can be written as*

$$|||e|||^2_{\mathrm{b}} \leqslant C \sum_{e=1}^{N_{\mathrm{el}}} h_e^{2(k-1)} |\phi|^2_{H^{k+1}(\Omega_e)}, \tag{163}$$

where C is a constant.

Proof. As in the error analyses in Section 3.3, we take advantage of the decomposition of the error (80) and the Galerkin orthogonality (157) and write

$$\begin{aligned} m|||e^h|||^2_{\mathrm{b}} &\leqslant B_{\mathrm{b}}(e^h, e^h), \\ &= B_{\mathrm{b}}(e^h, e - \eta), \\ &\leqslant -B_{\mathrm{b}}(e^h, \eta), \\ &\leqslant |B_{\mathrm{b}}(e^h, \eta)|. \end{aligned} \tag{164}$$

We then can continue the inequality (164) as

$$m|||e^h|||^2_{\mathrm{b}} \leqslant |((EI)^{1/2} e^h_{,xx}, (EI)^{1/2} \eta_{,xx})_{\bar{\Omega}}| + |[\![e^h_{,x}]\!] \langle EI \eta_{,xx} \rangle_{\bar{\Gamma}}| + |\langle EI e^h_{,xx} \rangle [\![\eta_{,x}]\!]_{\bar{\Gamma}}| + |\tau [\![e^h_{,x}]\!] [\![\eta_{,x}]\!]_{\bar{\Gamma}}| + |e^h_{,x} \cdot nEI \eta_{,xx}|_{\Gamma_h}| + |EI e^h_{,xx} \eta_{,x} \cdot n|_{\Gamma_h}| + |\tau_h e^h_{,x} \cdot n \eta_{,x} \cdot n|_{\Gamma_h}|. \tag{165}$$

Making repeated use of the ε-inequality (83), utilizing (98), the interpolation estimate (A.13) and the trace inequality (A.18), we obtain

$$\frac{m}{2} |||e^h|||^2_{\mathrm{b}} \leqslant \frac{EI}{m} \|\eta_{,xx}\|^2_{\bar{\Omega}} + \left\{ \frac{(EI)^2}{m} \|\tau^{-1/2} \langle \eta_{,xx} \rangle\|^2_{\bar{\Gamma}} + \frac{(EI)^2}{m} \|\tau_h^{-1/2} \eta_{,xx}\|^2_{\Gamma_h} \right\} + \left\{ \frac{CEI}{m} \|h_e^{-1/2} [\![\eta, x]\!]\|^2_{\bar{\Gamma}} + \frac{CEI}{m} \|h_e^{-1/2} \eta_{,x}\|^2_{\Gamma_h} \right\} + \left\{ \frac{1}{m} \|\tau^{1/2} [\![\eta, x]\!]\|^2_{\bar{\Gamma}} + \frac{1}{m} \|\tau_h^{1/2} \eta, x\|^2_{\Gamma_h} \right\}. \tag{166}$$

We can estimate the terms on the right-hand side of (166) as

$$\frac{(EI)^2}{m} \|\tau^{-1/2} \langle \eta_{,xx} \rangle\|^2_{\bar{\Gamma}} + \frac{(EI)^2}{m} \|\tau_h^{-1/2} \eta_{,xx}\|^2_{\Gamma_h} \leqslant C \sum_{e=1}^{N_{\mathrm{el}}} h_e (h_e^{-1} \|\eta_{,xx}\|^2_{\Omega_e} + h_e \|\eta_{,xxx}\|^2_{\Omega_e}), \tag{167}$$

$$\frac{EI}{m} \|h_e^{-1/2} [\![\eta_{,x}]\!]\|^2_{\bar{\Gamma}} + \frac{EI}{m} \|h_e^{-1/2} \eta_{,x}\|^2_{\Gamma_h} \leqslant C \sum_{e=1}^{N_{\mathrm{el}}} h_e^{-1} (h_e^{-1} \|\eta_{,x}\|^2_{\Omega_e} + h_e \|\eta_{,xx}\|^2_{\Omega_e}), \tag{168}$$

$$\frac{1}{m}\|\tau^{1/2}[\![\eta_{,x}]\!]\|_{\Gamma}^2+\frac{1}{m}\|\tau_h^{1/2}\eta_{,x}\|_{\Gamma_h}^2\leqslant C\sum_{e=1}^{N_{\mathrm{el}}}h_e^{-1}(h_e^{-1}\|\eta_{,x}\|_{\Omega_e}^2+h_e\|\eta_{,xx}\|_{\Omega_e}^2),\tag{169}$$

where we have used (98), inequality (108) and trace inequality (A.18). Therefore, we can write for (166)

$$\frac{m}{2}|||e^h|||_{\mathrm{b}}^2\leqslant C\sum_{e=1}^{N_{\mathrm{el}}}\{\|\eta_{,xx}\|_{\Omega_e}^2+h_e(h_e^{-1}\|\eta_{,xx}\|_{\Omega_e}^2+h_e\|\eta_{,xxx}\|_{\Omega_e}^2)+h_e^{-1}(h_e^{-1}\|\eta_{,x}\|_{\Omega_e}^2+h_e\|\eta_{,xx}\|_{\Omega_e}^2)$$
$$+h_e^{-1}(h_e^{-1}\|\eta_{,x}\|_{\Omega_e}^2+h_e\|\eta_{,xx}\|_{\Omega_e}^2)\}.\tag{170}$$

From Appendix A, inequalities (A.12) and (A.13), we can deduce the interpolation estimates

$$\|\eta_{,xx}\|_{\Omega_e}^2\leqslant\|\eta\|_{H^2(\Omega_e)}^2\leqslant Ch_e^{2k-2}|\phi|_{H^{k+1}(\Omega_e)}^2,\tag{171}$$

$$\|\eta_{,xx}\|_{\Omega_e}\leqslant\|\eta\|_{H^2(\Omega_e)}\leqslant Ch_e^{k-1}|\phi|_{H^{k+1}(\Omega_e)},\tag{172}$$

$$\|\eta_{,xx}\|_{H^1(\Omega_e)}\leqslant\|\eta\|_{H^3(\Omega_e)}\leqslant Ch_e^{k-2}|\phi|_{H^{k+1}(\Omega_e)},\tag{173}$$

$$\|\eta_{,x}\|_{\Omega_e}\leqslant\|\eta\|_{H^1(\Omega_e)}\leqslant Ch_e^{k}|\phi|_{H^{k+1}(\Omega_e)},\tag{174}$$

$$\|\eta_{,x}\|_{H^1(\Omega_e)}\leqslant\|\eta\|_{H^2(\Omega_e)}\leqslant Ch_e^{k-1}|\phi|_{H^{k+1}(\Omega_e)}.\tag{175}$$

We then obtain the result

$$|||e^h|||_{\mathrm{b}}^2\leqslant C\sum_{e=1}^{N_{\mathrm{el}}}h_e^{2(k-1)}|\phi|_{H^{k+1}(\Omega_e)}^2.\tag{176}$$

Using similar arguments to bound $|||\eta|||_{\mathrm{b}}^2$ and the triangle inequality, we conclude

$$|||e|||_{\mathrm{b}}^2\leqslant C\sum_{e=1}^{N_{\mathrm{el}}}h_e^{2(k-1)}|\phi|_{H^{k+1}(\Omega_e)}^2.\quad\square\tag{177}$$

4.1.5. Convergence in L^2-norm

We wish to prove convergence of the C/DG method (146) in the L^2-norm for the homogeneous Dirichlet problem, i.e., for the case $\Gamma=\Gamma_g=\Gamma_h$ and $g=h=0$. Let us first quote the following theorem (see Theorem 2.1 in [27], and Theorems 5.1 and 5.4 in Section 2 of [33] for a proof):

Theorem 4.2. *The mapping $P:C^\infty(\Omega)\to C^\infty(\Omega)\times C^\infty(\partial\Omega)\times C^\infty(\partial\Omega)$ defined by $P\phi=(\phi_{,xxxx},\phi,\phi_{,n})$ and completed by continuity is a homeomorphism of $H^s(\Omega)$ onto $H^{s-4}(\Omega)\times H^{s-1/2}(\partial\Omega)\times H^{s-3/2}(\partial\Omega)$ for all $s\geqslant 4$, and there exist constants α_s and β_s such that*

$$\|\phi\|_{H^s(\Omega)}\leqslant\alpha_s\{\|\phi_{,xxxx}\|_{H^{s-4}(\Omega)}+\|\phi\|_{H^{s-1/2}(\partial\Omega)}+\|\phi_{,n}\|_{H^{s-3/2}(\partial\Omega)}\}\leqslant\beta_s\|\phi\|_{H^s(\Omega)}.\tag{178}$$

Note that we have introduced in the above theorem the notation $\phi_{,n}=\phi_{,x}\cdot n$ for a normal derivative. For the bilinear form (147), the following proposition holds:

Proposition 4.3. *There exists a constant $0<C<\infty$ such that*

$$B_{\mathrm{b}}(w^h,v^h)\leqslant C|||w^h|||_{\mathrm{b}}|||v^h|||_{\mathrm{b}}\quad\forall w^h,v^h\in\mathscr{V}^h(\Omega),\tag{179}$$

where C is independent of h_e.

Proof. We can obtain (179) by using the Cauchy–Schwarz inequality [81]

$$|(a,b)| \leqslant \|a\|\|b\|, \tag{180}$$

which holds for suitably defined a and b, on each term of the bilinear form, namely

$$\begin{aligned} B_{\mathrm{b}}(w^h, v^h) &\leqslant |B_{\mathrm{b}}(w^h, v^h)|, \\ &\leqslant |(w^h_{,xx}, EIv^h_{,xx})_{\tilde{\Omega}}| + |\langle\!\langle w^h_{,x}\rangle\!\rangle\langle EIv^h_{,xx}\rangle_{\tilde{\Gamma}}| + |\langle EIw^h_{,xx}\rangle\langle\!\langle v^h_{,x}\rangle\!\rangle_{\tilde{\Gamma}}| \\ &\quad + |\tau\langle\!\langle w^h_{,x}\rangle\!\rangle\langle\!\langle v^h_{,x}\rangle\!\rangle_{\tilde{\Gamma}}| + |w^h_{,x}\cdot nEIv^h_{,xx}|_{\Gamma_h}| + |EIw^h_{,xx}v^h_{,x}\cdot n|_{\Gamma_h}| + |\tau_h w^h_{,x}\cdot nv^h_{,x}\cdot n|_{\Gamma_h}|, \\ &\leqslant \|(EI)^{1/2}w^h_{,xx}\|_{\tilde{\Omega}}\|(EI)^{1/2}v^h_{,xx}\|_{\tilde{\Omega}} + \|\tau^{1/2}\langle\!\langle w^h_{,x}\rangle\!\rangle\|_{\tilde{\Gamma}}\|\tau^{-1/2}\langle EIv^h_{,xx}\rangle\|_{\tilde{\Gamma}} \\ &\quad + \|\tau^{-1/2}\langle EIw^h_{,xx}\rangle\|_{\tilde{\Gamma}}\|\tau^{1/2}\langle\!\langle v^h_{,x}\rangle\!\rangle\|_{\tilde{\Gamma}} + \|\tau^{1/2}\langle\!\langle w^h_{,x}\rangle\!\rangle\|_{\tilde{\Gamma}}\|\tau^{1/2}\langle\!\langle v^h_{,x}\rangle\!\rangle\|_{\tilde{\Gamma}} \\ &\quad + \|\tau_h^{1/2}w^h_{,x}\|_{\Gamma_h}\|\tau_h^{-1/2}EIv^h_{,xx}\|_{\Gamma_h} + \|\tau_h^{-1/2}EIw^h_{,xx}\|_{\Gamma_h}\|\tau_h^{1/2}v^h_{,x}\|_{\Gamma_h} + \|\tau_h^{1/2}w^h_{,x}\|_{\Gamma_h}\|\tau_h^{1/2}v^h_{,x}\|_{\Gamma_h}. \end{aligned} \tag{181}$$

Using the Cauchy–Schwarz inequality again in the form [81]

$$\sum_i |a_ib_i| \leqslant \left(\sum_i |a_i|^2\right)^{1/2}\left(\sum_i |b_j|^{1/2}\right)^{1/2}, \tag{182}$$

we have

$$\begin{aligned} B_{\mathrm{b}}(w^h, v^h) &\leqslant \{\|(EI)^{1/2}w^h_{,xx}\|^2_{\tilde{\Omega}} + \|\tau^{1/2}\langle\!\langle w^h_{,x}\rangle\!\rangle\|^2_{\tilde{\Gamma}} + \|\tau^{-1/2}\langle EIw^h_{,xx}\rangle\|^2_{\tilde{\Gamma}} + \|\tau^{1/2}\langle\!\langle w^h_{,x}\rangle\!\rangle\|^2_{\tilde{\Gamma}} + \|\tau_h^{1/2}w^h_{,x}\|^2_{\Gamma_h} \\ &\quad + \|\tau_h^{-1/2}EIw^h_{,xx}\|^2_{\Gamma_h} + \|\tau_h^{1/2}w^h_{,x}\|^2_{\Gamma_h}\}^{1/2}\{\|(EI)^{1/2}v^h_{,xx}\|^2_{\tilde{\Omega}} + \|\tau^{-1/2}\langle EIv^h_{,xx}\rangle\|^2_{\tilde{\Gamma}} + \|\tau^{1/2}\langle\!\langle v^h_{,x}\rangle\!\rangle\|^2_{\tilde{\Gamma}} \\ &\quad + \|\tau^{1/2}\langle\!\langle v^h_{,x}\rangle\!\rangle\|^2_{\tilde{\Gamma}} + \|\tau_h^{-1/2}EIv^h_{,xx}\|^2_{\Gamma_h} + \|\tau_h^{1/2}v^h_{,x}\|^2_{\Gamma_h} + \|\tau_h^{1/2}v^h_{,x}\|^2_{\Gamma_h}\}^{1/2}. \end{aligned} \tag{183}$$

Similar to the approach in Section 3.3.2, using trace inequality (A.18) and inverse estimate. (A.17), we obtain

$$\begin{aligned} B_{\mathrm{b}}(w^h, v^h) &\leqslant C\{\|(EI)^{1/2}w^h_{,xx}\|^2_{\tilde{\Omega}} + \|\tau^{1/2}\langle\!\langle w^h_{,x}\rangle\!\rangle\|^2_{\tilde{\Gamma}} + \|\tau_h^{1/2}w^h_{,x}\|^2_{\Gamma_h}\}^{1/2}\{\|(EI)^{1/2}v^h_{,xx}\|^2_{\tilde{\Omega}} + \|\tau^{1/2}\langle\!\langle v^h_{,x}\rangle\!\rangle\|^2_{\tilde{\Gamma}} \\ &\quad + \|\tau_h^{1/2}v^h_{,x}\|^2_{\Gamma_h}\}^{1/2} = C|||w^h|||_{\mathrm{b}}|||v^h|||_{\mathrm{b}}, \end{aligned} \tag{184}$$

where C is independent of h_e. □

Remark 4.1. Proposition 4.3 can be generalized as follows: Assume, ϕ, $\phi_d \in H^{k+3}(\Omega)$ are, respectively, exact solutions of the given boundary-value problem and a certain "dual problem" to be defined subsequently. Let the collection of finite element spaces $\{\mathscr{V}^h\}$ be quasi-uniform. Then there exists $h_0 = h_0(\phi, \phi_d)$ and a constant $\tilde{C}$ independent of ϕ, ϕ_d and h_e such that, $\forall h_e \leqslant h_0$,

$$\|\eta_{,xxx}\|^2_{\Omega_e} \leqslant \tilde{C}h_e^{-2}\|\eta_{,xx}\|^2_{\Omega_e}, \tag{185}$$

$$\|\eta_{d,xxx}\|^2_{\Omega_e} \leqslant \tilde{C}h_e^{-2}\|\eta_{d,xx}\|^2_{\Omega_e}, \tag{186}$$

where $\eta = \phi - \tilde{\phi}^h$ and $\eta_d = \phi_d - \tilde{\phi}^h_d$ are the interpolation errors. This result is due to Arnold et al. [87], and has been employed by Hughes et al. [88]. With (185), (186), (98), (108), the inverse estimate (A.17), and the trace inequality (A.18), we can show that

$$B_{\mathrm{b}}(\eta_d, e^h) \leqslant C|||\eta_d|||_{\mathrm{b}}|||e^h|||_{\mathrm{b}}, \tag{187}$$

$$B_{\mathrm{b}}(\eta_d, \eta) \leqslant C|||\eta_d|||_{\mathrm{b}}|||\eta|||_{\mathrm{b}}, \tag{188}$$

where $e^h = \tilde{\phi}^h - \phi^h$ and C is a constant independent of ϕ, ϕ_d, and h_e.

We can now state the following

Theorem 4.3. *For a homogeneous Dirichlet problem, the error of the C/DG method* (146) *converges optimally in the L^2-norm $\forall k \geqslant 3$, namely*

$$\|e\| \leqslant Ch^{k+1}|\phi|_{H^{k+1}(\Omega)}, \tag{189}$$

where $h = \max_e h_e$ and where we have extended definition (76) *to the case of seminorms.*

Proof. Consider the homogeneous Dirichlet problem (i.e., the dual problem):

$$EI\phi_{d_{,xxxx}} = f_d \quad \text{in } \Omega, \tag{190}$$

$$\phi_d = 0 \quad \text{on } \Gamma, \tag{191}$$

$$\phi_{d_x} \cdot n = 0 \quad \text{on } \Gamma. \tag{192}$$

From Theorem 4.2 we have $\forall s \geqslant 4$ the regularity estimate

$$\|\phi_d\|_{H^s(\Omega)} \leqslant \alpha_s \|f_d\|_{H^{s-4}(\Omega)}. \tag{193}$$

Note from the decomposition of the error (80) that $\tilde{\phi}^h \in \mathscr{S}^h$. We can write for the interpolation error, see (176) and (177),

$$|||\eta_d|||_{\mathrm{b}} = |||\phi_d - \tilde{\phi}^h_d|||_{\mathrm{b}} \leqslant Ch^{s-2}\|\phi_d\|_{H^s(\Omega)}. \tag{194}$$

As $e \in \mathscr{V} = H^1_0(\Omega) = \{w | w \in H^1(\Omega),\ w = 0 \text{ on } \Gamma\}$, we can write $B_{\mathrm{b}}(e, \phi_d) = (e, f_d)$, and therefore

$$\begin{aligned}
(e, f_d) &= B_{\mathrm{b}}(e, \phi_d), \\
&= B_{\mathrm{b}}(\phi_d, e), \\
&= B_{\mathrm{b}}(\phi_d - \tilde{\phi}^h_d, e), \\
&= B_{\mathrm{b}}(\eta_d, e^h + \eta), \\
&= B_{\mathrm{b}}(\eta_d, e^h) + B_{\mathrm{b}}(\eta_d, \eta), \\
&\leqslant C|||\eta_d|||_{\mathrm{b}}(|||e^h|||_{\mathrm{b}} + |||\eta|||_{\mathrm{b}}), \\
&\leqslant Ch^{s-2}\|\phi_d\|_{H^s(\Omega)}(|||e^h|||_{\mathrm{b}} + |||\eta|||_{\mathrm{b}}), \\
&\leqslant Ch^{s-2}\|f_d\|_{H^{s-4}(\Omega)}(|||e^h|||_{\mathrm{b}} + |||\eta|||_{\mathrm{b}}),
\end{aligned} \tag{195}$$

where we have used the symmetry of the bilinear form and the Galerkin orthogonality condition (157). Let $f_d = e$ and $s = 4$. Then (195) becomes

$$\|e\| \leqslant Ch^2(|||e^h|||_{\mathrm{b}} + |||\eta|||_{\mathrm{b}}) \leqslant Ch^{k+1}|\phi|_{H^{k+1}(\Omega)}. \quad \square \tag{196}$$

Remark 4.2. Another way to prove an L^2-estimate is to adopt the approach used by Baker [27] in which an alternative energy norm is introduced which includes derivative terms on element interfaces. In our case this would amount to the second derivative. Stability can still be established in terms of this norm by using the trace inequality and inverse estimates. However, one can easily establish continuity on the space $\mathscr{V}$ rather than $\mathscr{V}^h$ (cf. Proposition 4.3) which obviates the need for the inverse estimate for interpolation errors (cf. Remark 4.1). We refer to Baker [27] for details.

4.2. Poisson–Kirchhoff plate theory

The Poisson–Kirchhoff plate theory is a two-dimensional generalization of the Bernoulli–Euler beam theory. In this section, we perform an error analysis for the thin plate and will see that the convergence results are the same as for the one-dimensional thin beam case.

4.2.1. Model problem

Let $\Omega \subset \mathbb{R}^2$ be an open, bounded domain and let Γ be its boundary, assumed smooth for the time being. Let Γ_g, Γ_h, Γ_M and Γ_Q denote again the displacement, slope, moment and shear force boundaries, respectively. We let $\Gamma = \overline{\Gamma_g \cup \Gamma_Q} = \overline{\Gamma_h \cup \Gamma_M}$, $\Gamma_g \cap \Gamma_Q = \emptyset$, and $\Gamma_h \cap \Gamma_M = \emptyset$. For simplicity we assume $\Gamma_g = \Gamma_h$ and $\Gamma_Q = \Gamma_M$. Let s be the unit tangent vector to Γ such that $\boldsymbol{n} \times \boldsymbol{s} = \boldsymbol{e}_3$, the unit basis vector in the positive out-of-plane direction. The strong form of the Poisson–Kirchhoff plate bending problem can be written in indicial notation as

$$(C_{\alpha\beta\gamma\delta}\phi_{,\gamma\delta})_{,\beta\alpha} = f \quad \text{in } \Omega, \tag{197}$$

$$\phi = g \quad \text{on } \Gamma_g, \tag{198}$$

$$\phi_{,\alpha} n_\alpha = h_\alpha n_\alpha = h_n \quad \text{on } \Gamma_h, \tag{199}$$

$$C_{\alpha\beta\gamma\delta}\phi_{,\gamma\delta} n_\beta n_\alpha = M_\alpha n_\alpha = M_n \quad \text{on } \Gamma_M, \tag{200}$$

$$-(C_{\alpha\beta\gamma\delta}\phi_{,\gamma\delta} n_\beta s_\alpha)_{,s} - (C_{\alpha\beta\gamma\delta}\phi_{,\gamma\delta})_{,\beta} n_\alpha = Q \quad \text{on } \Gamma_Q, \tag{201}$$

where $1 \leqslant \alpha, \beta, \gamma, \delta \leqslant 2$. Eq. (197) is the equilibrium of moment for the plate, ϕ is the displacement perpendicular to the plate, $C_{\alpha\beta\gamma\delta}$ are the elastic coefficients and f is a given distributed load. The prescribed boundary displacement, slope, moment and shear force are denoted by g, h_n, M_n and Q, respectively. The components of the outward normals to element boundaries are denoted by n_α. One can express the normal derivative as $\phi_{,n} = \phi_{,\alpha} n_\alpha$ and the tangential derivative as $\phi_{,s} = \phi_{,\alpha} s_\alpha$. Note that in the Poisson–Kirchhoff theory, there are two boundary conditions at each point: either transverse displacement (198) or shear, Q (201), and either normal slope (199) or normal moment (200). This may be contrasted with the Reissner–Mindlin thick plate theory in which the tangential slope, $h_s = h_\alpha s_\alpha$, or the twisting moment, $M_s = M_\alpha s_\alpha$, need be additionally specified. Consequently, in the present case, $\boldsymbol{h} = h_n \boldsymbol{n}$ and $\boldsymbol{M} = M_n \boldsymbol{n}$. The reader is directed to Hughes [10] for elaboration and sign conventions on the components. Let us assume in the following that the elastic coefficients $C_{\alpha\beta\gamma\delta}$ are constant. For plane stress, they are

$$C_{\alpha\beta\gamma\delta} = \frac{t^3}{12}[\mu(\delta_{\alpha\gamma}\delta_{\beta\delta} + \delta_{\alpha\delta}\delta_{\beta\gamma}) + \bar{\lambda}\delta_{\alpha\beta}\delta_{\gamma\delta}], \tag{202}$$

where t is the thickness of the plate, $\delta_{\alpha\beta}$ is the Kronecker delta and

$$\mu = \frac{E}{2(1+\nu)}, \tag{203}$$

$$\bar{\lambda} = \frac{\nu E}{1-\nu^2}. \tag{204}$$

In the above, E is the elastic modulus and ν is Poisson's ratio.

At this point we introduce a direct notation for problem (197)–(201), which will stress the similarities between the C/DG methods for the thin plate and the thin beam. The components of the fourth-order tensor $\boldsymbol{C}$ and of the moment and slope vectors $\boldsymbol{M}$ and $\boldsymbol{h}$ are defined as

$$[\boldsymbol{C}]_{\alpha\beta\gamma\delta} = C_{\alpha\beta\gamma\delta}, \tag{205}$$

$$[\boldsymbol{M}]_\alpha = M_\alpha, \tag{206}$$

$$[\boldsymbol{h}]_\alpha = h_\alpha. \tag{207}$$

Similarly, the components of the first- and second-order differential operators $\boldsymbol{D}$ and $\boldsymbol{D}^2$ are defined as

$$[\boldsymbol{D}\phi]_\alpha = \phi_{,\alpha}, \tag{208}$$

$$[\boldsymbol{D}^2\phi]_{\alpha\beta} = \phi_{,\alpha\beta}. \tag{209}$$

We can now rewrite (197)–(201) in direct notation as

$$\boldsymbol{D}^2 : (\boldsymbol{C} : \boldsymbol{D}^2\phi) = f \quad \text{in } \Omega, \tag{210}$$

$$\phi = g \quad \text{on } \Gamma_g, \tag{211}$$

$$\boldsymbol{D}\phi \cdot \boldsymbol{n} = h_n \quad \text{on } \Gamma_h, \tag{212}$$

$$((\boldsymbol{C} : \boldsymbol{D}^2\phi) \cdot \boldsymbol{n}) \cdot \boldsymbol{n} = M_n \quad \text{on } \Gamma_M, \tag{213}$$

$$-(\boldsymbol{D}[((\boldsymbol{C} : \boldsymbol{D}^2\phi) \cdot \boldsymbol{n}) \cdot \boldsymbol{s}]) \cdot \boldsymbol{s} - [\boldsymbol{D} \cdot (\boldsymbol{C} : \boldsymbol{D}^2\phi)] \cdot \boldsymbol{n} = Q \quad \text{on } \Gamma_Q. \tag{214}$$

4.2.2. Method

Considering the partition (24) of the domain into finite elements, let us choose functions which are continuous on Ω, but discontinuous in first- and higher-order derivatives across interior boundaries by adopting the spaces (144) and (145) for our approximations. We propose the following C/DG method for the solution of the Poisson–Kirchhoff plate problem (210)–(214): Find $\phi^h \in \mathscr{S}^h$ such that

$$B_{\mathrm{p}}(w^h, \phi^h) = L_{\mathrm{p}}(w^h) \quad \forall w^h \in \mathscr{V}^h, \tag{215}$$

where

$$\begin{aligned} B_{\mathrm{p}}(w^h, \phi^h) = {} & (\boldsymbol{D}^2 w^h, \boldsymbol{C} : \boldsymbol{D}^2\phi^h)_{\tilde{\Omega}} - (\llbracket \boldsymbol{D}w^h \rrbracket, \langle (\boldsymbol{C} : \boldsymbol{D}^2\phi^h) \cdot \boldsymbol{n} \rangle)_{\tilde{\Gamma}} - (\langle (\boldsymbol{C} : \boldsymbol{D}^2 w^h) \cdot \boldsymbol{n} \rangle, \llbracket \boldsymbol{D}\phi^h \rrbracket)_{\tilde{\Gamma}} \\ & + (\tau \llbracket \boldsymbol{D}w^h \rrbracket, \llbracket \boldsymbol{D}\phi^h \rrbracket)_{\tilde{\Gamma}} - (w^h_{,n}\boldsymbol{n}, (\boldsymbol{C} : \boldsymbol{D}^2\phi^h) \cdot \boldsymbol{n})_{\Gamma_h} - ((\boldsymbol{C} : \boldsymbol{D}^2 w^h) \cdot \boldsymbol{n}, \phi^h_{,n}\boldsymbol{n})_{\Gamma_h} \\ & + (\tau_h w^h_{,n}\boldsymbol{n}, \phi^h_{,n}\boldsymbol{n})_{\Gamma_h} \end{aligned} \tag{216}$$

and

$$L_{\mathrm{p}}(w^h) = (w^h, f)_{\tilde{\Omega}} + (w^h, Q)_{\Gamma_Q} + (w^h_{,n}\boldsymbol{n}, M_n\boldsymbol{n})_{\Gamma_M} - ((\boldsymbol{C} : \boldsymbol{D}^2 w^h) \cdot \boldsymbol{n}, h_n\boldsymbol{n})_{\Gamma_h} + (\tau_h w^h_{,n}\boldsymbol{n}, h_n\boldsymbol{n})_{\Gamma_h}, \tag{217}$$

where, by continuity of the finite element functions,

$$\llbracket \boldsymbol{D}w^h \rrbracket = \llbracket w^h_{,n} \rrbracket \boldsymbol{n} \quad \text{on } \tilde{\Gamma}, \tag{218}$$

$$\llbracket \boldsymbol{D}\phi^h \rrbracket = \llbracket \phi^h_{,n} \rrbracket \boldsymbol{n} \quad \text{on } \tilde{\Gamma}, \tag{219}$$

We also note that since $\Gamma_g = \Gamma_h$,

$$\boldsymbol{D}w^h = w^h_{,n}\boldsymbol{n} \quad \text{on } \Gamma_h. \tag{220}$$

The inner product on $\tilde{\Omega}$ in (216) is defined as

$$(\boldsymbol{D}^2 w^h, \boldsymbol{C} : \boldsymbol{D}^2\phi^h)_{\tilde{\Omega}} = \int_{\tilde{\Omega}} (\boldsymbol{D}^2 w^h) : (\boldsymbol{C} : \boldsymbol{D}^2\phi^h)\,\mathrm{d}\Omega. \tag{221}$$

Note that, as for the Bernoulli–Euler beam, the relationships (142) and (143) hold. The normals n in (216) and (217) are the element outward normals on exterior boundaries, whereas on interior boundaries $\tilde{\Gamma}$ we consider the normal pointing from the element with lower element number e to the element with higher element number, although this choice is arbitrary. For dimensional consistency, the stabilization parameters are of the order

$$\tau = \mathcal{O}(|\boldsymbol{C}|/h_e), \tag{222}$$

$$\tau_h = \mathcal{O}(|\boldsymbol{C}|/h_e), \tag{223}$$

where the norm for the fourth-order tensor can be defined as

$$|\boldsymbol{C}| = \sup_{\substack{\boldsymbol{A}\in\mathbb{R}^d\times\mathbb{R}^d \\ \boldsymbol{A}\neq\boldsymbol{0}}} \frac{|\boldsymbol{C}:\boldsymbol{A}|}{|\boldsymbol{A}|}. \tag{224}$$

4.2.3. Error analysis

The error analysis for the Poisson–Kirchhoff plate theory follows along the lines of the developments in Section 4.1.3. We first prove consistency and stability, which in turn imply convergence of the C/DG method.

Consistency. We integrate (215) by parts and obtain

$$\begin{aligned}
0 &= B_{\mathrm{p}}(w^h,\phi^h) - L_{\mathrm{p}}(w^h),\\
&= (w^h,[\boldsymbol{D}^2:(\boldsymbol{C}:\boldsymbol{D}^2\phi^h) - f])_{\tilde{\Omega}}\\
&\quad - (\langle w^h\rangle,[\![(\boldsymbol{D}\cdot(\boldsymbol{C}:\boldsymbol{D}^2\phi^h)]\cdot\boldsymbol{n}]\!])_{\tilde{\Gamma}} + (\langle\boldsymbol{D}w^h\rangle,[\![(\boldsymbol{C}:\boldsymbol{D}^2\phi^h)\cdot\boldsymbol{n}]\!])_{\tilde{\Gamma}}\\
&\quad - (\langle(\boldsymbol{C}:\boldsymbol{D}^2w^h)\cdot\boldsymbol{n}\rangle + \tau[\![\boldsymbol{D}w^h]\!],[\![\boldsymbol{D}\phi^h]\!])_{\tilde{\Gamma}}\\
&\quad - (w^h,\{(\boldsymbol{D}[((\boldsymbol{C}:\boldsymbol{D}^2\phi^h)\cdot\boldsymbol{n})\cdot\boldsymbol{s}])\cdot\boldsymbol{s} + [\boldsymbol{D}\cdot(\boldsymbol{C}:\boldsymbol{D}^2\phi^h)]\cdot\boldsymbol{n} + Q\})_{\Gamma_Q}\\
&\quad + (w^h_{,n}\boldsymbol{n},[(\boldsymbol{C}:\boldsymbol{D}^2\phi^h)\cdot\boldsymbol{n} - M_n\boldsymbol{n}])_{\Gamma_M} - ((\boldsymbol{C}:\boldsymbol{D}^2w^h)\cdot\boldsymbol{n} + \tau_h\boldsymbol{D}w^h,\phi^h_{,n} - h_n)_{\Gamma_h}.
\end{aligned} \tag{225}$$

We can substitute the exact solution ϕ for ϕ^h in (215), which leads to the Galerkin orthogonality condition for the thin plate case, viz.

$$B_{\mathrm{p}}(w^h,e) = 0 \quad \forall w^h \in \mathscr{V}^h(\Omega). \tag{226}$$

Stability. Let us define

$$|||w^h|||_{\mathrm{p}}^2 = \|\boldsymbol{C}^{1/2}:\boldsymbol{D}^2w^h\|_{\tilde{\Omega}}^2 + \|\tau^{1/2}[\![\boldsymbol{D}w^h]\!]\|_{\tilde{\Gamma}}^2 + \|\tau_h^{1/2}\boldsymbol{D}w^h\|_{\Gamma_h}^2. \tag{227}$$

Proposition 4.4. $|||\cdot|||_{\mathrm{p}}$ *is a norm on* $\mathscr{V}^h$.

Proof. For the same reasons as in the previous proof of Proposition 4.1, there are no non-trivial functions for which (227) could vanish. □

Proposition 4.5. *The C/DG method* (215) *is stable in the energy norm* (227), *that is, there exists a positive constant m such that*

$$B_{\mathrm{p}} = (w^h,w^h) \geqslant m|||w^h|||_{\mathrm{p}}^2 \quad \forall w^h \in \mathscr{V}^h(\Omega). \tag{228}$$

Proof. From the definition (216) we have

$$B_{\mathrm{p}}(w^h,w^h) \geqslant \|\boldsymbol{C}^{1/2}:\boldsymbol{D}^2w^h\|^2_{\bar{\Omega}} + \|\tau^{1/2}[\![\boldsymbol{D}w^h]\!]\|^2_{\bar{\Gamma}} + \|\tau_h^{1/2}\boldsymbol{D}w^h\|^2_{\Gamma_h} - 2(|([\![\boldsymbol{D}w^h]\!],\langle(\boldsymbol{C}:\boldsymbol{D}^2w^h)\cdot\boldsymbol{n}\rangle)_{\bar{\Gamma}}| + |(\boldsymbol{D}w^h,(\boldsymbol{C}:\boldsymbol{D}^2w^h)\cdot\boldsymbol{n})_{\Gamma_h}|). \tag{229}$$

Following the same steps as in Section 4.1.3, i.e., invoking the ε-inequality (83), inequality (98), trace inequality (A.18) and inverse estimate (A.17), we conclude

$$B_{\mathrm{p}}(w^h,w^h) \geqslant \sum_{e=1}^{N_{\mathrm{el}}}\left(1-\frac{\varepsilon C|\boldsymbol{C}|}{h_e}\right)\|\boldsymbol{C}^{1/2}:\boldsymbol{D}^2w^h\|^2_{\Omega_e} + \left(1-\frac{1}{\varepsilon\tau}\right)\|\tau^{1/2}[\![\boldsymbol{D}w^h]\!]\|^2_{\bar{\Gamma}} + \left(1-\frac{1}{\varepsilon\tau_h}\right)\|\tau_h^{1/2}\boldsymbol{D}w^h\|^2_{\bar{\Gamma}} \geqslant m|||w^h|||^2_{\mathrm{p}}. \tag{230}$$

In particular, assuming that $\tau=\tau_h$, we can prove (228) for $m=1/2$ if we choose $\varepsilon|_{\Omega_e}=h_e/(2C|\boldsymbol{C}|)$, in which case we obtain $\tau=\tau_h=4C|\boldsymbol{C}|/h_e$. □

4.2.4. Convergence in energy norm

Theorem 4.4. *Assume that the consistency condition* (226) *and stability condition* (228) *of the method hold. Given that the conditions are satisfied for the interpolation estimates* (A.12), (A.13) *and the trace inequality* (A.18) *holds, the error estimate for the C/DG method* (215) *can be written as*

$$|||e|||^2_{\mathrm{p}} \leqslant C\sum_{e=1}^{N_{\mathrm{el}}} h_e^{2(k-1)}|\phi|^2_{H^{k+1}(\Omega_e)}, \tag{231}$$

where C is a constant.

Proof. We can write, by the same arguments as in Section 4.1.3, invoking the Galerkin orthogonality condition (226),

$$\begin{aligned} m|||e^h|||^2_{\mathrm{p}} &\leqslant B_{\mathrm{p}}(e^h,e^h),\\ &= B_{\mathrm{p}}(e^h,e-\eta),\\ &\leqslant -B_{\mathrm{p}}(e^h,\eta),\\ &\leqslant |B_{\mathrm{p}}(e^h,\eta)|,\\ &\leqslant |(\boldsymbol{C}^{1/2}:\boldsymbol{D}^2e^h,\boldsymbol{C}^{1/2}:\boldsymbol{D}^2\eta)_{\bar{\Omega}}| + |([\![\boldsymbol{D}e^h]\!],\langle(\boldsymbol{C}:\boldsymbol{D}^2\eta)\cdot\boldsymbol{n}\rangle)_{\bar{\Gamma}}|\\ &\quad + |(\langle(\boldsymbol{C}:\boldsymbol{D}^2e^h)\cdot\boldsymbol{n}\rangle,[\![\boldsymbol{D}_\eta]\!])_{\bar{\Gamma}}| + |\tau[\![\boldsymbol{D}e^h]\!],[\![\boldsymbol{D}\eta]\!])_{\bar{\Gamma}}|\\ &\quad + |(\boldsymbol{D}e^h,(\boldsymbol{C}:\boldsymbol{D}^2\eta)\cdot\boldsymbol{n})_{\Gamma_h}| + |((\boldsymbol{C}:\boldsymbol{D}^2e^h)\cdot\boldsymbol{n},\boldsymbol{D}\eta)_{\Gamma_h}| + |(\tau_h\boldsymbol{D}e^h,\boldsymbol{D}\eta)_{\Gamma_h}|. \end{aligned} \tag{232}$$

Note also that since $\Gamma_g=\Gamma_h$,

$$\eta=\phi-\tilde{\phi}^h=g-g=0 \quad \text{on } \Gamma_h, \tag{233}$$

and thus

$$\eta_{,s}=0, \quad \boldsymbol{D}\eta=\eta_{,n}\boldsymbol{n} \quad \text{on } \Gamma_h. \tag{234}$$

Making use of inequalities (83), (98), (A.13), (A.17) and (A.18), we have

$$\frac{m}{2}|||e^h|||^2_{\mathrm{p}} \leqslant \frac{|\boldsymbol{C}|}{m}\|\boldsymbol{D}^2\eta\|^2_{\bar{\Omega}} + \left\{\frac{|\boldsymbol{C}|^2}{m}\|\tau^{-1/2}\langle(\boldsymbol{D}^2\eta)\cdot\boldsymbol{n}\rangle\|^2_{\bar{\Gamma}} + \frac{|\boldsymbol{C}|^2}{m}\|\tau_h^{-1/2}(\boldsymbol{D}^2\eta)\cdot\boldsymbol{n}\|^2_{\Gamma_h}\right\} + \left\{\frac{C|\boldsymbol{C}|}{m}\|h_e^{-1/2}[\![\boldsymbol{D}\eta]\!]\|^2_{\bar{\Gamma}} + \frac{C|\boldsymbol{C}|}{m}\|h_e^{-1/2}\boldsymbol{D}\eta\|^2_{\Gamma_h}\right\} + \left\{\frac{1}{m}\|\tau^{1/2}[\![\boldsymbol{D}\eta]\!]\|^2_{\bar{\Gamma}} + \frac{1}{m}\|\tau_h^{1/2}\boldsymbol{D}\eta\|^2_{\Gamma_h}\right\}. \tag{235}$$

We obtain for the terms on the right-hand side of (235) with (98), (108) and (A.18)

$$\frac{|C|^2}{m}\|\tau^{-1/2}\langle(D^2\eta)n\rangle\|_{\bar{\Gamma}}^2+\frac{|C|^2}{m}\|\tau_h^{-1/2}(D^2\eta)n\|_{\Gamma_h}^2\leqslant C\sum_{e=1}^{N_{\mathrm{el}}}h_e(h_e^{-1}\|D^2\eta\|_{\Omega_e}^2+h_e\|D^3\eta\|_{\Omega_e}^2), \tag{236}$$

$$\frac{|C|}{m}\|h_e^{-1/2}[\![D\eta]\!]\|_{\bar{\Gamma}}^2+\frac{|C|}{m}\|h_e^{-1/2}D\eta\|_{\Gamma_h}^2\leqslant C\sum_{e=1}^{N_{\mathrm{el}}}h_e^{-1}(h_e^{-1}\|D\eta\|_{\Omega_e}^2+h_e\|D^2\eta\|_{\Omega_e}^2), \tag{237}$$

$$\frac{1}{m}\|\tau^{1/2}[\![D\eta]\!]\|_{\bar{\Gamma}}^2+\frac{1}{m}\|\tau_h^{1/2}D\eta\|_{\Gamma_h}^2\leqslant C\sum_{e=1}^{N_{\mathrm{el}}}h_e^{-1}(h_e^{-1}\|D\eta\|_{\Omega_e}^2+h_e\|D^2\eta\|_{\Omega_e}^2). \tag{238}$$

Therefore, we can estimate (235) as

$$\begin{aligned}\frac{m}{2}|||e^h|||_{\mathrm{p}}^2\leqslant C\sum_{e=1}^{N_{\mathrm{el}}}\{&\|D^2\eta\|_{\Omega_e}^2+h_e(h_e^{-1}\|D^2\eta\|_{\Omega_e}^2+h_e\|D^3\eta\|_{\Omega_e}^2)+h_e^{-1}(h_e^{-1}\|D\eta\|_{\Omega_e}^2+h_e\|D^2\eta\|_{\Omega_e}^2)\\&+h_e^{-1}(h_e^{-1}\|D\eta\|_{\Omega_e}^2+h_e\|D^2\eta\|_{\Omega_e}^2)\}.\end{aligned} \tag{239}$$

From Appendix A, inequalities (A.12) and (A.13), we can deduce the interpolation estimates

$$\|D^2\eta\|_{\Omega_e}^2\leqslant\|\eta\|_{H^2(\Omega_e)}^2\leqslant Ch_e^{2k-2}|\phi|_{H^{k+1}(\Omega_e)}^2, \tag{240}$$

$$\|D^2\eta\|_{\Omega_e}\leqslant\|\eta\|_{H^2(\Omega_e)}\leqslant Ch_e^{k-1}|\phi|_{H^{k+1}(\Omega_e)}, \tag{241}$$

$$\|D^2\eta\|_{H^1(\Omega_e)}\leqslant\|\eta\|_{H^3(\Omega_e)}\leqslant Ch_e^{k-2}|\phi|_{H^{k+1}(\Omega_e)}, \tag{242}$$

$$\|D\eta\|_{\Omega_e}\leqslant\|\eta\|_{H^1(\Omega_e)}\leqslant Ch_e^{k}|\phi|_{H^{k+1}(\Omega_e)}, \tag{243}$$

$$\|D\eta\|_{H^1(\Omega_e)}\leqslant\|\eta\|_{H^2(\Omega_e)}\leqslant Ch_e^{k-1}|\phi|_{H^{k+1}(\Omega_e)} \tag{244}$$

and write

$$|||e^h|||_{\mathrm{p}}^2\leqslant C\sum_{e=1}^{N_{\mathrm{el}}}h_e^{2(k-1)}|\phi|_{H^{k+1}(\Omega_e)}^2. \tag{245}$$

Using similar arguments to bound $|||\eta|||_{\mathrm{p}}^2$ and the triangle inequality, we conclude

$$|||e|||_{\mathrm{p}}^2\leqslant C\sum_{e=1}^{N_{\mathrm{el}}}h_e^{2(k-1)}|\phi|_{H^{k+1}(\Omega_e)}^2. \quad \square \tag{246}$$

4.2.5. Convergence in L^2-norm

The proof of convergence of the C/DG method (215) in the L^2-norm for the homogeneous Dirichlet problem is analogous to the proof for the thin beam case in Section 4.1.3. For this reason we restrict our attention to the main points and refer to the previous developments for further details. We quote again from Theorem 2.1 in Baker [27] for the purpose of this proof for the thin plate.

Theorem 4.5. *The mapping* $P:C^\infty(\Omega)\to C^\infty(\Omega)\times C^\infty(\partial\Omega)\times C^\infty(\partial\Omega)$ *defined by* $P\phi=(D^2:D^2\phi,\phi,D\phi\cdot n)$ *and completed by continuity is a homeomorphism of* $H^s(\Omega)$ *onto* $H^{s-4}(\Omega)\times H^{s-1/2}(\partial\Omega)\times H^{s-3/2}(\partial\Omega)$ *for all* $s\geqslant 4$, *and there exist constants* α_s and β_s *such that*

$$\|\phi\|_{H^s(\Omega)}\leqslant\alpha_s\{\|D^2:D^2\phi\|_{H^{s-4}(\Omega)}+\|\phi\|_{H^{s-1/2}(\partial\Omega)}+\|D\phi\cdot n\|_{H^{s-3/2}(\partial\Omega)}\}\leqslant\beta_s\|\phi\|_{H^s(\Omega)}. \tag{247}$$

For the bilinear form (216), we have the following

Proposition 4.6. *There exists a constant* $0 < C < \infty$ *such that*

$$B_{\mathrm{p}}(w^h, v^h) \leqslant C|||w^h|||_{\mathrm{p}}|||v^h|||_{\mathrm{p}} \quad \forall w^h, v^h \in \mathscr{V}^h, \tag{248}$$

where C *is independent of* h_e.

Proof. The proof follows by the same arguments used to prove Proposition 4.3. □

Remark 4.3. As in Remark 4.1, one can employ inverse estimates for the interpolation errors [87] and establish the following generalization of Proposition 4.6:

$$B_{\mathrm{p}}(\eta_d, e^h) \leqslant C|||\eta_d|||_{\mathrm{p}}|||e^h|||_{\mathrm{p}}, \tag{249}$$

$$B_{\mathrm{p}}(\eta_d, \eta) \leqslant C|||\eta_d|||_{\mathrm{p}}|||\eta|||_{\mathrm{p}}, \tag{250}$$

where η_d is the interpolation error of the dual problem.

Theorem 4.6. *For a homogeneous Dirichlet problem, the error of the C/DG method* (215) *converges optimally in the* L^2*-norm* $\forall k \geqslant 3$, *namely*

$$\|e\| \leqslant Ch^{k+1}|\phi|_{H^{k+1}(\Omega)}. \tag{251}$$

Proof. Consider the homogeneous Dirichlet problem (i.e., the dual problem)

$$\boldsymbol{D}^2 : \boldsymbol{D}^2\phi_d = f_d \quad \text{in } \Omega, \tag{252}$$

$$\phi_d = 0 \quad \text{on } \Gamma, \tag{253}$$

$$\boldsymbol{D}\phi_d \cdot \boldsymbol{n} = 0 \quad \text{on } \Gamma. \tag{254}$$

From Theorem 4.5 we have $\forall s \geqslant 4$ the regularity estimate

$$\|\phi_d\|_{H^s(\Omega)} \leqslant \alpha_s \|f_d\|_{H^{s-4}(\Omega)}, \tag{255}$$

and from (245) and (246) and the decomposition of the error (80) we can obtain

$$|||\eta_d|||_{\mathrm{p}} = |||\phi_d - \tilde{\phi}_d^h|||_{\mathrm{p}} \leqslant Ch^{s-2}\|\phi_d\|_{H^s(\Omega)}. \tag{256}$$

As $e \in \mathscr{V} = H_0^1(\Omega)$, we can write $B_{\mathrm{p}}(e, \phi_d) = (e, f_d)$, and therefore

$$\begin{aligned}
(e, f) &= B_{\mathrm{p}}(e, \phi_d), \\
&= B_{\mathrm{p}}(\phi_d, e), \\
&= B_{\mathrm{p}}(\phi_d - \tilde{\phi}_d^h, e), \\
&= B_{\mathrm{p}}(\eta_d, e^h + \eta), \\
&= B_{\mathrm{p}}(\eta_d, e^h) + B_{\mathrm{p}}(\eta_d, \eta), \qquad (257) \\
&\leqslant C|||\eta_d|||_{\mathrm{p}}(|||e^h|||_{\mathrm{p}} + |||\eta|||_{\mathrm{p}}), \\
&\leqslant Ch^{s-2}\|\phi_d\|_{H^s(\Omega)}(|||e^h|||_{\mathrm{p}} + |||\eta|||_{\mathrm{p}}), \\
&\leqslant Ch^{s-2}\|f_d\|_{H^{s-4}(\Omega)}(|||e^h|||_{\mathrm{p}} + |||\eta|||_{\mathrm{p}}), \qquad (258)
\end{aligned}$$

where we have used the symmetry of the bilinear form and the Galerkin orthogonality condition (226). With $f_d = e$ and $s = 4$ we can conclude from (258) and (245)

$$\|e\| \leqslant Ch^2(|||e^h|||_{\mathrm{p}} + |||\eta|||_{\mathrm{p}}) \leqslant Ch^{k+1}|\phi|_{H^{k+1}(\Omega)}. \quad \square \tag{259}$$

5. C/DG methods for strain gradient theory

5.1. Background

The most widely used theories of continuum solid mechanics involve non-polar materials that are also simple in the sense of Noll [89]. Material point rotations are neglected and the Cauchy stress is assumed to be a functional of the deformation only through its first gradient. However, an interest in polar materials has existed at least since the pioneering work of the Cosserats [90,91]. The rotational degrees of freedom introduce couple stresses and body couples. Rich theories of such continua were worked out in the 1960s [3,4,92]. The terms "micropolar" and "micromorphic" continua were coined to refer to solids in which the directors attached to material points are respectively rigid and deformable [93]. Such theories have applications in electrically polarized media, granular materials and in biological tissues, among other areas. Since they introduce a length scale "Cosserat continua" have been proposed as regularized descriptions of softening materials [94], which otherwise demonstrate deformations localized onto bands of vanishing width.

Turning attention to higher-order gradients of deformation, the earliest references appear to belong to Cauchy [95]. Such continua were termed "materials of grade n" by Truesdell and Noll [89], referring to the order of the highest derivative of the deformation. Linear and nonlinear elasticity were considered in light of the role played by the second gradient of displacement; i.e., the strain gradient, by Truesdell and Toupin [92], and later by Toupin [3]. The balance laws included a higher-order stress—couple stress in this case—and hence required higher-order boundary conditions on the couple stress traction and strain. Assuming a stored energy function, the couple stress was related via formal procedures to the strain gradient. Shortly after, Mindlin [4] proposed a linear theory that encompassed the theories of the Cosserats and of Toupin as special cases. The formalism of Toupin and Mindlin was recently extended to the deformation and flow theories of plasticity [12], motivated by experimental observations of the apparent length scale dependence of plasticity in metals when deformations vary at scales of the order of a micron [96–98]. Variants of this strain gradient plasticity theory have also appeared [99,100]. These theories have been widely applied to studying length scale-dependent deformation phenomena in metals. Polar and higher-order continuum theories have been applied to layered materials, composites and granular media in addition to polycrystalline metals.

Solution of the initial and boundary value problems posed in terms of the higher-order theories is not straightforward: the governing differential equation and boundary conditions are complicated [3] and analytic solutions are restricted to the simplest cases. Computational difficulties also arise. While boundary conditions are easier to treat in the variational setting, requirements of regularity dictate that, with the CG method, the displacement must be a C^1 function over the domain. The degrees of freedom include nodal displacements and displacement gradients. The situation is partially analogous to classical Bernoulli–Euler beam and Poisson–Kirchhoff plate theories in one and two spatial dimensions respectively.

The higher-order stress and strain gradient correspond to moment and curvature in the beam and plate theories. Finite element formulations incorporating C^1 displacement fields are therefore a natural first choice for strain gradient theories. As is easily appreciated, however, the computational cost is high; the large number of degrees of freedom soon place such formulations beyond the realm of practicality. Finite element formulations for the Fleck–Hutchinson strain gradient plasticity theory have been developed with

plate elements as a basis but were generally found to perform poorly [101]. Mixed and hybrid formulations have also been developed in the same work and elsewhere [19], and applied to strain gradient plasticity or elasticity problems. While some of the developed elements have been subjected to the Patch test and other benchmark problems, a rigorous numerical analysis is missing. Mathematical proofs of consistency and stability have not been demonstrated, and the rate of convergence has not been established.

Meshless methods confer an arbitrary degree of smoothness on solutions and have been applied to strain gradient theories [102,103]. While an analysis of a class of meshless methods has appeared recently [104,105], the connection to higher-order elliptic problems has not been made.

In this section a class of C/DG Methods is presented for higher-order gradient theories that trace their roots to the work of Toupin [3]. The application of C/DG methods to higher-order continuum theories demonstrates the growing relevance of these numerical methods. The section begins with the strong form of the problem. A weak form is then presented that leads to the C/DG method, and its equivalence with the strong form of the higher-order continuum theory is demonstrated. A numerical analysis of the method is then presented covering the usual ground of consistency, stability and hence, rate of convergence. Optimal error estimates are derived in the energy and L^2 norms. A shear layer example is considered and numerical solutions using the C/DG method are compared with the exact solution.

5.2. One-dimensional Toupin–Mindlin strain gradient theory

Toupin and Mindlin included higher-order stresses and strains in their theory of linear elasticity, which serves today as the foundation of more advanced strain gradient plasticity formulations [3,4,12]. Let us introduce a one-dimensional model problem following their concepts.

5.2.1. Model problem

Let $\Omega \subset \mathbb{R}$ be an open, bounded domain and Γ its boundary. Let Γ_g, Γ_q, Γ_t and Γ_r denote the displacement, displacement gradient, couple stress and traction boundaries, respectively.

The strong form of the problem can be written as

$$\sigma_{,x} - \bar{\sigma}_{,xx} + f = 0 \quad \text{in } \Omega, \tag{260}$$

$$\phi = g \quad \text{on } \Gamma_g, \tag{261}$$

$$\phi_{,x} \cdot n = q \quad \text{on } \Gamma_q, \tag{262}$$

$$\bar{\sigma} = r \quad \text{on } \Gamma_r, \tag{263}$$

$$(\sigma - \bar{\sigma}_{,x}) \cdot n = t \quad \text{on } \Gamma_t. \tag{264}$$

We have $\overline{\Gamma_g \cup \Gamma_t} = \Gamma$, $\Gamma_g \cap \Gamma_t = \emptyset$, $\overline{\Gamma_q \cup \Gamma_r} = \Gamma$, $\Gamma_q \cap \Gamma_r = \emptyset$, and f, g, q, r and t are given data. The constitutive equations for the stress σ and higher-order stress $\bar{\sigma}$ can be expressed as

$$\sigma = \mu \phi_{,x}, \tag{265}$$

$$\bar{\sigma} = \mu l^2 \phi_{,xx}, \tag{266}$$

where μ is a material parameter and l a length scale. We can rewrite (260)–(264) with (265) and (266) as

$$(\mu \phi_{,x})_{,x} - (\mu l^2 \phi_{,xx})_{,xx} + f = 0 \quad \text{in } \Omega, \tag{267}$$

$$\phi = g \quad \text{on } \Gamma_g, \tag{268}$$

$$\phi_{,x} \cdot n = q \quad \text{on } \Gamma_q, \tag{269}$$

$$\mu l^2 \phi_{,xx} = r \quad \text{on } \Gamma_r, \tag{270}$$

$$\mu \phi_{,x} \cdot n - (\mu l^2 \phi_{,xx})_{,x} \cdot n = t \quad \text{on } \Gamma_t. \tag{271}$$

From a mathematical point of view, the one-dimensional Toupin–Mindlin strain gradient theory is a generalization of the Bernoulli–Euler beam theory, involving in addition to the fourth-order derivative also a second-order derivative, see (137) for a comparison.

5.2.2. Method

Let us consider the standard partition (24) of the domain into finite elements and let us choose the spaces (144) and (145) for our approximation functions, i.e., let the functions again be continuous on the entire domain, but discontinuous in first and higher-order derivatives across interior boundaries. The C/DG method for the one-dimensional Toupin–Mindlin strain gradient theory (267)–(271) can be written as: Find $\phi^h \in \mathscr{S}^h$ such that

$$B_s(w^h, \phi^h) = L_s(w^h) \quad \forall w^h \in \mathscr{V}^h, \tag{272}$$

where the bilinear form is defined as

$$\begin{aligned} B_s(w^h, \phi^h) = {} & (w^h_{,x}, \mu \phi^h_{,x})_{\tilde{\Omega}} + (w^h_{,xx}, \mu l^2 \phi^h_{,xx})_{\tilde{\Omega}} - [\![w^h_{,x}]\!] \langle \mu l^2 \phi^h_{,xx} \rangle_{\tilde{\Gamma}} - \langle \mu l^2 w^h_{,xx} \rangle [\![\phi^h_{,x}]\!]_{\tilde{\Gamma}} \\ & + \tau [\![w^h_{,x}]\!] [\![\phi^h_{,x}]\!]_{\tilde{\Gamma}} - w^h_{,x} \cdot n \mu l^2 \phi^h_{,xx}|_{\Gamma_q} - \mu l^2 w^h_{,xx} \phi^h_{,x} \cdot n|_{\Gamma_q} + \tau_q w^h_{,x} \cdot n \phi^h_{,x} \cdot n|_{\Gamma_q} \end{aligned} \tag{273}$$

and the linear form as

$$L_s(w^h) = (w^h, f)_{\tilde{\Omega}} + w^h_{,x} \cdot n r|_{\Gamma_r} - \mu l^2 w^h_{,xx} q|_{\Gamma_q} + w^h t|_{\Gamma_t} + \tau_q w^h_{,x} \cdot n q|_{\Gamma_q}. \tag{274}$$

In (273) and (274), τ and τ_q denote the stabilization parameters on interior boundaries and on the exterior displacement gradient boundary, respectively.

5.2.3. Error analysis

The error analysis of the C/DG method (272) is a generalization of the analysis in Section 4.1.3, accounting for the additional terms from the second derivative in the bilinear form of the strain gradient formulation. Let us assume for simplicity that μ and μl^2 are continuous on Ω.

Consistency. We start by integrating (272) by parts, viz.

$$\begin{aligned} 0 &= B_s(w^h, \phi^h) - L_s(w^h) \\ &= (w^h, [(\mu \phi^h_{,x})_{,x} - (\mu l^2 \phi^h_{,xx})_{,xx} + f])_{\tilde{\Omega}} - \langle \mu l^2 w^h_{,xx} \rangle [\![\phi^h_{,x}]\!]_{\tilde{\Gamma}} + \langle w^h_{,x} \rangle [\![\mu l^2 \phi^h_{,xx}]\!]_{\tilde{\Gamma}} \\ &\quad - \langle w^h \rangle [\![\mu \phi^h_{,x} - (\mu l^2 \phi^h_{,xx})_{,x}]\!]_{\tilde{\Gamma}} - \mu l^2 w^h_{,xx} [\phi^h_{,x} \cdot n - q]_{\Gamma_q} + w^h_{,x} \cdot n [\mu l^2 \phi^h_{,xx} - r]_{\Gamma_r} \\ &\quad - w^h [\mu \phi^h_{,x} \cdot n - (\mu l^2 \phi^h_{,xx})_{,x} \cdot n - t]_{\Gamma_t} + \tau [\![w^h_{,x}]\!] [\![\phi^h_{,x}]\!]_{\tilde{\Gamma}} + \tau_q w^h_{,x} \cdot n [\phi^h_{,x} \cdot n - q]_{\Gamma_q}. \end{aligned} \tag{275}$$

From (275) we deduce the Euler–Lagrange equations

$$(\mu \phi^h_{,x})_{,x} - (\mu l^2 \phi^h_{,xx})_{,xx} + f = 0 \quad \text{in } \tilde{\Omega}, \tag{276}$$

$$\phi^h_{,x} \cdot n = q \quad \text{on } \Gamma_q, \tag{277}$$

$$\mu l^2 \phi^h_{,xx} = r \quad \text{on } \Gamma_r, \tag{278}$$

$$\mu\phi^h_{,x}\cdot n-(\mu l^2\phi^h_{,xx})_{,x}\cdot n=t\quad\text{on }\Gamma_t, \tag{279}$$

$$[\![\phi^h_{,x}]\!]=0\quad\text{on }\tilde{\Gamma}, \tag{280}$$

$$[\![\mu l^2\phi^h_{,xx}]\!]=0\quad\text{on }\tilde{\Gamma}, \tag{281}$$

$$[\![\mu\phi^h_{,x}-(\mu l^2\phi^h_{,xx})_{,x}]\!]=0\quad\text{on }\tilde{\Gamma}. \tag{282}$$

Eq. (276) is the governing partial differential equation (267) on element interiors, (277)–(279) are the boundary conditions, (280) implies the continuity of the displacement gradient, (281) the continuity of the couple stress and (282) the continuity of the traction across interior boundaries. From the substitution of ϕ for ϕ^h in (272) results the Galerkin orthogonality condition

$$B_s(w^h,e)=0\quad\forall w^h\in\mathscr{V}^h(\Omega). \tag{283}$$

Stability. Let us define the energy norm for the one-dimensional Toupin–Mindlin strain gradient problem as

$$|||w^h|||_s^2=\|\mu^{1/2}w^h_{,x}\|^2_{\tilde{\Omega}}+\|(\mu l^2)^{1/2}w^h_{,xx}\|^2_{\tilde{\Omega}}+\|\tau^{1/2}[\![w^h_{,x}]\!]\|^2_{\tilde{\Gamma}}+\|\tau_q^{1/2}w^h_{,x}\|^2_{\Gamma_q}. \tag{284}$$

Proposition 5.1. *$|||\cdot|||_s^2$ is a norm on $\mathscr{V}^h$.*

Proof. There are again no non-trivial functions for which (284) could vanish (see the proof of Proposition 4.1). □

Proposition 5.2. *The C/DG method* (272) *is stable in the energy norm* (284), *that is, there exists a positive constant m such that*

$$B_s(w^h,w^h)\geqslant m|||w^h|||_s^2\quad\forall w^h\in\mathscr{V}^h(\Omega). \tag{285}$$

Proof. The proof follows directly from the proof of Proposition 4.2, as all terms of (273) are, up to the material parameter and length scale, identical to the terms in (147), except for the first term, and for this term we have

$$(w^h_{,x},\mu w^h_{,x})_{\tilde{\Omega}}=\|\mu^{1/2}w^h_{,x}\|^2_{\tilde{\Omega}}, \tag{286}$$

and the result (285) follows for $m=1/2$ if we assume that $\tau=\tau_q=4C\mu l^2/h_e$. □

5.2.4. Convergence in energy norm

Theorem 5.1. *Assume that the consistency condition* (283) *and stability condition* (285) *of the method hold. Given that the conditions are satisfied for the interpolation estimates* (A.12), (A.13) *and the trace inequality* (A.18) *holds, the error estimate for the C/DG method* (272) *can be written as*

$$|||e|||_s^2\leqslant C\sum_{e=1}^{N_{\mathrm{el}}}h_e^{2(k-1)}|\phi|^2_{H^{k+1}(\Omega_e)}, \tag{287}$$

where C is a constant.

Proof. Invoking the decomposition of the error (80) and the Galerkin orthogonality (283), we have

$$\begin{aligned} m|||e^h|||_s^2 &\leqslant B_s(e^h, e^h), \\ &= B_s(e^h, e - \eta), \\ &\leqslant -B_s(e^h, \eta), \\ &\leqslant |B_s(e^h, \eta)|. \end{aligned} \tag{288}$$

We then can continue the inequality (288) as

$$\begin{aligned} m|||e^h|||_s^2 \leqslant\ & |(\mu^{1/2} e^h_{,x}, \mu^{1/2}\eta_{,x})_{\bar{\Omega}}| + |((\mu l^2)^{1/2} e^h_{,xx}, (\mu l^2)^{1/2}\eta_{,xx})_{\bar{\Omega}}| + |[\![e^h_{,x}]\!]\langle \mu l^2 \eta_{,xx}\rangle_{\bar{\Gamma}}| + |\langle \mu l^2 e^h_{,xx}\rangle [\![\eta_{,x}]\!]_{\bar{\Gamma}}| \\ &+ |\tau [\![e^h_{,x}]\!][\![\eta_{,x}]\!]_{\bar{\Gamma}}| + |e^h_{,x} \cdot n \mu l^2 \eta_{,xx}|_{\Gamma_q}| + |\mu l^2 e^h_{,xx}\eta_{,x} \cdot n|_{\Gamma_q}| + |\tau_q e^h_{,x} \cdot n \eta_{,x} \cdot n|_{\Gamma_q}|. \end{aligned} \tag{289}$$

Following the same steps as in the convergence proof in Section 4.1.3, we obtain

$$\begin{aligned} \frac{m}{2}|||e^h|||_s^2 \leqslant\ & \frac{\mu}{m}\|\eta_{,x}\|^2_{\bar{\Omega}} + \frac{\mu l^2}{m}\|\eta_{,xx}\|^2_{\bar{\Omega}} + \left\{ \frac{(\mu l^2)^2}{m}\|\tau^{-1/2}\langle \eta_{,xx}\rangle\|^2_{\bar{\Gamma}} + \frac{(\mu l^2)^2}{m}\|\tau_q^{-1/2}\eta_{,xx}\|^2_{\Gamma_q} \right\} \\ &+ \left\{ \frac{C\mu l^2}{m}\|h_e^{-1/2}[\![\eta_{,x}]\!]\|^2_{\bar{\Gamma}} + \frac{C\mu l^2}{m}\|h_e^{-1/2}\eta_{,x}\|^2_{\Gamma_q} \right\} + \left\{ \frac{1}{m}\|\tau^{1/2}[\![\eta_{,x}]\!]\|^2_{\bar{\Gamma}} + \frac{1}{m}\|\tau_q^{1/2}\eta_{,x}\|^2_{\Gamma_q} \right\} \end{aligned} \tag{290}$$

and then

$$\begin{aligned} \frac{m}{2}|||e^h|||_s^2 \leqslant C\sum_{e=1}^{N_{\mathrm{el}}} \{ & \|\eta_{,x}\|^2_{\Omega_e} + \|\eta_{,xx}\|^2_{\Omega_e} + h_e(h_e^{-1}\|\eta_{,xx}\|^2_{\Omega_e} + h_e\|\eta_{,xxx}\|^2_{\Omega_e}) + h_e^{-1}(h_e^{-1}\|\eta_{,x}\|^2_{\Omega_e} + h_e\|\eta_{,xx}\|^2_{\Omega_e}) \\ &+ h_e^{-1}(h_e^{-1}\|\eta_{,x}\|^2_{\Omega_e} + h_e\|\eta_{,xx}\|^2_{\Omega_e})\}. \end{aligned} \tag{291}$$

Using relationships (171)–(175) as well as

$$\|\eta_{,x}\|^2_{\Omega_e} \leqslant \|\eta\|^2_{H^1(\Omega_e)} \leqslant C h_e^{2k}|\phi|^2_{H^{k+1}(\Omega_e)}, \tag{292}$$

which has been derived from (A.12) and (A.13) in Appendix A, yields

$$|||e^h|||_s^2 \leqslant C\sum_{e=1}^{N_{\mathrm{el}}} h_e^{2(k-1)}|\phi|^2_{H^{k+1}(\Omega_e)}. \tag{293}$$

Employing similar arguments to bound $|||\eta|||_s^2$ and the triangle inequality, we obtain the result

$$|||e|||_s^2 \leqslant C\sum_{e=1}^{N_{\mathrm{el}}} h_e^{2(k-1)}|\phi|^2_{H^{k+1}(\Omega_e)}. \quad \square \tag{294}$$

5.2.5. Convergence in L^2-norm

For the homogeneous Dirichlet problem (i.e., for the case $\Gamma = \Gamma_g = \Gamma_q$ and $g = q = 0$) we prove convergence of the C/DG method (272) in the L^2-norm. We can write the following theorem (see Theorems 5.1 and 5.4 in Section 2 of Lions and Magenes [33] for a proof):

Theorem 5.2. *The mapping $P : C^\infty(\Omega) \to C^\infty(\Omega) \times C^\infty(\partial\Omega) \times C^\infty(\partial\Omega)$ defined by $P\phi = (\phi_{,xx} - \phi_{,xxxx}, \phi, \phi_{,n})$ and completed by continuity is a homeomorphism of $H^s(\Omega)$ onto $H^{s-4}(\Omega) \times H^{s-1/2}(\partial\Omega) \times H^{s-3/2}(\partial\Omega)$ for all $s \geqslant 4$, and there exist constants α_s and β_s such that*

$$\|\phi\|_{H^s(\Omega)} \leqslant \alpha_s\{\|\phi_{,xx} - \phi_{,xxxx}\|_{H^{s-4}(\Omega)} + \|\phi\|_{H^{s-1/2}(\partial\Omega)} + \|\phi_{,n}\|_{H^{s-3/2}(\partial\Omega)}\} \leqslant \beta_s\|\phi\|_{H^s(\Omega)}. \tag{295}$$

Proposition 5.3. *There exists a constant* $0 < C < \infty$ *such that*

$$B_s(w^h, v^h) \leqslant C|||w^h|||_s|||v^h|||_s \quad \forall w^h, v^h \in \mathscr{V}^h, \tag{296}$$

where C *is independent of* h_e.

Proof. Eq. (296) follows from the Cauchy–Schwarz inequality by first applying it in the form (180) to each term of the bilinear form, namely

$$\begin{aligned}
B_s(w^h, v^h) &\leqslant |B_s(w^h, v^h)|, \\
&\leqslant |(w^h_{,x}, \mu v^h_{,x})_{\bar{\Omega}}| + |(w^h_{,xx}, \mu l^2 v^h_{,xx})_{\bar{\Omega}}| + |[\![w^h_{,x}]\!]\langle \mu l^2 v^h_{,xx}\rangle_{\bar{\Gamma}}| + |\langle \mu l^2 w^h_{,xx}\rangle [\![v^h_{,x}]\!]_{\bar{\Gamma}}| \\
&\quad + |\tau [\![w^h_{,x}]\!][\![v^h_{,x}]\!]_{\bar{\Gamma}}| + |w^h_{,x} \cdot n \mu l^2 v^h_{,xx}|_{\Gamma_q}| + |\mu l^2 w^h_{,xx} v^h_{,x} \cdot n|_{\Gamma_q}| + |\tau_q w^h_{,x} \cdot n v^h_{,x} \cdot n|_{\Gamma_q}|, \\
&\leqslant \|\mu^{1/2} w^h_{,x}\|_{\bar{\Omega}} \|\mu^{1/2} v^h_{,x}\|_{\bar{\Omega}} + \|(\mu l^2)^{1/2} w^h_{,xx}\|_{\bar{\Omega}} \|(\mu l^2)^{1/2} v^h_{,xx}\|_{\bar{\Omega}} \\
&\quad + \|\tau^{1/2} [\![w^h_{,x}]\!]\|_{\bar{\Gamma}} \|\tau^{-1/2} \langle \mu l^2 v^h_{,xx}\rangle\|_{\bar{\Gamma}} + \|\tau^{-1/2} \langle \mu l^2 w^h_{,xx}\rangle\|_{\bar{\Gamma}} \|\tau^{1/2} [\![v^h_{,x}]\!]\|_{\bar{\Gamma}} \\
&\quad + \|\tau^{1/2} [\![w^h_{,x}]\!]\|_{\bar{\Gamma}} \|\tau^{1/2} [\![v^h_{,x}]\!]\|_{\bar{\Gamma}} + \|\tau_q^{1/2} w^h_{,x}\|_{\Gamma_q} \|\tau_q^{-1/2} \mu l^2 v^h_{,xx}\|_{\Gamma_q} \\
&\quad + \|\tau_q^{-1/2} \mu l^2 w^h_{,xx}\|_{\Gamma_q} \|\tau_q^{1/2} v^h_{,x}\|_{\Gamma_q} + \|\tau_q^{1/2} w^h_{,x}\|_{\Gamma_q} \|\tau_q^{1/2} v^h_{,x}\|_{\Gamma_q},
\end{aligned} \tag{297}$$

and then again in the form (182), resulting in

$$\begin{aligned}
B_s(w^h, v^h) &\leqslant \{\|\mu^{1/2} w^h_{,x}\|^2_{\bar{\Omega}} + \|(\mu l^2)^{1/2} w^h_{,xx}\|^2_{\bar{\Omega}} + \|\tau^{1/2} [\![w^h_{,x}]\!]\|^2_{\bar{\Gamma}} + \|\tau^{-1/2} \langle \mu l^2 w^h_{,xx}\rangle\|^2_{\bar{\Gamma}} + \|\tau^{1/2} [\![w^h_{,x}]\!]\|^2_{\bar{\Gamma}} \\
&\quad + \|\tau_q^{1/2} w^h_{,x}\|^2_{\Gamma_q} + \|\tau_q^{-1/2} \mu l^2 w^h_{,xx}\|^2_{\Gamma_q} + \|\tau_q^{1/2} w^h_{,x}\|^2_{\Gamma_q}\}^{1/2} \{\|\mu^{1/2} v^h_{,x}\|^2_{\bar{\Omega}} + \|(\mu l^2)^{1/2} v^h_{,xx}\|^2_{\bar{\Omega}} \\
&\quad + \|\tau^{-1/2} \langle \mu l^2 v^h_{,xx}\rangle\|^2_{\bar{\Gamma}} + \|\tau^{1/2} [\![v^h_{,x}]\!]\|^2_{\bar{\Gamma}} + \|\tau^{1/2} [\![v^h_{,x}]\!]\|^2_{\bar{\Gamma}} + \|\tau_q^{-1/2} \mu l^2 v^h_{,xx}\|^2_{\Gamma_q} \\
&\quad + \|\tau_q^{1/2} v^h_{,x}\|^2_{\Gamma_q} + \|\tau_q^{1/2} v^h_{,x}\|^2_{\Gamma_q}\}^{1/2}.
\end{aligned} \tag{298}$$

With (A.18) and (A.17) we find

$$\begin{aligned}
B_s(w^h, v^h) &\leqslant C\{\|\mu^{1/2} w^h_{,x}\|^2_{\bar{\Omega}} + \|(\mu l^2)^{1/2} w^h_{,xx}\|^2_{\bar{\Omega}} + \|\tau^{1/2} [\![w^h_{,x}]\!]\|^2_{\bar{\Gamma}} + \|\tau_q^{1/2} w^h_{,x}\|^2_{\Gamma_q}\}^{1/2} \{\|\mu^{1/2} v^h_{,x}\|^2_{\bar{\Omega}} \\
&\quad + \|(\mu l^2)^{1/2} v^h_{,xx}\|^2_{\bar{\Omega}} + \|\tau^{1/2} [\![v^h_{,x}]\!]\|^2_{\bar{\Gamma}} + \|\tau_q^{1/2} v^h_{,x}\|^2_{\Gamma_q}\}^{1/2} = C|||w^h|||_s|||v^h|||_s,
\end{aligned} \tag{299}$$

where C is independent of h_e. □

Remark 5.1. As in Remarks 4.1 and 4.3 one can employ inverse estimates for the interpolation errors, due to Arnold et al. [87], leading to the following generalizations of Proposition 5.3:

$$B_s(\eta_d, e^h) \leqslant C|||\eta_d|||_s|||e^h|||_s, \tag{300}$$

$$B_s(\eta_d, \eta) \leqslant C|||\eta_d|||_s|||\eta|||_s, \tag{301}$$

where $\eta_d = \phi_d - \tilde{\phi}_d$ is the interpolation error of the dual problem.

Theorem 5.3. *For a homogeneous Dirichlet problem, the error of the C/DG method* (272) *converges optimally in the* L^2*-norm* $\forall k \geqslant 3$, *namely*

$$\|e\| \leqslant Ch^{k+1} |\phi|_{H^{k+1}(\Omega)}. \tag{302}$$

Proof. Consider the homogeneous Dirichlet problem (i.e., the dual problem):

$$\mu \phi_{d_{,xx}} - \mu l^2 \phi_{d_{,xxxx}} = f_d \quad \text{in } \Omega, \tag{303}$$

$$\phi_d = 0 \quad \text{on } \Gamma, \tag{304}$$

$$\phi_{d_{,x}} \cdot n = 0 \quad \text{on } \Gamma. \tag{305}$$

From Theorem 5.2 we have $\forall s \geqslant 4$ the regularity estimate

$$\|\phi_d\|_{H^s(\Omega)} \leqslant \alpha_s \|f_d\|_{H^{s-4}(\Omega)}. \tag{306}$$

We invoke the decomposition of the error (80) and note that $\tilde{\phi}^h \in \mathscr{S}^h$. From (293) and (294) we can conclude

$$\|\eta_d\|_s = |||\phi_d - \tilde{\phi}_d^h|||_s \leqslant Ch^{s-2}\|\phi_d\|_{H^s(\Omega)}. \tag{307}$$

As $e \in \mathscr{V} = H_0^1(\Omega)$, we have $B_s(e, \phi_d) = (e, f_d)$, and therefore

$$\begin{aligned}(e, f_d) &= B_s(e, \phi_d) = B_s(\phi_d, e) = B_s(\phi_d - \tilde{\phi}_d^h, e) = B_s(\eta_d, e^h + \eta) \\ &= B_s(\eta_d, e^h) + B_s(\eta_d, \eta) \leqslant C|||\eta_d|||_s(|||e^h|||_s + |||\eta|||_s) \\ &\leqslant Ch^{s-2}\|\phi_d\|_{H^s(\Omega)}(|||e^h|||_s + |||\eta|||_s) \leqslant Ch^{s-2}\|f_d\|_{H^{s-4}(\Omega)}(|||e^h|||_s + |||\eta|||_s),\end{aligned} \tag{308}$$

where we have used the symmetry of the bilinear form and the Galerkin orthogonality condition (283). With $f_d = e$ and $s = 4$, we obtain from (308) that

$$\|e\| \leqslant Ch^2(|||e^h|||_s + |||\eta|||_s) \leqslant Ch^{k+1}|\phi|_{H^{k+1}(\Omega)}. \quad \square \tag{309}$$

6. Numerical validation

In the preceding two sections we have analytically investigated C/DG methods for the Bernoulli–Euler beam theory, the Poisson–Kirchhoff plate theory and the one-dimensional Toupin–Mindlin strain gradient theory. In this section we wish to test these formulations numerically. For this purpose we introduce specific boundary value model problems and perform a convergence study for diferent load cases, orders of interpolation and discretizations. We end this section with a comparison of the numerical findings with our analytical results.

6.1. Bernoulli–Euler beam theory

We have chosen a simple cantilever beam model for testing the C/DG method under three different loading conditions, namely loaded by an end moment, an end shear force and a distributed force. The exact solution is known in all cases, and for each case we will compare the approximate solution of the C/DG method with the exact solution. We first introduce the three model problems and their exact solutions. Then, we perform a convergence study for different orders of interpolation. Last, we give an intermediate summary of the numerical results for the Bernoulli–Euler beam theory.

6.1.1. Model problems

Let us consider a Bernoulli–Euler cantilever beam of unit length. The first load case we want to simulate is a moment end load acting on the free end of the beam (see Fig. 12), for which the boundary value problem can be formulated as

$$(EI\phi_{,xx})_{,xx} = 0 \quad \text{in }]0;1[, \tag{310}$$

$$\phi(0) = 0, \tag{311}$$

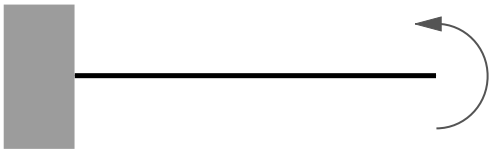

Fig. 12. Bernoulli–Euler beam loaded by end moment.

$$\phi_{,x}(0) = 0, \tag{312}$$

$$EI\phi_{,xx}(1) = M, \tag{313}$$

$$(EI\phi_{,xx})_{,x}(1) = 0. \tag{314}$$

The exact solution for this problem is

$$\phi(x) = \frac{1}{2}\frac{M}{EI}x^2. \tag{315}$$

For the second load case of a shear force acting at the free end (see Fig. 13), the boundary value problem can be stated as

$$(EI\phi_{,xx})_{,xx} = 0 \quad \text{in }]0;1[, \tag{316}$$

$$\phi(0) = 0, \tag{317}$$

$$\phi_{,x}(0) = 0, \tag{318}$$

$$EI\phi_{,xx}(1) = 0, \tag{319}$$

$$(EI\phi_{,xx})_{,x}(1) = Q. \tag{320}$$

The exact solution for this problem for constant EI is

$$\phi(x) = \frac{1}{2}\frac{Q}{EI}\left(\frac{1}{3}x^3 - x^2\right). \tag{321}$$

The third load case involves a distributed force over the entire length of the beam (see Fig. 14). The strong form of the corresponding boundary value problem can be written as

$$(EI\phi_{,xx})_{,xx} = f \quad \text{in }]0;1[, \tag{322}$$

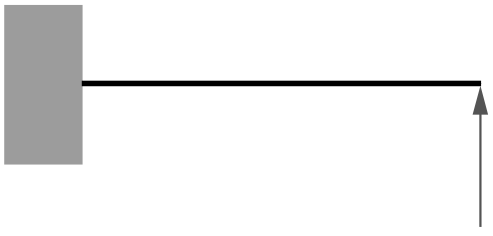

Fig. 13. Bernoulli–Euler beam loaded by end shear force.

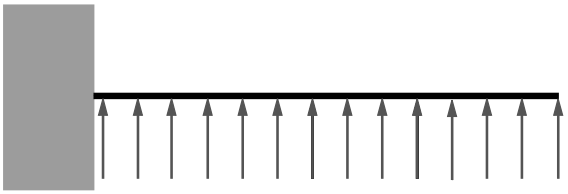

Fig. 14. Bernoulli–Euler beam with distributed load.

$$\phi(0) = 0, \tag{323}$$

$$\phi_{,x}(0) = 0, \tag{324}$$

$$EI\phi_{,xx}(1) = 0, \tag{325}$$

$$(EI\phi_{,xx})_{,x}(1) = 0. \tag{326}$$

The exact solution for this problem for constant EI is

$$\phi(x) = \frac{1}{24}\frac{f}{EI}(x^4 - 4x^3 + 6x^2). \tag{327}$$

6.1.2. Convergence study

The convergence rates of the C/DG method (146) are investigated for the three model problems introduced in Section 6.1.1 for linear ($k = 1$), quadratic ($k = 2$) and cubic ($k = 3$) interpolation. We have employed a uniform mesh, which has been successively refined.

6.1.2.1. Linear interpolation. The convergence rates of the error in the energy norm and in the L^2-norm are shown for the moment end load case and linear interpolation in Fig. 15, where $N_{\mathrm{el}} = 1/h$ serves as a parameter to indicate the degree of mesh refinement. For this load case we obtain nodally superconvergent behavior, which can be seen in Fig. 16, where we have plotted the normalized displacements of the exact and approximate solutions over the length of the beam for a discretization into two elements. For other discretizations we would obtain similar nodally superconvergent behavior.

In Figs. 17 and 18, convergence rates are plotted for the shear end load and distributed load cases, respectively, in the energy norm, in the L^2-norm and pointwise for the tip node at $x = 1$. As we would have expected from the analytical results, Figs. 15, 17 and 18 show the boundedness of the error in the energy norm. In the L^2-norm we obtain quadratic convergence rates in all load cases, which are optimal. Also pointwise we have quadratic convergence rates at the tip node.

Note that for linear interpolation, the choice of the correct stabilization constants is crucial for obtaining convergence (see Appendix B for an analytical procedure to find the correct stabilization constants). For a random choice of the stabilization constants, convergence is lost for linear interpolation, as the stabilization terms in (146) are the only terms in the formulation which contribute to the left-hand side matrix and therefore determine the solution.

6.1.2.2. Quadratic interpolation. We have repeated the convergence analyses for the model problems from Section 6.1.1 for quadratic interpolation functions. Fig. 19 illustrates that the C/DG approximation is exact for the end moment load case. Recall from Section 6.1.1 that the analytic solution for this load case is quadratic, and our quadratic finite element functions are capable of reproducing the exact solution.

The convergence rates of the error in the energy norm, in the L^2-norm and pointwise at the tip node are shown in Fig. 20 for the end shear force load case, and in Fig. 21 for the distributed force load case.

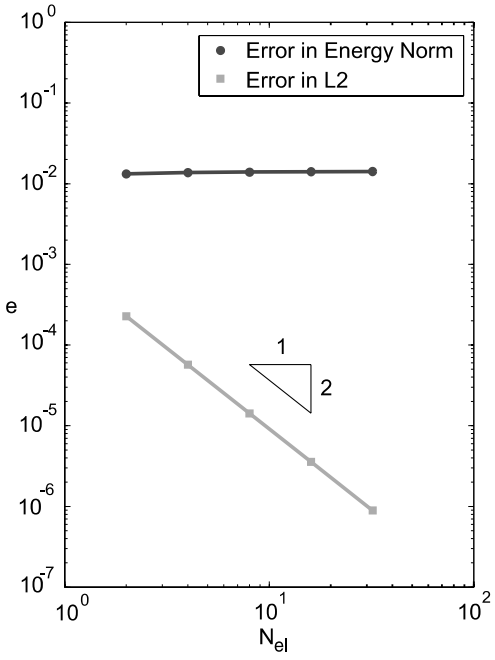

Fig. 15. Convergence rates for M-load case ($k = 1$).

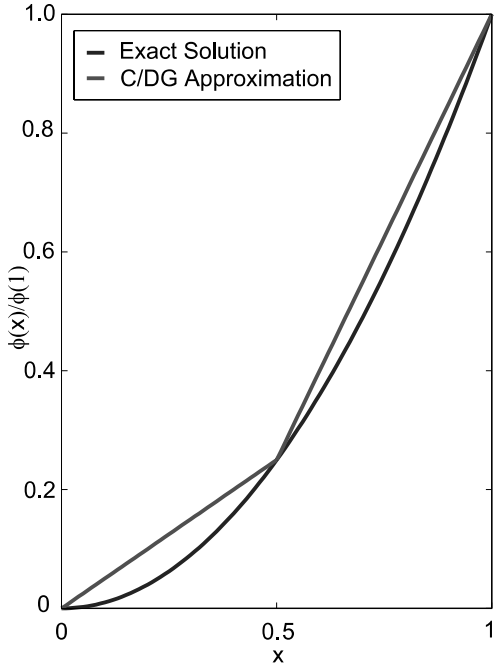

Fig. 16. Nodal superconvergence for M-load case ($k = 1$).

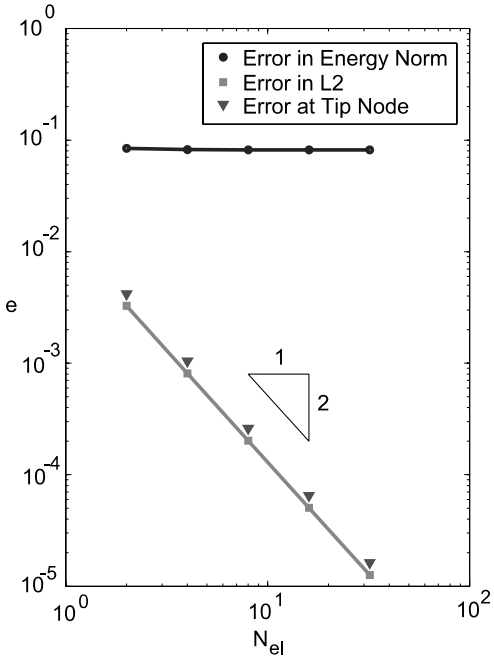

Fig. 17. Convergence rates for Q-load case ($k = 1$).

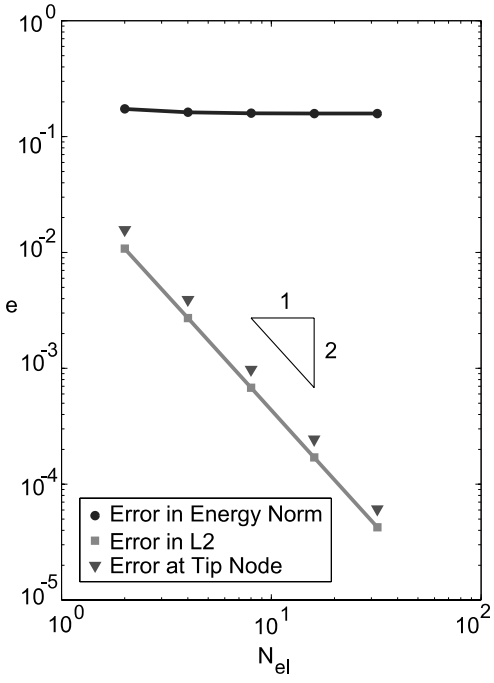

Fig. 18. Convergence rates for f-load case ($k = 1$).

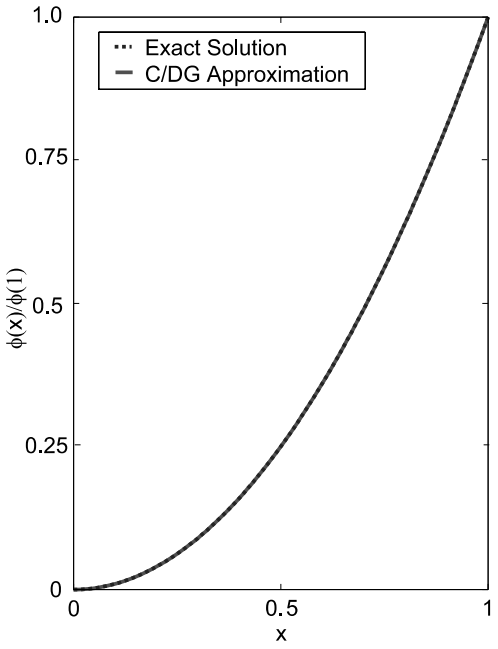

Fig. 19. C/DG method is exact for M-load case ($k = 2$).

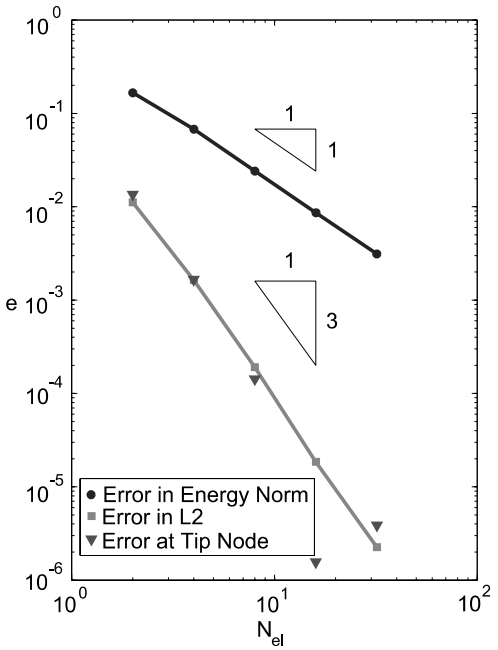

Fig. 20. Convergence rates for Q-load case ($k = 2$).

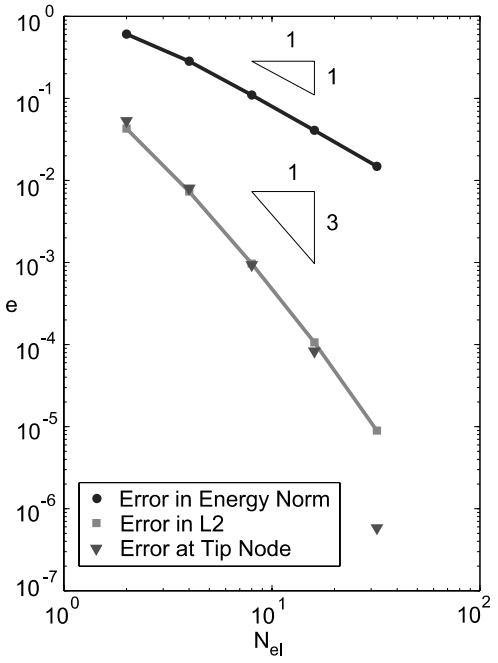

Fig. 21. Convergence rates for f-load case ($k = 2$).

We can see from these figures that the C/DG method converges at optimal rate in the energy norm, in the L^2-norm and pointwise at the tip node for our choice of the stabilization constants, which have been determined numerically. The computations have been performed with the value $C = 1.46$ for both stabilization constants, see Appendix B. In particular, in the energy norm, we have

$$|||e|||_{\mathrm{b}} \propto h^1, \tag{328}$$

and in the L^2-norm, we find

$$\|e\| \propto h^3. \tag{329}$$

For arbitrary choice of the stabilization constants, the C/DG method is still convergent, but convergence rates are not necessarily optimal.

6.1.2.3. Cubic interpolation. Recall from Section 6.1.1 that the analytic solutions for the end moment and end shear force load cases are quadratic and cubic, respectively, and our cubic finite element space is capable of reproducing the exact solutions in these two load cases. For the distributed force load case, the convergence rates in the energy norm and in the L^2-norm are displayed in Fig. 22. The C/DG method yields superconvergent behavior at the boundary and interior boundary nodes for this load case, and even for coarse discretizations the approximate and exact solution are virtually identical, see Fig. 23 as an example for a discretization into two elements.

We can see from Fig. 22 that the C/DG method converges at optimal rate in the energy norm and in the L^2-norm for our choice of the stabilization constants, which have been determined numerically to be $C = 3.62$ for both parameters. In the energy norm, we find

$$|||e|||_{\mathrm{b}} \propto h^2, \tag{330}$$

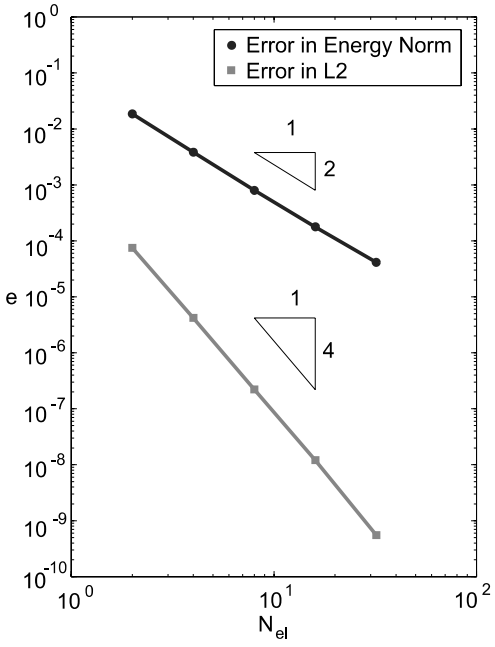

Fig. 22. Convergence rates for f-load case ($k = 3$).

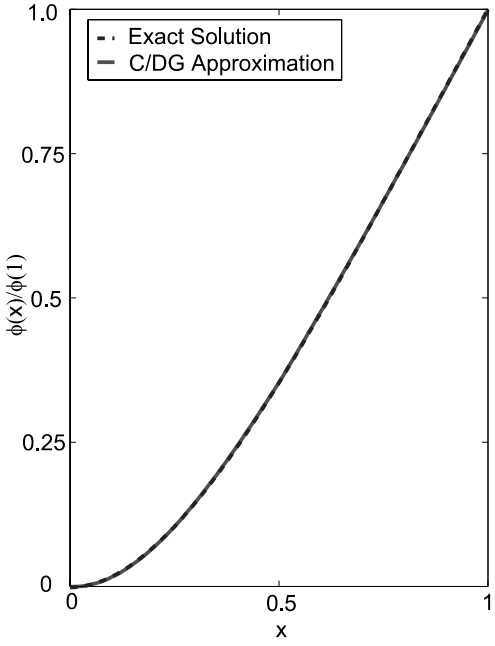

Fig. 23. Nodal superconvergence for f-load case ($k = 3$).

and in the L^2-norm, we have

$$\|e\| \propto h^4. \tag{331}$$

When one chooses the stabilization constants arbitrarily, but selects the same ones for τ and τ_h, convergence rates are often still optimal for cubic interpolation, and the nodal superconvergence property is retained. For some choices, however, convergence rates can be suboptimal.

6.1.3. Summary for Bernoulli–Euler beam theory

Our numerical findings confirm the results of the error analysis in Section 4.1.3. In particular, the convergence rate in the energy norm is optimal for all orders of interpolation, namely

$$|||e|||_{\mathrm{b}} \propto h^{k-1}. \tag{332}$$

Our numerical results further suggest that the convergence rate in the L^2-norm is also optimal for all orders of interpolation, even though the proof in Section 4.1.3 required an order of interpolation of cubic or higher, viz.

$$\|e\| \propto h^{k+1}. \tag{333}$$

Table 4 gives a summary of the convergence rates in the energy norm and in the L^2-norm for the different model problems and all orders of interpolation considered. We can see from the table that whenever the finite element space contains polynomials of the order of the exact solution, the C/DG approximation is identical to the exact solution. For linear and cubic interpolation, we obtain nodally superconvergent behavior (indicated by numbers in boldface type in Table 4) whenever the finite element space contains polynomials of one order less than the polynomial of the exact solution. For quadratic interpolation, however, this is not the case. Similar results of different behavior for even and odd orders of interpolation have been reported in other situations for the DG method [61], which are consistent with our findings.

6.2. Poisson–Kirchhoff plate theory

We wish to validate in this section the analytical results for the C/DG method (215) for a square and circular plate with different loading and boundary conditions. In both cases the exact solution will be symmetric, and therefore it will be sufficient to consider just one quarter of the plate for the simulation and to apply appropriate conditions on the symmetry boundaries. We employ quadrilateral quadratic and cubic elements as shown in Figs. 24 and 25 and monitor the center point deflection for successively refined meshes.

Table 4
Convergence rates (panel a) in energy norm and (panel b) in L^2-norm for linear, quadratic and cubic interpolation for M, Q and f-load cases. Nodal superconvergence is indicated by numbers in boldface type

	Linear	Quadratic	Cubic
Energy norm			
M	**0**	Exact	Exact
Q	0	1	Exact
f	0	1	**2**
L^2-norm			
M	**2**	Exact	Exact
Q	2	3	exact
f	2	3	**4**

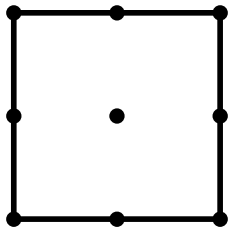

Fig. 24. Quadratic element.

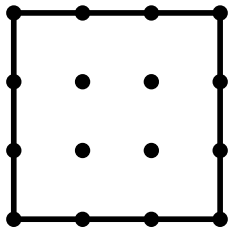

Fig. 25. Cubic element.

6.2.1. Square plate

The loading conditions for our simulation of the square plate are shown in Figs. 26 and 27. Both for the distributed load case and the center point load case we employ two types of boundary conditions: simply supported (i.e., zero displacement and moment on the exterior boundary) and clamped (i.e., zero displacement and slope on the exterior boundary). Figs. 28 and 29 show the deformation of the plate for the two types of boundary conditions for the distributed load case, and Figs. 30 and 31 for the center point load case.

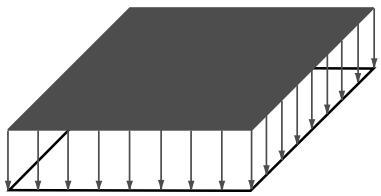

Fig. 26. Square plate with distributed load.

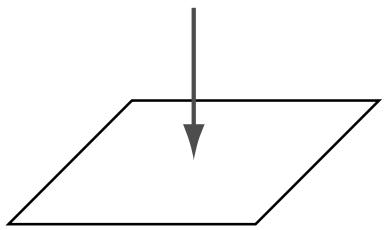

Fig. 27. Square plate with center point load.

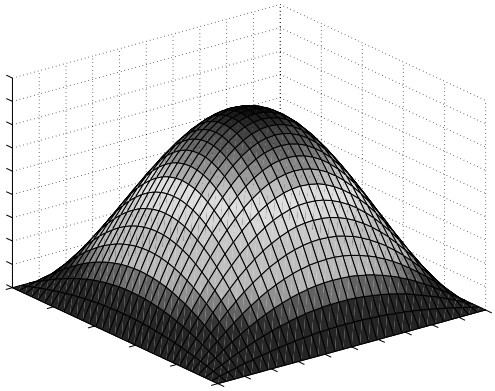

Fig. 28. Illustration of deformation for simply supported plate with distributed load.

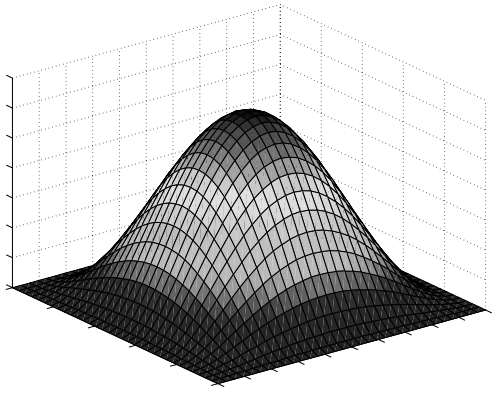

Fig. 29. Illustration of deformation for clamped plate with distributed load.

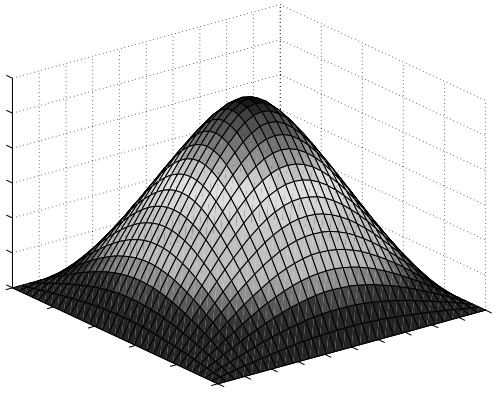

Fig. 30. Illustration of deformation for simply supported plate with center point load.

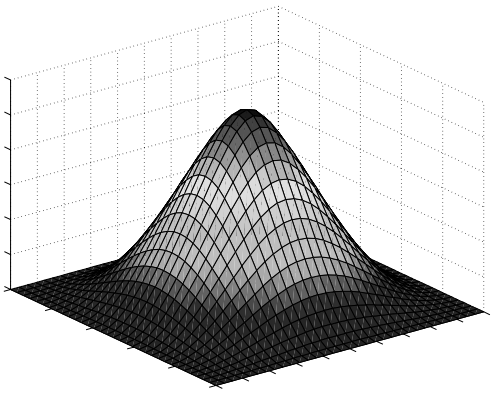

Fig. 31. Illustration of deformation for clamped plate with center point load.

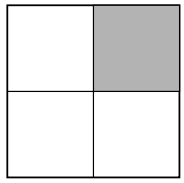

Subdivision of Quarter Plate into $N \times N$ Elements

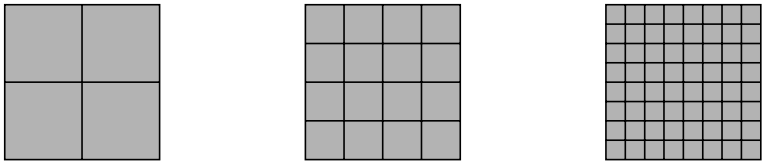

$N = 2$ $N = 4$ $N = 8$

Fig. 32. Mesh refinement for square plate.

We are interested in the convergence behavior of the center point deflection for different discretizations, and we have adopted the parameter N to indicate the degree of mesh refinement of the quarter plate considered, see Fig. 32.

6.2.1.1. Distributed load. The convergence behavior of the center point displacement for the square plate under a distributed load is shown for quadratic and cubic interpolation in Fig. 33 for simply supported boundary conditions and in Fig. 34 for the clamped plate. We have normalized the approximate center point deflection in the plots against the series solution (see the work of Timoshenko and Woinowski-Krieger [8] and Nádai [7] for series solutions). One can see that both the quadratic and the cubic elements converge, that in both cases the approximations are very accurate and that the cubic element converges more rapidly to the exact solution than the quadratic element. It is interesting to note that the quadratic element underestimates the center point deflection whereas the cubic element overestimates it.

The convergence of the center bending moment is shown in Fig. 35 for the simply supported plate and distributed load. Both quadratic and cubic elements converge, and again the quadratic element approxi-

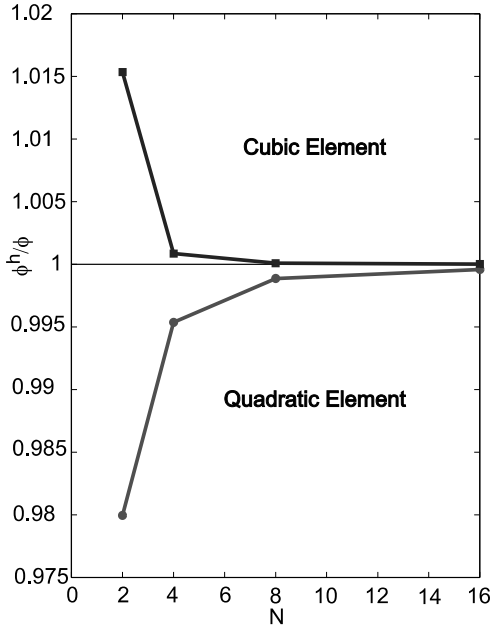

Fig. 33. Convergence of center point displacement for simply supported plate with distributed load.

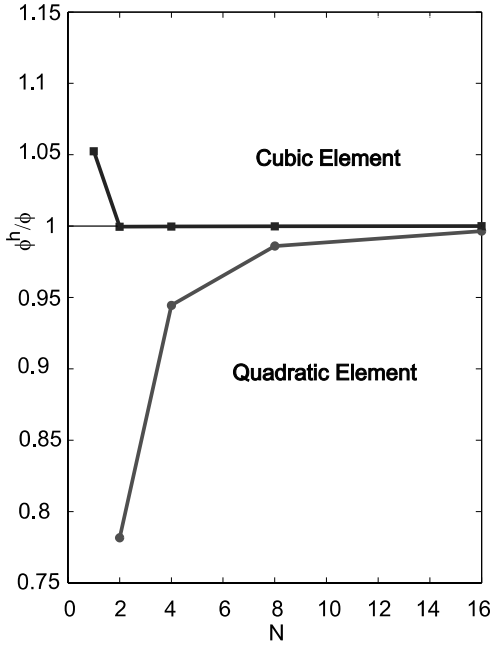

Fig. 34. Convergence of center point displacement for clamped plate with distributed load.

mates the center bending moment from below whereas the cubic element converges from above. Note that the moments have been calculated by differentiating the approximation functions and multiplying with the

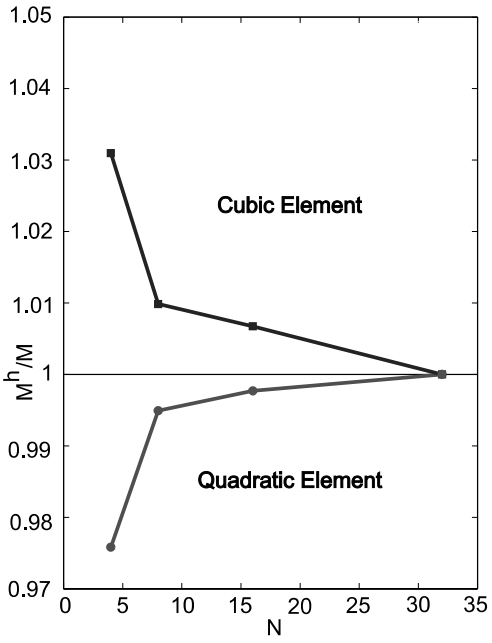

Fig. 35. Convergence of center bending moment for simply supported plate with distributed load.

nodal values. Moments can alternatively be calculated by introducing an auxiliary problem, see Hughes et al. [106] for details.

6.2.1.2. Center point load. The convergence results for the quadratic and cubic elements are displayed for the center point load in Fig. 36 for the simply supported plate and in Fig. 37 for the clamped plate. Under this loading condition both elements converge, as in the distributed load case, however, both elements approximate the center point defection now from below.

6.2.2. Circular plate

The circular plate is an interesting problem in that the discretization of its domain is non-uniform. We wish to consider the case of a distributed load (see Fig. 38) for clamped and simply supported boundary conditions. The exact solution for this loading condition is symmetric as for the previous cases, and we will only consider one quarter of the plate for the simulation. The parameter N serves again as an indicator for the degree of mesh refinement, see Fig. 39 for an illustration.

6.2.2.1. Distributed load. We have performed a convergence study at the center point for the quadratic element under distributed loading condition for the simply supported plate (Fig. 40) and for the clamped plate (Fig. 41). Also for the non-uniform meshes employed (see Fig. 39) we obtain good convergence results, the ratio of the C/DG approximation versus the exact solution approaches unity rapidly and the quadratic element underestimates the center point deflection.

6.2.3. Summary for Poisson–Kirchhoff plate theory

Our convergence study showed that both the quadratic and cubic elements converge and that good accuracy is obtained even for coarse discretizations. The numerical experiments seem to suggest that the stabilization constants are not critical for convergence if chosen large enough. For an analytical framework

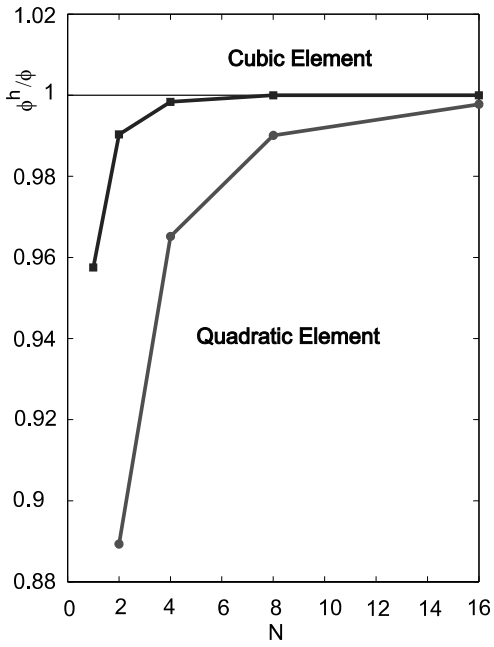

Fig. 36. Convergence of center point displacement for simply supported plate with center point load.

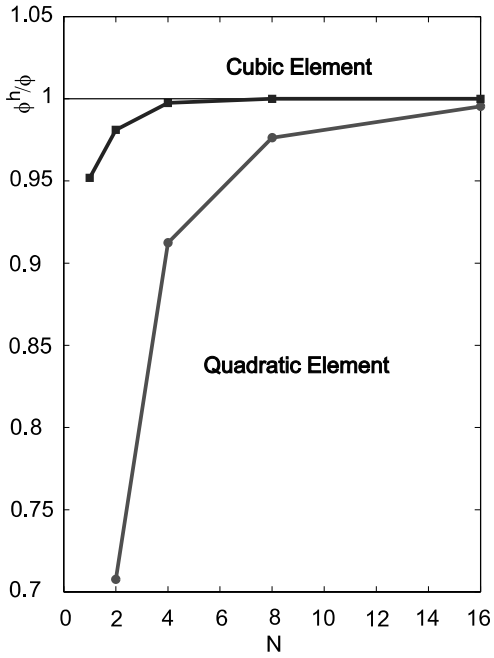

Fig. 37. Convergence of center point displacement for clamped plate with center point load.

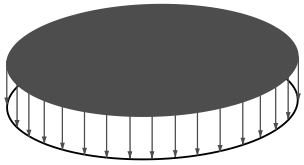

Fig. 38. Circular plate with distributed load.

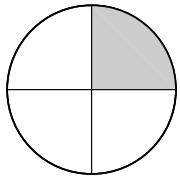

Subdivision of Quarter Plate into Elements

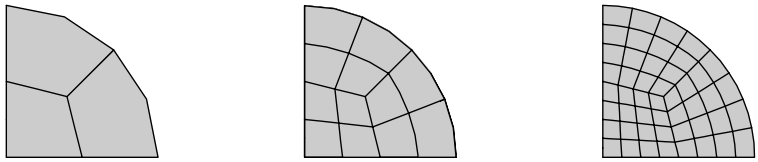

$N = 2$ $N = 4$ $N = 8$

Fig. 39. Mesh refinement for circular plate.

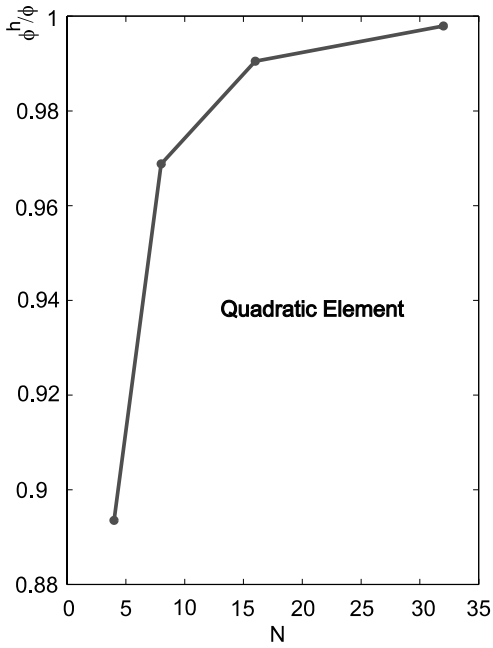

Fig. 40. Convergence of center point displacement for simply supported circular plate with distributed load.

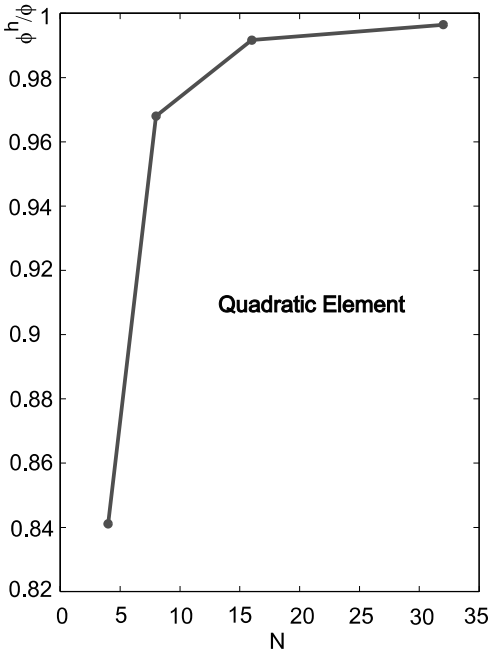

Fig. 41. Convergence of center point displacement for clamped circular plate with distributed load.

for deriving the stabilization constants see Harari and Hughes [107]. Their results indicate that the constants for quadratic and cubic interpolation can be quite large. As yet we have been unable to find a linear plate element with satisfactory convergence behavior.

6.3. Shear layer problem with the Toupin–Mindlin theory

We wish to consider a Toupin–Mindlin shear layer as model problem to validate our C/DG method (272) for a strain gradient theory. Let us introduce the model problem, its exact solution, present a convergence study and compare the numerical findings with our results of the error analysis.

6.3.1. Model problem

We want to simulate a shear-deformable body which is fixed on its left and upon which a traction acts on its right as shown in Fig. 42. In particular, in this problem the length from the attachment to where the traction acts is assumed to be L. The problem can be formulated as

$$(\mu\phi_{,x})_{,x} - (\mu l^2\phi_{,xx})_{,xx} + f = 0 \quad \text{in }]0;L[, \tag{334}$$

$$\phi(0) = 0, \tag{335}$$

$$\phi_{,x}(0) = 0, \tag{336}$$

$$\phi_{,x}(L) = 0, \tag{337}$$

$$\mu\phi_{,x}(L) - \mu l^2\phi_{,xxx}(L) = t, \tag{338}$$

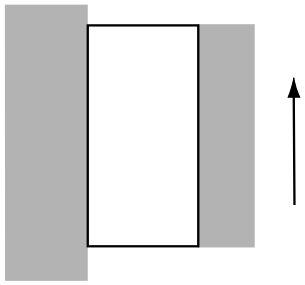

Fig. 42. Shear layer attached on the left side ($x = 0$) with traction acting on the right side ($x = L$).

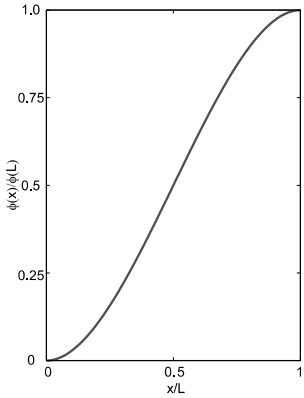

Fig. 43. Exact solution for Toupin–Mindlin shear layer model problem.

and the exact solution to this problem can be expressed as

$$\phi(x) = \frac{tl}{\mu(e^{L/l}+1)}(1 - e^{L/l} + e^{(L-x)/l} - e^{x/l}) + \frac{t}{\mu}x \tag{339}$$

and is illustrated in Fig. 43.

6.3.2. Convergence study

The convergence rates for linear interpolation can be seen in Fig. 44, where we have again $N_{\mathrm{el}} = 1/h$. The error in the energy norm is bounded as we would expect from our analytical findings. In the L^2-norm and pointwise at $x = L$ we have quadratic convergence, which is optimal. Fig. 45 shows the ratio of the approximate C/DG solution to the exact solution for successive mesh refinements, and while the error for very coarse discretizations can be considerable, we converge rapidly to the exact solution.

The convergence rates for quadratic interpolation and cubic interpolation are presented in Figs. 46 and 47. We obtain linear (quadratic) convergence for quadratic (cubic) interpolation in the energy norm, respectively. In the L^2-norm as well as pointwise at $x = L$, we obtain a convergence rate of three and four for quadratic and cubic interpolation, respectively.

6.3.3. Summary for Toupin–Mindlin shear layer

Our numerical observations confirm our analytical results in that all orders of interpolation considered lead to optimal convergence rates in the energy norm. In the L^2-norm we were able to confirm the analytical

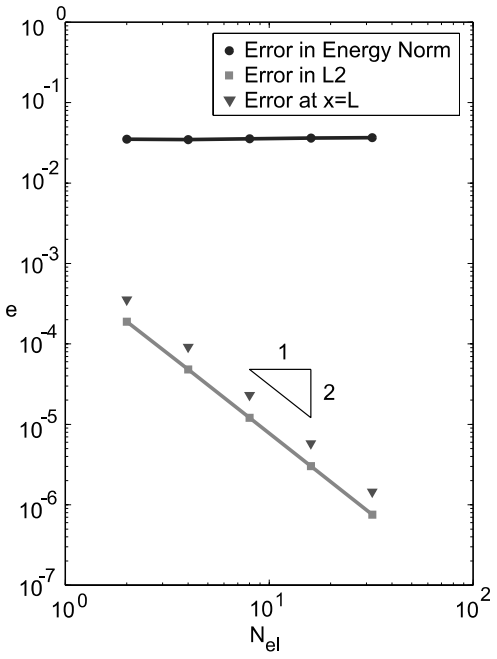

Fig. 44. Convergence rates for linear element ($k = 1$).

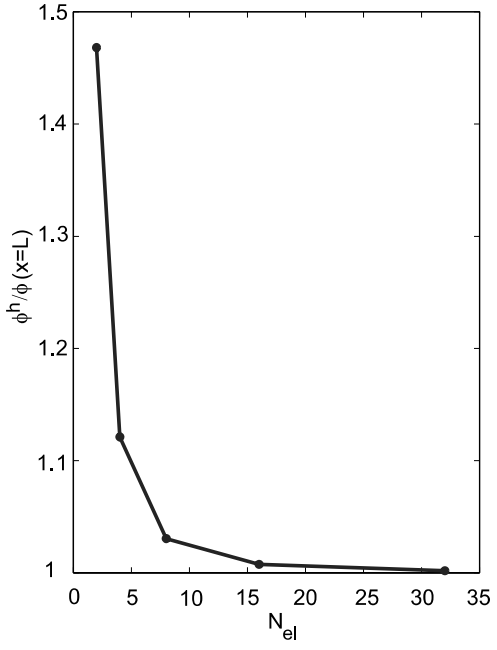

Fig. 45. Normalized displacement at $x = L$ for linear element ($k = 1$).

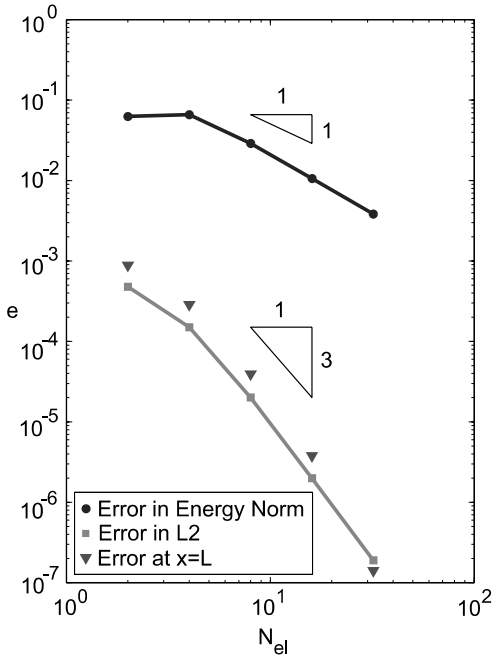

Fig. 46. Convergence rates for quadratic element ($k = 2$).

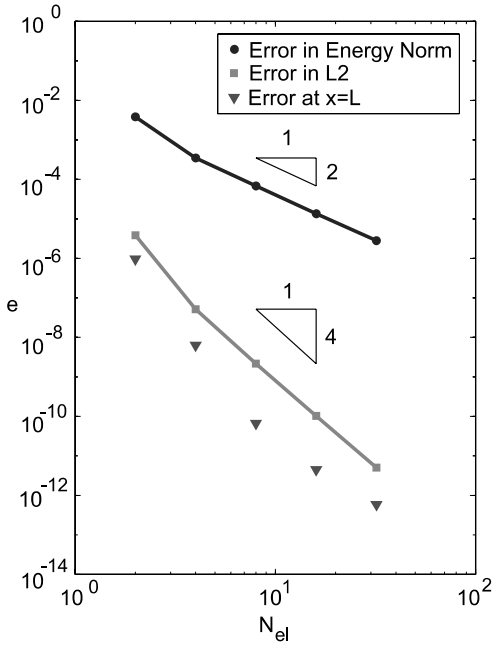

Fig. 47. Convergence rates for cubic element ($k = 3$).

result of optimal convergence for cubic interpolation, and in addition we showed that also for linear and quadratic interpolation we obtain optimal convergence rates in the L^2-norm, even though the proof did not hold in those cases.

As in the case of the Bernoulli–Euler beam theory, we need to invoke the correct stabilization constants for optimal convergence rates and in order to obtain any convergence for linear interpolation. The C/DG method converges independent of the choice for the stabilization constants for quadratic and cubic interpolation, but convergence rates may be suboptimal.

6.4. Numerical results

Let us briefly summarize the numerical observations for the Bernoulli–Euler beam theory, the Poisson–Kirchhoff plate theory and the Toupin–Mindlin shear layer. In the one-dimensional examples, we numerically obtained optimal convergence rates both in the energy norm and in the L^2-norm. For two-dimensional problems, we achieved convergence for quadratic and cubic interpolation only. The choice of the stabilization constants is not critical for convergence if chosen large enough for quadratic and cubic interpolation, but is critical for linear interpolation in order to ensure optimal convergence rates.

7. Conclusions

Traditional approaches for solving fourth-order elliptic problems within the framework of CG methods are problematic: C^1-continuous methods are intractable for three-dimensional problems and mixed methods involve independent fields leading to an increased number of unknowns and stability constraints on the combination of interpolation functions. Current shell formulations are complex, and no formulations exist for three-dimensional strain gradient theories.

The objective of this paper was to establish a simple and variationally consistent approach for the solution of fourth-order elliptic problems. The C/DG method we have introduced for this purpose exhibits the following features:

1. It is formulated in the primary variable only. We have eliminated all derived quantities such as rotations or displacement gradients from the description, as well as all Lagrange multipliers.
2. Only C^0-continuous approximation functions of low order (linear, quadratic, cubic) have been employed, leading to straightforward implementations of the method.
3. The method is consistent, stable, convergent and simple.

The C/DG method was presented for the examples of thin bending theories and a strain gradient theory, and suggests a new framework for solving fourth- and higher-order elliptic problems, namely the combination of stabilized CG and DG methods. The concepts and methods developed in this paper are easily generalizable to other situations and offer the opportunity to derive formulations for new classes of problems and for problems abandoned in the past due to their complexity.

7.1. Summary of main results

Let us briefly summarize the main findings. We have given an overview of basic finite element techniques such as the CG method, the DG method and stabilization, which provide the foundation for our developments. We have presented analyses of these methods for the advection, diffusion and advection–diffusion model problems, which have highlighted the strengths and weaknesses of each technique. Based on these findings we have explored a new approach for solving fourth-order elliptic problems which has been termed

the C/DG method. It combines the advantageous features of the underlying basic finite element techniques, namely a formulation in the primary variable only with C^0-continuous approximation functions, and the weak enforcement of continuity of the first- and higher-order derivatives via stabilizing residual terms on interior boundaries. These stabilizing terms have crucial importance for the convergence of the method. We have performed an error analysis of the C/DG method for Bernoulli–Euler beam theory, for Poisson–Kirchhoff plate theory and for a Toupin–Mindlin strain gradient theory. In each case, we have obtained optimal convergence rate behavior, which has been verified numerically for simple example model problems.

Based on our results, we can draw the conclusion that the C/DG method is an attractive and competitive approach for solving fourth-order elliptic problems. It allows for formulations for thin bending theories for plates and shells with displacements as only degrees of freedom, avoiding rotational degrees of freedom. For strain gradient theories in elasticity and plasticity, the C/DG method permits formulations in the primary variable only, eliminating displacement gradients and Lagrange multipliers and thereby enhancing efficiency for two-dimensional problems and offering for the first time an approach which is amenable to three-dimensional generalizations.

7.2. Directions for future work

The work presented in this paper has introduced a new framework for solving fourth-order elliptic problems, and the analytical results as well as some simple numerical validation examples warrant further exploration of the potential of the C/DG method. In particular, we suggest to consider the following areas for future work.

Analytically, it is interesting to investigate the convergence behavior of the C/DG method in the L^2-norm for linear and quadratic interpolation. Numerically, further tests of the C/DG method should explore its convergence rates for more advanced model problems and compare them against the results from traditional approaches for fourth-order elliptic problems. As for the application areas, the design of methods for shell analysis as well as for strain gradient theories in two and three dimensions and for materials with discontinuous material behavior are expected to uncover the full potential of the C/DG method. So far, no formulation for linear interpolation has been devised for two dimensional problems, and further exploration in this direction is worthwhile. The stabilization terms in the formulation are of crucial importance, and continued investigation into the determination of their form and the constants in one and two dimensions, both numerically and analytically, is called for. Clearly, much research remains to be done before the C/DG method may be considered to be applicable to real-world engineering problems.

Acknowledgements

This work was supported by ONR under grant no. N00014-99-1-0122-P00002 and by NASA under grant no. NCC2-5363-2 at Stanford University. The work of Krishna Garikipati at University of Michigan was supported by NSF under grant CMS#0087019. Gerald Engel received partial support from Cusanuswerk, Hermann–Reissner–Stiftung, Flughafen Frankfurt Main Stiftung, and Studentenwerk Stuttgart Stiftung. Mats Larson was supported by STINT. The authors gratefully acknowledge the above support.

Appendix A. Inequalities

Appendix A first states the basic definitions of a finite element, of degrees of freedom, of basis functions, of an interpolant as well as of affine-equivalent finite elements, which are needed for the definition of

regularity. Then, interpolation estimates are given. Appendix A is concluded with important inverse estimates and a basic trace inequality. The interpolation estimates, the inverse estimates and the trace inequality are extensively used in the error analyses throughout this paper. The references for the following definitions and theorems are Brenner and Scott [32] and Ciarlet [108].

A.1. Basic definitions

To set the stage for the developments in this appendix we first wish to define a finite element, degrees of freedom, basis functions, an interpolant, affine-equivalent elements as well as regularity.

Definition A.1. A *finite element* in $\mathbb{R}^d$ is a triple (Ω, P, Σ) where

- $\Omega \subset \mathbb{R}^d$ is closed and has a non-empty interior and a Lipschitz-continuous boundary,
- P is a finite-dimensional space of real-valued functions on Ω with $N = \dim P$,
- Σ is a set of N linear forms ψ_i, $1 \leqslant i \leqslant N$, defined over the space P, and it is assumed that the set Σ is P-unisolvent, i.e., given any real scalars c_i, $1 \leqslant i \leqslant N$, there exists a unique function $w \in P$ that satisfies $\psi(w) = c_i$, $1 \leqslant i \leqslant N$.

Definition A.2. The linear forms ψ_i, $1 \leqslant i \leqslant N$, are called *degrees of freedom* of the finite element and, due to the P-unisolvency of Σ, it is easy to see that they are linearly independent. Therefore, Σ is a basis for the dual of P, which we will denote by P'.

Definition A.3. Always because of the P-unisolvency of Σ, it is clear that there exist N functions $w_i \in P$, $1 \leqslant i \leqslant N$, that satisfy $\psi_j(w_i) = \delta_{ij}$, $1 \leqslant j \leqslant N$. Therefore, the identity

$$w = \sum_{i=1}^{N} \psi_i(w) w_i \quad \forall w \in P \tag{A.1}$$

holds. The functions w_i, $1 \leqslant i \leqslant N$, are called *basis functions* of the finite element.

We can now state the definition of an interpolant, which has great importance in both interpolation and approximation theory.

Definition A.4. Given (Ω, P, Σ) and a function $v : \Omega \to \mathbb{R}$ smooth enough to have the degrees of freedom $\psi_i(v)$, $1 \leqslant i \leqslant N$, well defined, we define the P-interpolant of the function v as

$$\Pi v = \sum_{i=1}^{N} \psi_i(v) w_i. \tag{A.2}$$

Due to the P-unisolvency of Σ, the P-interpolant is the unique function satisfying

$$\Pi v \in P \quad \text{and} \quad \psi_i(\Pi v) = \psi_i(v), \quad 1 \leqslant i \leqslant N. \tag{A.3}$$

Definition A.5. For $\boldsymbol{x} \in \mathbb{R}^d$, let $F(x) = \boldsymbol{A}\boldsymbol{x} + \boldsymbol{b}$ be an affine map (A non-singular). We say that the finite elements (Ω, P, Σ) and $(\hat{\Omega}, \hat{P}, \hat{\Sigma})$ are *affine-equivalent* if

- $\hat{\Omega} = F(\Omega)$,
- $\hat{P} = \{\hat{w} : \hat{\Omega} \to \mathbb{R} | \hat{w} = w \circ F, w \in P\}$,
- $\hat{\Sigma} = \{\hat{\psi}_i \in \hat{P}' | \hat{\psi}_i(w \circ F) = \psi_i(w), w \in P\}$.

Definition A.6. Given a family of finite elements $(\Omega_e, P_e, \Sigma_e)$, let

$$h_e = \operatorname{diam}(\Omega_e) \tag{A.4}$$

and

$$\rho_e = \sup\{\operatorname{diam}(S), S \text{ is a ball contained in } \Omega_e\}. \tag{A.5}$$

We say that the family of finite elements is *regular* if

- there exists a constant α such that

$$\frac{h_e}{\rho_e} \leqslant \alpha, \tag{A.6}$$

- the family (h_e) is bounded and 0 is its only accumulation point, which we indicate, with an abuse of notation, as

$$h_e \to 0. \tag{A.7}$$

A.2. Interpolation estimates

Theorem A.1. *Let $(\hat{\Omega}, \hat{P}, \hat{\Sigma})$ be a finite element and s the greatest order of the partial derivatives occurring in the definition of $\hat{\Sigma}$. Furthermore, assume that for some integers $m \geqslant 0$ and $k \geqslant 0$ it is also*

$$H^{k+1}(\hat{\Omega}) \hookrightarrow C^s(\hat{\Omega}), \tag{A.8}$$

$$H^{k+1}(\hat{\Omega}) \hookrightarrow H^m(\hat{\Omega}), \tag{A.9}$$

$$P_k(\hat{\Omega}) \subset \hat{P} \subset H^m(\hat{\Omega}), \tag{A.10}$$

where $C^s(\Omega)$ denotes the space of all real-valued s-times continuously differentiable functions on $\Omega \subset \mathbb{R}^d$, $\hookrightarrow$ is the symbol indicating inclusion with continuous injection, and $P_k(\hat{\Omega})$ is the space of all polynomials of degree $\leqslant k$ defined over $\hat{\Omega}$. Then there exists a constant C, depending only on $\hat{\Omega}$, $\hat{P}$ and $\hat{\Sigma}$, such that for all affine-equivalent finite elements in the family $(\Omega_e, P_e, \Sigma_e)$, i.e., $\forall e$ we have

$$|v - \Pi_e v|_{H^m(\Omega_e)} \leqslant C \frac{h_e^{k+1}}{\rho_e^m} |v|_{H^{k+1}(\Omega_e)} \quad \forall v \in H^{k+1}(\Omega_e), \tag{A.11}$$

where $\Pi_e v$ indicates the *P_e-interpolant of v*.

A simpler version of this theorem can also be proven by considering the case of a regular affine family of elements as in Definition A.6. We have in this case

Theorem A.2. *Let $(\Omega_e, P_e, \Sigma_e)$ be an affine family of finite elements whose reference finite element $(\hat{\Omega}, \hat{P}, \hat{\Sigma})$ satisfies conditions* (A.8)–(A.10), *and assume in addition that the family is regular. Then there exists a constant C, depending only on $\hat{\Omega}$, $\hat{P}$ and $\hat{\Sigma}$, such that for all finite elements in the family we have*

$$|v - \Pi_e v|_{H^m(\Omega_e)} \leqslant C h_e^{k+1-m} |v|_{H^{k+1}(\Omega_e)} \quad \forall v \in H^{k+1}(\Omega_e). \tag{A.12}$$

Remarks.

1. Under the given assumptions it is possible to prove a stronger version of Theorem A.2, for which (A.12) is replaced by

$$\|v - \Pi_e v\|_{H^m(\Omega_e)} \leqslant C h_e^{k+1-m} |v|_{H^{k+1}(\Omega_e)} \quad \forall v \in H^{k+1}(\Omega_e). \tag{A.13}$$

2. The above theorems are the particularization of the analogous results holding in Sobolev spaces, i.e., for $v \in W_p^{k+1}(\Omega_e)$, $p \in [1, \infty]$, the proof of which can be found in Ciarlet [108].

A.3. Inverse estimates

We now examine the relationship between different seminorms on a finite element space. For some local results, see Brenner and Scott [32], as Ciarlet [108] reports only global results, from which these here need to be extracted.

Theorem A.3. *Let (Ω, P, Σ) be a finite element, $(\hat{\Omega}, \hat{P}, \hat{\Sigma})$ its reference element and l, m two positive integers such that*

$$l \leqslant m, \tag{A.14}$$

$$\hat{P} \subset H^l(\hat{\Omega}) \cap H^m(\hat{\Omega}). \tag{A.15}$$

Then there exists a constant C_{I}, depending only on $\hat{\Omega}$, $\hat{P}$, l and m such that

$$|v|_{H^m(\Omega_e)} \leqslant C_{\mathrm{I}} h_e^{l-m} |v|_{H^l(\Omega_e)} \quad \forall v \in P. \tag{A.16}$$

Remarks

1. As in the section on interpolation estimates, under the same assumptions, a stronger theorem, holding for norms rather than seminorms, can be proven, viz.

$$\|v\|_{H^m(\Omega_e)} \leqslant C_{\mathrm{I}} h_e^{l-m} \|v\|_{H^l(\Omega_e)} \quad \forall v \in P. \tag{A.17}$$

2. Also, again as in the previous section, the above theorem is the particularization of the analogous result holding in Sobolev rather than Hilbert spaces.

A.4. Trace inequality

To conclude, we report an important theorem [109,110] which gives a relevant and very useful bound for the L^2-norm of a function on an element boundary in terms of norms of the same function in the interior of the element.

Theorem A.4. *Let $\Omega \subset \mathbb{R}^d$ have a Lipschitz boundary. Then there is a constant C such that*

$$\|v\|_{\partial\Omega_e}^2 \leqslant C(h_e^{-1} \|v\|_{\Omega_e}^2 + h_e \|\nabla v\|_{\Omega_e}^2) \quad \forall v \in H^1(\Omega_e). \tag{A.18}$$

See [109, 110] for details.

Appendix B. Stabilization parameter

In this appendix, we give a definition of the stabilization parameter which has been used in the numerical examples. For linear interpolation, we present an approach for analytically determining the stabilization constants appearing in the definition of the stabilization parameters in one dimension. For the

determination of the stabilization constants in other cases, we refer to the work of Harari and Hughes [107]. An alternative to the analytical approach for finding the stabilization constants is their numerical determination, see [111,112] for details.

B.1. Definition of stabilization parameter

From dimensional considerations, we can write the stabilization parameter as follows:

- for the Bernoulli–Euler beam theory, we have

$$\tau = C\frac{EI}{h_e}, \tag{B.1}$$

- for the Poisson–Kirchhoff plate theory, we have

$$\tau = C\frac{Et^3}{12(1-\nu^2)h_e}, \tag{B.2}$$

- for the one-dimensional Toupin–Mindlin strain gradient theory, we have

$$\tau = C\frac{\mu l^2}{h_e}. \tag{B.3}$$

In the above, the C's are constants which depend on the order of interpolation. For one-dimensional problems, the element characteristic length h_e is identical to the element length for uniform discretizations, and can be defined as the distance between the centroids of the elements adjacent to the interior boundary under consideration for non-uniform discretizations. For two-dimensional problems, we have used the distance between the centroids of the elements adjacent to the interior boundary under consideration as depicted in Fig. 48.

B.2. Determination of constants for linear interpolation

For the case of a Bernoulli–Euler beam loaded by an end moment, the exact solution is quadratic (see Section 6.1.1) and we would hope that a nodally superconvergent method can be designed for this load case

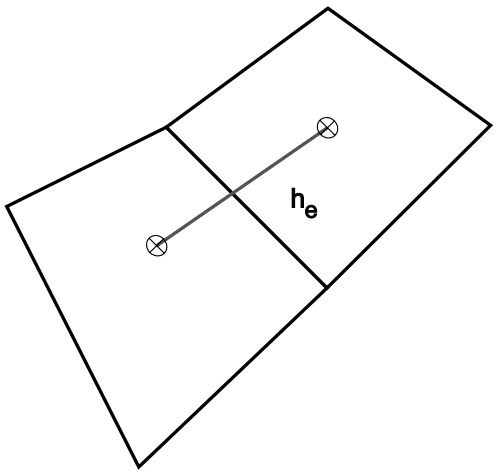

Fig. 48. Definition of h_e.

for linear interpolation functions. Let us consider model problem (310)–(314) with a discretization into uniform elements of length h.

Let us choose for the purpose of determining the stabilization constants the trial solution and weighting function spaces for our approximation as

$$\mathscr{S}^h = \left\{ \phi^h \in H^1(\Omega) |\ \phi^h|_{\Omega_e} \in P_k(\Omega_e)\ \forall \Omega_e \in \mathscr{P}(\Omega) \right\}, \tag{B.4}$$

$$\mathscr{V}^h = \left\{ w^h \in H^1(\Omega) |\ w^h|_{\Omega_e} \in P_k(\Omega_e)\ \forall \Omega_e \in \mathscr{P}(\Omega) \right\}. \tag{B.5}$$

Note that in definition (B.4) we do not require the trial solution functions to satisfy the displacement boundary condition, and we do not require the weighting functions to satisfy the homogeneous counterpart of the displacement boundary condition in (B.5). Rather, we wish to enforce the displacement boundary condition weakly, and therefore we add stabilizing terms on the displacement boundary to the variational equation, multiplied by a stabilization parameter

$$\tau_g = \mathscr{O}(EI/h^3). \tag{B.6}$$

Omitting all terms involving higher-order derivatives in (146), as these terms vanish for linear interpolation, we obtain

$$\tau [\![w^h_{,x}]\!] [\![\phi^h_{,x}]\!]_{\tilde{\Gamma}} + \tau_h w^h_{,x}(0) \phi^h_{,x}(0) + \tau_g w^h(0) \phi^h(0) = w^h_{,x}(1) M. \tag{B.7}$$

The first interface stabilization term leads for the example of interface node i to the interface matrix

$$\frac{\tau}{h^2} \begin{bmatrix} 1 & -2 & 1 \\ -2 & 4 & -2 \\ 1 & -2 & 1 \end{bmatrix} \begin{matrix} \\ i, \\ \\ \end{matrix} \tag{B.8}$$

which is assembled in the global stiffness matrix instead of element contributions for the two elements adjacent to the interface i. After assembly, a typical row i for a discretization into at least four elements, away from the matrix contributions due to the boundary terms, reads

$$\frac{\tau}{h^2} (\phi_{i-2} - 4\phi_{i-1} + 6\phi_i - 4\phi_{i+1} + \phi_{i+2}) = 0, \tag{B.9}$$

where the ϕ_i denote the value of ϕ at node i. Note that (B.9) coincides for $\tau = EI/h$ with the second-order accurate central finite difference operator for a fourth derivative [113], viz.

$$EI \left(\frac{\partial^4 \phi}{\partial x^4} \right)_i = \frac{EI}{h^4} (\phi_{i-2} - 4\phi_{i-1} + 6\phi_i - 4\phi_{i+1} + \phi_{i+2}), \tag{B.10}$$

the only difference between (B.9) and (B.10) being one order of h, which is due to the fact that the finite element formulation is an integral statement over the domain. We have indicated in (B.10) at which node the derivative is evaluated by the subscript i on the bracket. The interface stabilization terms are the only contribution to the stiffness matrix, apart from the boundary condition stiffness terms.

Let us now consider a discretization of the domain into four uniform elements. It will be possible to construct a method which exhibits superconvergent behavior at every node for linear approximation functions for the end moment load case. The contribution to the stiffness matrix due to the boundary condition terms are for linear interpolation for the displacement boundary condition

$$\tau_g \begin{bmatrix} 1 & 0 \\ 0 & 0 \end{bmatrix} \tag{B.11}$$

in the first element, and for the slope boundary condition

$$\frac{\tau_h}{h^2}\begin{bmatrix} 1 & -1 \\ -1 & 1 \end{bmatrix} \tag{B.12}$$

also in the first element. Choosing for $\tau_g = EI/h^3$ and for $\tau_h = CEI/h$, where C is a constant that needs to be determined, the matrix system for the discretization into four uniform elements reads

$$\frac{EI}{h^3}\begin{bmatrix} 2+C & -2-C & 1 & 0 & 0 \\ -2-C & 5+C & -4 & 1 & 0 \\ 1 & -4 & 6 & -4 & 1 \\ 0 & 1 & -4 & 5 & -2 \\ 0 & 0 & 1 & -2 & 1 \end{bmatrix}\begin{pmatrix} \phi_1 \\ \phi_2 \\ \phi_3 \\ \phi_4 \\ \phi_5 \end{pmatrix} = \begin{pmatrix} 0 \\ 0 \\ 0 \\ -M/h \\ M/h \end{pmatrix}. \tag{B.13}$$

Note that the left-hand side of the fifth row in (B.13) coincides with the second-order accurate central finite difference operator for a second derivative at node 4, viz.

$$EI\left(\frac{\partial^2\phi}{\partial x^2}\right)_4 = \frac{EI}{h^2}(\phi_3 - 2\phi_4 + \phi_5) = M, \tag{B.14}$$

whereas the left-hand side of the fourth row coincides with the second-order accurate backward finite difference operator for a second derivative at node 5, namely

$$EI\left(\frac{\partial^2\phi}{\partial x^2}\right)_5 = \frac{EI}{h^2}(-\phi_2 + 4\phi_3 - 5\phi_4 + 2\phi_5) = M. \tag{B.15}$$

Therefore, from a finite difference point of view, the last two rows of the matrix system (B.13) both satisfy the approximation of the moment boundary condition (313) with second-order accuracy.

We now seek to also satisfy the other three boundary conditions to second-order accuracy in a finite difference sense. Using the exact solution

$$\phi_i = \frac{1}{2}\frac{M}{EI}x_i^2 \tag{B.16}$$

at nodes $i = 1$–4, we obtain from the first two rows of (B.13) the equations

$$(-2-C)\frac{Mh^2}{2} + \frac{M(2h)^2}{2} = 0, \tag{B.17}$$

$$(5+C)\frac{Mh^2}{2} - 4\frac{M(2h)^2}{2} + \frac{M(3h)^2}{2} = 0. \tag{B.18}$$

Both equations are identically satisfied for $C = 2$. With this value of C, the first two rows of (B.13) read

$$4\phi_1 - 4\phi_2 + \phi_3 = 0, \tag{B.19}$$

$$-4\phi_1 + 7\phi_2 - 4\phi_3 + \phi_4 = 0. \tag{B.20}$$

These equations can be interpreted as follows: one can view (B.19) as the addition of the two parts

$$\phi_1 = 0 \tag{B.21}$$

and

$$3\phi_1 - 4\phi_2 + \phi_3 = 0, \tag{B.22}$$

where (B.21) is the enforcement of the displacement boundary condition (311), and (B.22) is the enforcement of the slope boundary condition (312), as the left-hand side coincides with the second-order accurate forward finite difference operator for a first derivative at node 1, viz.

$$EI\left(\frac{\partial\phi}{\partial x}\right)_1 = -\frac{EI}{h}(3\phi_1 - 4\phi_2 + \phi_3) = 0. \tag{B.23}$$

Similarly, one can interpret Eq. (B.20) as a linear combination of the two parts

$$3\phi_1 - 4\phi_2 + \phi_3 = 0, \tag{B.24}$$

$$-\phi_1 + 3\phi_2 - 3\phi_3 + \phi_4 = 0. \tag{B.25}$$

The left-hand side of (B.24) is again the second-order accurate forward finite difference approximation for a first derivative at node 1 and therefore enforces again the slope boundary condition (312), whereas the left-hand side of (B.25) is the forward finite difference approximation of a third derivative at node 1, namely

$$EI\left(\frac{\partial^3\phi}{\partial x^3}\right)_1 = \frac{EI}{h^3}(-\phi_1 + 3\phi_2 - 3\phi_3 + \phi_4) = 0. \tag{B.26}$$

Note that (B.26) is only first-order accurate. This enforces a shear force boundary condition similar to (314), but instead of the required shear force boundary condition at $x = 1$, it enforces a shear force boundary condition at $x = 0$. In this case, however, this is admissible, because due to the loading of the beam with an end moment only, the shear force is identically zero over the entire beam.

As can be seen in Section 6.1.2, the choice of

$$\tau = \frac{EI}{h}, \tag{B.27}$$

$$\tau_h = 2\frac{EI}{h}, \tag{B.28}$$

leads to a method which is superconvergent at every node for the end moment load case, and which will converge at optimal rate in the energy norm and in the L^2-norm for linear interpolation. For the cases of an end shear force and a distributed load, nodal superconvergence will be lost, but the method will still be converging at optimal rates. Enforcing the displacement boundary condition strongly does not alter the results.

Appendix C. Implementation of DG methods

Implementation of DG and C/DG methods into existing programs for finite element-based CG methods requires some modifications. The added terms of the DG or C/DG methods involve interaction between contiguous elements. Thus it is necessary to implement a search algorithm which can detect the individual interface between the contiguous elements, as well as, identify the segments for imposition of boundary condition terms. For the Bernoulli–Euler beam theory and the one-dimensional Toupin–Mindlin strain gradient theory the interfaces are merely end points of contiguous elements, whereas for the Poisson–Kirchhoff plate theory the interfaces are segments defining element edges. A three dimensional formulation would use faces as the interface segments. Our search results in a list where each entry gives the pair of elements to use and a list of associated vertex nodes sufficient to describe the interface segment (1 for a point interface; 2 for a line interface; 3 for a face interface). A pass through this array will describe all interfaces to be processed for a DG or a C/DG method.

In a DG method variables are often used which do not involve nodal unknowns. Thus, it is desirable to define element variables as two classes: *nodal* variables and *element* variables. In this way one can accomodate CG formulations which include element Lagrange multiplier terms (e.g., to invoke incompressibility at an element level) as well as DG formulations in which approximation is given in terms of element variables only. In the FEAP system a parameter is used to define the number of element parameters and a second parameter to define the number of parameters at each node. Additionally, a new class of element types is needed to compute the interface contributions (the FEAP library now consists of `ELMTnn` and `IELMTnn` classes, the former treating the domain terms of elements and the latter the interface terms [114]). Data is passed to each interface element for both elements associated to it (as identified by the search described above). For boundary segments the data for only one element is provided. Thus, with this data structure, it is possible to compute all the necessary contributions from both the interface and boundary terms. Output from the interface elements is identical to that from typical domain elements and thus may be processed using the available modules (e.g., those to assemble element arrays into global arrays and solve the resulting equations).

In our formulation a direct solution of the assembled equations is performed using a profile (skyline) method [115]. In order to properly assemble the coefficient matrix it is necessary to determine the profile from all the terms in a DG or C/DG method. This is accomplished by processing the usual domain equations of individual elements (as in any finite element CG method) as well as considering the interface equations associated with element pairs. The actual profile in the matrix is obtained by first computing the maximum column height for each equation and then converting it to a pointer for locating terms in the coefficient matrix stored as a single subscript array [115]. The algorithms already in the program for individual elements also are used for the interface pairs. Again the interface pairs identified in the search process play a crucial role in the determination of the profile.

References

[1] E. Zauderer, Partial Differential Equations of Applied Mathematics, second ed., Wiley, New York, 1989.
[2] Encyclopaedia Britannica, 2001, Solids Mechanics/History/Beams, Columns, Plates, and Shells, http://www.britannica.com.
[3] R.A. Toupin, Elastic materials with couple-stresses, Archive for Rational Mechanics and Analysis 11 (1962) 385–414.
[4] R.D. Mindlin, Micro-structure in linear elasticity, Archive for Rational Mechanics and Analysis 16 (1964) 51–78.
[5] I.S. Sokolnikoff, Mathematical Theory of Elasticity, second ed., Krieger Publishing, Malabar, FL, 1983.
[6] S. Timoshenko, J.N. Goodier, Theory of Elasticity, second ed., McGraw-Hill, New York, 1951.
[7] A. Nádai, Die elastischen Platten, Springer, Berlin, 1925.
[8] S. Timoshenko, S. Woinowsky-Krieger, Theory of Plates and Shells, second ed., McGraw-Hill, New York, 1959.
[9] A.C. Ugural, Stresses in Plates and Shells, McGraw-Hill, New York, 1981.
[10] T.J.R. Hughes, The Finite Element Method: Linear Static and Dynamic Finite Element Analysis, Dover, Mineola, New York, 2000.
[11] O.C. Zienkiewicz, R.L. Taylor, The Finite Element Method, fifth ed., Butterworth-Heinemann, Oxford, 2000.
[12] N.A. Fleck, J.W. Hutchinson, Strain gradient plasticity, Advances in Applied Mechanics 33 (1997) 295–361.
[13] M. Fortin, F. Brezzi, Mixed and Hybrid Finite Element Methods, Springer, New York, 1991.
[14] I. Babuška, Error-bounds for finite element method, Numerische Mathematik 16 (1970/1971) 322–333.
[15] F. Brezzi, On the existence, uniqueness and approximation of saddle-point problems arising from lagrangian multipliers, Revue Française d'Automation, Information, Recherche Opérationnelle, Séries Rouge 8 (R-2) (1974) 129–151.
[16] D.S Malkus, T.J.R. Hughes, Mixed finite-element methods—reduced and selective integration techniques: Unification of concepts, Computer Methods in Applied Mechanics and Engineering 15 (1) (1978) 63–81.
[17] T.J.R. Hughes, L.P. Franca, A mixed finite element formulation for Reissner–Mindlin plate theory: Uniform convergence of all higher-order spaces, Computer Methods in Applied Mechanics and Engineering 67 (2) (1988) 223–240.
[18] D.N. Arnold, R.S. Falk, A uniformly accurate finite element method for the Reissner–Mindlin plate, SIAM Journal on Numerical Analysis 26 (6) (1989) 1276–1290.
[19] J.Y. Shu, W.E. King, N.A. Fleck, Finite elements for materials with strain gradient effects, International Journal for Numerical Methods in Engineering 44 (3) (1999) 73–391.

[20] J.L. Batoz, K.J. Bathe, L.W. Ho, A study of 3-node triangular plate bending elements, International Journal for Numerical Methods in Engineering 15 (12) (1980) 1771–1812.
[21] G. Strang, G.J. Fix, An Analysis of the Finite Element Method, Prentice-Hall, Englewood Cliffs, NJ, 1973.
[22] R. Phaal, C.R. Calladine, A simple class of finite-elements for plate and shell problems. 1. Elements for beams and thin flat plates, International Journal for Numerical Methods in Engineering 35 (5) (1992) 955–977.
[23] R. Phaal, C.R. Calladine, A simple class of finite-elements for plate and shell problems. 2. An element for thin shells with only translational degrees of freedom, International Journal for Numerical Methods in Engineering 35 (5) (1992) 979–996.
[24] E. Oñate, M. Cervera, Derivation of thin plate bending elements with one degree of freedom per node: a simple three node triangle, Engineering Computations 10 (6) (1993) 543–561.
[25] E. Oñate, F. Zarate, Rotation-free triangular plate and shell elements, International Journal for Numerical Methods in Engineering 47 (1) (2000) 557–603.
[26] I. Babuška, M. Zlámal, Nonconforming elements in the finite element method with penalty, SIAM Journal on Numerical Analysis 10 (1973) 863–875.
[27] G.A. Baker, Finite element methods for elliptic equations using nonconforming elements, Mathematics of Computation 31 (137) (1977) 45–59.
[28] J.H. Argyris, Die Matrizentheorie der Statik, Ingenieur Archiv 25 (1957) 174–192.
[29] J.H. Argyris, Energy Theorems and Structural Analysis, Butterworth, London, 1960.
[30] O.C. Zienkiewicz, Y.K. Cheung, The Finite Element Method in Structural and Continuum Mechanics, McGraw-Hill, London, 1967.
[31] R. Courant, Variational methods for the solution of problems of equilibrium and vibrations, Bulletin of the American Mathematical Society 49 (1943) 1–23.
[32] S.C. Brenner, L.R. Scott, The Mathematical Theory of Finite Element Methods, Springer, New York, 1994.
[33] J.-L. Lions, E. Magenes, Non-Homogeneous Boundary Value Problems and Applications, vol. I, Springer, New York, 1972 (Translated from the French by P. Kenneth, Die Grundlehren der mathematischen Wissenschaften, Band 181).
[34] J.-L. Lions, E. Magenes, Non-Homogeneous Boundary Value Problems and Applications, vol. II, Springer, New York, 1972 (Translated from the French by P. Kenneth, Die Grundlehren der mathematischen Wissenschaften, Band 182).
[35] J.-L. Lions, E. Magenes, Non-Homogeneous Boundary Value Problems and Applications, vol. III, Springer, New York, 1973 (Translated from the French by P. Kenneth, Die Grundlehren der mathematischen Wissenschaften, Band 183).
[36] T.J.R. Hughes, G.M. Hulbert, Space–time finite element methods for elastodynamics: Formulations and error estimates, Computer Methods in Applied Mechanics and Engineering 66 (3) (1988) 339–363.
[37] G.M. Hulbert, T.J.R. Hughes, Space–time finite element methods for second-order hyperbolic equations, Computer Methods in Applied Mechanics and Engineering 84 (3) (1990) 327–348.
[38] W.H. Reed and T.R. Hill, Triangular mesh methods for the neutron transport equation, Technical Report LA-UR-73-479, Los Alamos Scientific Laboratory, Los Alamos, 1973.
[39] P. Lesaint, P.-A. Raviart, On a finite element method for solving the neutron transport equation, in: C. de Boor (Ed.), Mathematical Aspects of Finite Elements in Partial Differential Equations, Academic Press, New York, 1974, pp. 89–123.
[40] P. Lesaint, Sur la résolution des systèmes hyperboliques du premier ordre par des méthodes d'eléments finis, Ph.D. thesis, Université de Paris VI, Paris, France, 1975.
[41] C. Johnson, U. Nävert, J. Pitkäranta, Finite element methods for linear hyperbolic problems, Computer Methods in Applied Mechanics and Engineering 45 (1984) 285–312.
[42] C. Johnson, J. Pitkäranta, An analysis of the discontinuous Galerkin method for a scalar hyperbolic equation, Mathematics of Computation 46 (173) (1986) 1–26.
[43] E.L. Wilson, R.L. Taylor, W.P. Doherty, J. Ghaboussi, Incompatible displacement models, in: S.J. Fenves, N. Perrone, A.R. Robinson, W.C. Schnobrick (Eds.), Numerical and Computer Models in Structural Mechanics, Academic Press, New York, 1973, pp. 43–57.
[44] P. Lesaint, On the convergence of Wilson's non-conforming element for solving the elastic problem, Computer Methods in Applied Mechanics and Engineering 7 (1976) 1–16.
[45] F. Kikuchi, Y. Ando, A new variational functional for the finite element method, Nuclear Engineering and Design 21 (1972) 95–113.
[46] B. Cockburn, C.W. Shu, TVB Runge–Kutta local projection discontinuous Galerkin finite element methods for conservation laws. II: General framework, Mathematics of Computation 52 (1989) 411–435.
[47] K.S. Bey, J.T. Oden, *hp*-version discontinuous Galerkin methods for hyperbolic conservation laws, Computer Methods in Applied Mechanics and Engineering 133 (1996) 259–286.
[48] P. Houston, C. Schwab, E. Suli, Stabilized *hp*-finite element methods for first-order hyperbolic problems, Technical Report 98/14, Oxford University Computing Laboratory, Oxford, England, November 1998.
[49] F. Bassi, S. Rebay, High-order accurate discontinuous finite element solution of the 2D Euler equations, Journal of Computational Physics 138 (1997) 251–285.

[50] F. Bassi, S. Rebay, A high-order accurate discontinuous finite element method for the numerical solution of the compressible Navier–Stokes equations, Journal of Computational Physics 131 (1997) 267–279.
[51] F. Brezzi, G. Manzini, D. Marini, P. Pietra, A. Russo, Discontinuous Galerkin approximations for elliptic problems, Numerical Methods for Partial Differential Equations 16 (4) (2000) 365–378.
[52] B. Cockburn, C.W. Shu, The local discontinuous Galerkin finite element method for time-dependent convection–diffusion systems, SIAM Journal on Numerical Analysis 35 (1998) 2440–2463.
[53] J.A. Nitsche, Über ein Variationsprinzip zur Lösung von Dirichlet-Problemen bei Verwendung von Teilräumen, die keinen Randbedingungen unterworfen sind, Abhandlungen aus dem Mathematischen Seminar der Universität Hamburg 36 (1971) 9–15.
[54] I. Babuška, The finite element method with penalty, Mathematics of Computation 27 (1973) 221–228.
[55] J. Douglas Jr., T. Dupont, Interior penalty procedures for elliptic and parabolic Galerkin methods, in: Computing Methods in Applied Sciences, Lecture Notes in Physics, vol. 58, Springer, Berlin, 1976, pp. 207–216.
[56] M.F. Wheeler, An elliptic collocation-finite element method with interior penalties, SIAM Journal on Numerical Analysis 15 (1) (1978) 152–161.
[57] P. Percell, M.F. Wheeler, A local residual finite element procedure for elliptic equations, SIAM Journal on Numerical Analysis 15 (4) (1978) 705–714.
[58] D.N. Arnold, An interior penalty finite element method with discontinuous elements, Ph.D. thesis, University of Chicago, Chicago, Illinois, 1979.
[59] D.N. Arnold, An interior penalty finite element method with discontinuous elements, SIAM Journal on Numerical Analysis 19 (4) (1982) 742–760.
[60] L.M. Delves, C.A. Hall, An implicit matching principle for global element calculations, Journal of the Institute of Mathematics and its Applications 23 (2) (1979) 223–234.
[61] C.E. Baumann, An *hp*-adaptive discontinuous finite element method for computational fluid mechanics, Ph.D. thesis, The University of Texas at Austin, Austin, Texas, 1997.
[62] I. Babuška, C.E. Baumann, J.T. Oden, A discontinuous *hp* finite element method for diffusion problems: 1-D analysis, Computers and Mathematics with Applications 37 (9) (1999) 103–122.
[63] J.T. Oden, I. Babuška, C.E. Baumann, A discontinuous *hp* finite element method for diffusion problems, Journal of Computational Physics 146 (2) (1998) 491–519.
[64] C.E. Baumann, J.T. Oden, A discontinuous *hp* finite element method for the Euler and Navier–Stokes equations, International Journal for Numerical Methods in Fluids 31 (1) (1999) 79–95.
[65] C.E. Baumann, J.T. Oden, A discontinuous *hp* finite element method for convection–diffusion problems, Computer Methods in Applied Mechanics and Engineering 175 (3–4) (1999) 311–341.
[66] C.E. Baumann, J.T. Oden, An adaptive-order discontinuous Galerkin method for the solution of the Euler equations of gas dynamics, International Journal for Numerical Methods in Engineering 47 (1–3) (2000) 61–73.
[67] S. Prudhomme, F. Pascal, J.T. Oden, A. Romkes, A priori error estimate for the Baumann–Oden version of the discontinuous Galerkin method, Comptes Rendus de I'Academie des Sciences, Serie I, Mathématique 332 (2001) 851–856.
[68] D.N. Arnold, F. Brezzi, B. Cockburn, D. Marini, Discontinuous Galerkin methods for elliptic problems, in: B. Cockburn, G.E. Karniadakis, C.-W. Shu (Eds.), Discontinuous Galerkin Methods, Lecture Notes in Computational Science and Engineering, vol. 11, Springer, Berlin, 2000, pp. 89–101.
[69] J. Freund, The space-continuous–discontinuous Galerkin method, Computer Methods in Applied Mechanics and Engineering 190 (26–27) (2001) 3461–3473.
[70] A.N. Brooks, T.J.R. Hughes, Streamline upwind/Petrov–Galerkin formulations for convection dominated flows with particular emphasis on the incompressible Navier–Stokes equations, Computer Methods in Applied Mechanics and Engineering 32 (1–3) (1982) 199–259.
[71] T.J.R. Hughes, L.P. Franca, G.M. Hulbert, A new finite element formulation for computational fluid dynamics. VIII. The Galerkin/least-squares method for advective–diffusive equations, Computer Methods in Applied Mechanics and Engineering 73 (2) (1989) 173–189.
[72] T.J.R. Hughes, Multiscale phenomena: Green's functions, the Dirichlet-to-Neumann formulation, subgrid scale models, bubbles and the origins of stabilized methods, Computer Methods in Applied Mechanics and Engineering 127 (1–4) (1995) 387–401.
[73] F. Brezzi, A. Russo, Choosing bubbles for advection–diffusion problems, Mathematical Models and Methods in Applied Sciences 4 (4) (1994) 571–587.
[74] F. Brezzi, L.P. Franca, T.J.R. Hughes, A. Russo, Stabilization techniques and subgrid scales capturing, in: The State of the Art in Numerical Analysis (York, 1996), Oxford University Press, New York, 1997, pp. 391–406.
[75] F. Brezzi, L.P. Franca, T.J.R. Hughes, A. Russo, $b = \int g$, Computer Methods in Applied Mechanics and Engineering 145 (3–4) (1997) 329–339.
[76] L.P. Franca, A. Russo, Unlocking with residual-free bubbles, Computer Methods in Applied Mechanics and Engineering 142 (3–4) (1997) 361–364.

[77] L.P. Franca, A. Russo, Mass lumping emanating from residual-free bubbles, Computer Methods in Applied Mechanics and Engineering 142 (3–4) (1997) 353–360.
[78] L.P. Franca, A. Russo, Approximation of the Stokes problem by residual-free macro-bubbles, East–West Journal of Numerical Mathematics 4 (4) (1996) 265–278.
[79] L.P. Franca, A. Russo, Deriving upwinding, mass lumping and selective reduced integration by residual-free bubbles, Applied Mathematics Letters 9 (5) (1996) 83–88.
[80] T. De Mulder, Stabilized finite element methods (SUPG, GLS) for incompressible flows, in: H. Deconinck (Ed.), Finite Element Methods for Compressible and Incompressible Flow, VKI Lecture Series Monographs Computational Fluid Dynamics, vol. SST5, Von Karman Institute, Rhode Saint Genese, Belgium, 1997.
[81] E. Kreyszig, Introductory Functional Analysis with Applications, Wiley, New York, 1989.
[82] L.P. Franca, S.L. Frey, T.J.R. Hughes, Stabilized finite element methods. I. Application to the advective–diffusive model, Computer Methods in Applied Mechanics and Engineering 95 (2) (1992) 253–276.
[83] J.T. Oden, L.F. Demkowicz, Applied Functional Analysis, CRC Press, Boca Raton, FL, 1996.
[84] T.J.R. Hughes, G. Engel, L. Mazzei, M.G. Larson, A comparison of discontinuous and continuous Galerkin methods based on error estimates, conservation, robustness and efficiency, in: B. Cockburn, G.E. Karniadakis, C.-W. Shu (Eds.), Discontinuous Galerkin Methods, Lecture Notes in Computational Science and Engineering, vol. 11, Springer, Berlin, 2000, pp. 135–146.
[85] R. Stenberg, On some techniques for approximating boundary conditions in the finite element method, Journal of Computational and Applied Mathematics 63 (1995) 139–148.
[86] R. Stenberg, Mortaring by a method of J.A. Nitsche, in: S. Idelsohn, E. Onate, E. Dvorkin (Eds.), Computational Mechanics—New Trends and Applications, CIMNE, Barcelona, Spain, 1998.
[87] D.N. Arnold, R. Falk, R. Scott, 1985, private communication.
[88] T.J.R. Hughes, L.P. Franca, M. Mallet, A new finite element formulation for computational fluid dynamics: VI. Convergence analysis of the generalized SUPG formulation for linear time-dependent multidimensional advective–diffusive systems, Computer Methods in Applied Mechanics and Engineering 63 (1) (1987) 97–112.
[89] C. Truesdell, W. Noll, The non-linear field theories of mechanics, in: Handbuch der Physik, vol. III/3, Springer, Berlin, 1965.
[90] E. Cosserat, F. Cosserat, Sur la mécanique génerale, Comptes Rendus de I'Academie des Sciences, Serie I, Mathématique 145 (1907) 1139–1142.
[91] E. Cosserat, F. Cosserat, Theorie des Corps Déformables, Hermann, Paris, 1909.
[92] C. Truesdell, R.A. Toupin, Principles of classical mechanics and field theory, in: Handbuch der Physik, vol III/1, Springer, Berlin, 1960.
[93] A.C. Eringen, Continuum Physics, vol. 4: Polar and Nonlocal Field Theories, New York, Academic Press, 1976.
[94] R. de Borst, L.J. Sluys, Localisation in a cosserat continuum under static and dynamic loading conditions, Computer Methods in Applied Mechanics and Engineering 90 (1991) 805–827.
[95] A.L. Cauchy, Note sur léquilibre et les mouvements vibratoires des corps solids, Comptes Rendus de I'Academie des Sciences. Serie I, Mathématique 32 (1851) 323–326.
[96] N.A. Stelmashenko, M.G. Walls, L.M. Brown, Y.V. Milman, Microindentation studies on W and Mo oriented single crystals, Acta Metallurgica et Materialia 41 (1993) 2855–2865.
[97] N.A. Fleck, G.M. Muller, M.F. Ashby, J.W. Hutchinson, Strain gradient plasticity: theory and experiment, Acta Metallurgica et Materialia 42 (1994) 475–487.
[98] J.S. Stolken, A.G. Evans, Microbend test method for measuring the plasticity length scale, Acta Materialia 46 (1998) 5109–5115.
[99] H. Gao, Y. Huang, W.D. Nix, Mechanism-based strain gradient plasticity. I. Theory, Journal of the Mechanics and Physics of Solids 47 (1999) 1239–1263.
[100] Y. Huang, H. Gao, W.D. Nix, J.W. Hutchinson, Mechanism-based strain gradient plasticity. II. Analysis, Journal of the Mechanics and Physics of Solids 48 (2000) 99–128.
[101] Z.C. Xia, J.W. Hutchinson, Crack tip fields in strain gradient plasticity, Journal of the Mechanics and Physics of Solids 44 (1996) 1621–1648.
[102] J.S. Chen, C.T. Wu, T. Belytschko, Regularization of material instabilities by mesh free approximations with intrinsic length scales, International Journal for Numerical Methods in Engineering 47 (2000) 1303–1322.
[103] H. Askes, J. Pamin, R. de Borst, Dispersion analysis and element-free Galerkin solutions of second- and fourth-order gradient-enhanced damage models, International Journal for Numerical Methods in Engineering 49 (2000) 811–832.
[104] S. Li, W.K. Liu, Reproducing kernel hierarchical partition of unity, part II: Applications, International Journal for Numerical Methods in Engineering 45 (1999) 289–317.
[105] S. Li, W.K. Liu, Reproducing kernel hierarchical partition of unity, part I: Formulation and theory, International Journal for Numerical Methods in Engineering 45 (1999) 251–288.
[106] T.J.R. Hughes, G. Engel, L. Mazzei, M.G. Larson, The continuous Galerkin method is locally conservative, Journal of Computational Physics 163 (2) (2000) 467–488.

[107] I. Harari, T.J.R. Hughes, What are C and h?: Inequalities for the analysis and design of finite element methods, Computer Methods in Applied Mechanics and Engineering 97 (2) (1992) 157–192.
[108] P.G. Ciarlet, Basic error estimates for elliptic problems, in: P.G. Ciarlet, J.L. Lions (Eds.), Finite Element Methods (Part 1), Handbook of Numerical Analysis, vol. II, North-Holland, Amsterdam, 1991.
[109] D.N. Arnold, An interior penalty finite element method with discontinuous elements, SIAM Journal on Numerical Analysis 19 (1982) 742–760.
[110] S. Agmon, Lectures on Elliptic Boundary Value Problems, Van Nostrand, Princeton, NJ, 1965.
[111] M. Lyly, Stabilized finite element methods for plate bending problems, Ph.D. thesis, Helsinki University of Technology, Espoo, Finland, 1999.
[112] M. Lyly, R. Stenberg, T. Vihinen, A stable bilinear element for the Reissner–Mindlin plate model, Computer Methods in Applied Mechanics and Engineering 110 (1993) 343–357.
[113] Ch. Hirsch, Numerical Computation of Internal and External Flows, Wiley, New York, 1988.
[114] R.L. Taylor, FEAP-A Finite Element Analysis Program, Programmer Manual, University of California Berkeley, http://www.ce.berkeley.edu/~rlt.
[115] R.L. Taylor, Solution of linear equations by a profile solver, Engineering Computations 4 (1985) 344–350.